Will nitrogen limitation and high CO_2 concentrations impact upon the sinking velocity of phytoplankton?

Amanda Mannfolk (nee. Pantorno)

Bachelor of Science

Honours Degree of a Bachelor of Science

Bachelor of Laws

A thesis submitted for the degree of Doctor of Philosophy at

Monash University in 2015

School of Biological Science

Copyright notice

TABLE OF CONTENTS

Abstract

The biological carbon pump in the ocean plays an important role in controlling atmospheric CO_2 levels. Approximately 1-3% of the yearly 50–60 Pg C of marine primary production settles in the deep ocean, where it is effectively sequestered for centuries to millennia. Central to the strength of the pump is the sinking velocity of phytoplankton cells and other organic debris. Stokes' Law indicates that the sinking velocity of a spherical cell will depend on its size and density, where larger, heavier cells will sink at a faster rate. Given that growth conditions can result in changes in cell size and macromolecular composition of phytoplankton, it might be expected that such changes could cause alterations in sinking velocity and carbon drawdown via the biological carbon pump.

In the future, phytoplankton cells in the open ocean are predicted to be more subject to nutrient limitation due to enhanced stratification reducing the upwelling of nutrients. This will be driven by the warming of surface waters and an increase in the difference between the temperature of the surface and deeper ocean. Therefore the effects of nitrogen limitation on the sinking velocity of *Emiliania huxleyi*, a coccolithophore responsible for significant phytoplankton blooms and biological drawdown of carbon was examined. Nitrogen limitation caused changes in macromolecular composition, especially lipid content and also alters coccosphere thickness. However, the overall density of the cells remained similar, and, as a consequence, cell size was the major determinant of sinking rate with N-limited cells in exponential phase sinking more slowly than N-replete cells. Cells in stationary phase showed the reverse trend with N-limited cells sinking faster, although not as fast as N-replete cells in exponential phase. N-limited cells produced more transparent

exopolymers (TEP), suggesting an increased capacity for aggregation and marine snow formation.

Phytoplankton cells are also expected to be to be exposed to higher concentrations of CO_2 in the future, potentially 1000 p.p.m. by the year 2100. Therefore, the effects of high CO_2 (1000 p.p.m.) on the sinking velocity of *E. huxleyi* were also examined. The high CO_2 did not alter the sinking velocity of *E. huxleyi* during the exponential growth phase. This was because the overall size and density of cells remained similar between high-CO_2 and ambient CO_2 grown cultures. The increased CO_2 concentration did however cause cells to increase their protoplast diameter and decrease their coccosphere radius, suggesting that cells were reducing their rate of calcification and channelling excess carbon into organic matter production. The high CO_2 also caused the cells to alter their macromolecular composition, increasing significantly the concentrations of lipids, carbohydrates and proteins. At stationary phase, the high CO_2 did not increase TEP production. However, by stationary phase, CO_2 equilibrium could not be maintained, so there were no differences in CO_2 concentrations between cultures. While this finding sheds no light on the role that TEP plays in sinking, it does further highlight the positive relationship between CO_2 concentrations and TEP production.

Phytoplankton cells will be exposed to many concurrent environmental changes in the future ocean. Therefore, the interactive effects of high CO_2 (1000 p.p.m.) and N-limitation on the sinking velocity of *Chaetoceros didymus*, a chain forming marine diatom, were examined. During the exponential growth phase, the N-limited/1000 p.p.m. CO_2 cells sank the fastest, followed by the N-replete/1000 p.p.m. CO_2 cells and then the N-limited/400

p.p.m. CO_2 cells. The N-replete/400 p.p.m. CO_2 cells sank at the slowest rate. The concentration of lipids and carbohydrates increased significantly in the N-replete/1000 p.p.m. CO_2 cells and increased further still when high CO_2 was combined with N-limitation, although this increase was not statistically significant. Despite this, there were no differences observed in density between any of the groups. It is likely, therefore, that the differences seen in sinking, during the exponential growth phase, were due to changes in the cells' physical size, either through increased chain- or spine-length. During stationary phase, the two N-limited cultures displayed the greatest sinking velocities while the slowest average sinking velocity was again seen in the N-replete/400 p.p.m. CO_2 cells. The N-limited/400 p.p.m. CO_2 cultures increased their sinking velocity because of an increase in cell volume caused by enhanced chain formation. In contrast the N-limited/1000 p.p.m. CO_2 cells increased their sinking velocity because of an increase in density. During stationary phase, TEP concentrations increased significantly in the two high CO_2 cultures, a 5 times increase being seen in the N-limited/1000 p.p.m. CO_2 cultures. This increase in TEP suggests a high capacity for marine snow formation in the future ocean.

These observations suggest that there will be changes in the efficiency of the biological carbon pump in the future, especially in areas that have increased nutrient stress caused by global climate change.

Declaration

This thesis contains no material which has been accepted for the award of any other degree or diploma at any university or equivalent institution and that, to the best of my knowledge and belief, this thesis contains no material previously published or written by another person, except where due reference is made in the text of the thesis.

Amanda Mannfolk (*nee*. Pantorno)

Acknowledgments

I would like to thank my supervisors Professor John Beardall and Dr Slobodanka Stojkovic for their continuous guidance, input and support throughout the completion of my project. Without their patience and willingness to spend time with me, this project could never have been completed.

I would like to thank the members of the Beardall Lab, past and present, with special mention to Daryl Holland who spent countless hours with me fixing the sinking machine and solving complex mathematical problems. His input of time was invaluable. I would also like to thank Stuart Larsen and Paulina Mikulic, for their continuous friendship and their willingness to problem solve with me. Their support helped me to get though many difficult periods. And I would also like to give a big thanks to the other friends I have made along the way who helped to make lab work fun.

I am also incredibly grateful to my family. I would like to thank Peter Mannfolk for his continuous love and for his incredible patience during the completion of my project. Thank you for helping me forget about work and ensuring that life was well rounded and wonderful. And finally, a big thanks to my little Millicent. Your cute little smile motivates me like nothing else.

Chapter 1.0: General Introduction

1.1 Climate Change and the Oceans

Since pre-industrial times, the concentration of carbon dioxide (CO_2) in the atmosphere has increased dramatically from approximately 280 parts per million (p.p.m.) in the 18th Century to 380 p.p.m in 2005 (Raven et al., 2005) and is currently (2015) at 404 p.p.m. The oceans have absorbed almost half of the emitted anthropogenic CO_2 since the beginning of the Industrial Revolution, approximately half by abiotic absorption, the remainder through the photosynthetic activities of algae (Raven et al., 2005). Therefore, without the oceans, the rise in atmospheric CO_2 concentration would be greatly exacerbated (Doney, 2006). Using large-scale simulations, predictions can be made about the likely extent of climate change. In order for these simulations to be accurate however, it is important to know whether the oceans will continue to draw down CO_2 at the same rate they always have or whether they will change their drawdown capabilities as a consequence of anthropogenic climate change. This latter scenario is possible because of the physico-chemical changes brought about by elevated CO_2. CO_2 entering the surface of the ocean decreases pH and causes ocean acidification. The pH in the ocean is predicted to decrease by 0.3 pH units from its present value by the year 2100 (Caldeira and Wickett, 2003), after already having decreased by approximately 0.1 pH units since pre-industrial times (Table 1.1) (Raven et al., 2005, Ruttimann, 2006, Riebesell et al., 2007). In addition to increased acidification as CO_2 concentrations increase, the oceans are expected to experience higher surface temperatures, enhanced stratification and a decreased mixed layer depth, all of which are expected to have some impacts on individual species, communities and ecosystems and potentially, the oceans' ability to draw down CO_2 (Raven et al., 2005, Riebesell et al., 2007).

Table 1.1: A Summary of predicted changes in the composition of seawater with increasing atmospheric carbon dioxide concentrations (Raven et al., 2005).

	Pre-industrial	**2005**	**3x pre-industrial**	**4x pre-industrial**
Atmospheric CO_2 Concentration (p.p.m.)	280	386	840	1120
CO_2 µmol/kg	9	13	28	38
Bicarbonate (HCO_3^-) µmol/kg	1768	1867	2070	2123
Carbonate ions (CO_3^{2-}) µmol/kg	225	185	103	81
Average Surface pH	8.18	8.07	7.77	7.65

1.2 Why is sinking important?

The oceanic "biological carbon pump" plays an important role in controlling atmospheric CO_2 levels. The pump involves photosynthetic phytoplankton fixing inorganic nutrients and CO_2 to produce organic matter and a proportion of the particulate organic matter so produced sinking to the deep ocean. As the sinking particles are transported through the water column, most of the organic carbon is remineralized and reused. A percentage, however, will sink into deep waters or settle in the sediment layer where, if beneath the main ocean thermocline, it could be effectively sequestered for centuries to millennia (Falkowski et al., 1998, Honjo et al., 2014). Globally, approximately 1 – 3% of net primary production will sink into deep waters or settle in the sediment (Falkowski et al., 1998, De La Rocha and Passow, 2007). In polar regions however, this percentage increases to anywhere between 30% and 100% of the net primary production (De La Rocha and Passow, 2007).

Once organic matter sinks, surface waters may become depleted of CO_2 over time. Carbon dioxide levels in the surface layer of the oceans, over a time scale of weeks to months, come to equilibrium

with the atmosphere, so as organic carbon is transported to deeper waters, CO_2 from the atmosphere is absorbed by the ocean (Smetacek, 1999). By removing carbon from the surface waters and taking it to greater depths, the pump increases the capacity of the oceans to act as a sink for atmospheric CO_2 (Raven et al., 2005). This pump therefore, plays a very important role in controlling atmospheric CO_2 levels and any changes in its strength because of changes in the sinking velocity of phytoplankton, could have significant consequences for the atmosphere.

1.3 Factors influencing a cell's sinking velocity – Stokes' Law

The velocity (μ) at which a spherical cell moves through the water column can be described by Stokes' Law;

$$\mu = 2gr^2 (\rho' - \rho)/9\eta \quad \text{(Equation 1.1)}$$

Where g is the gravitational acceleration, r is the cell radius, ρ' is the cell density, ρ is the density of the water and η is the viscosity of the water.

This law can be used to predict the sinking behaviour of phytoplankton. It indicates that the sinking velocity of a cell will vary depending on its radius and density, where larger, heavier cells will sink at a faster rate. The relationship will be distorted however, whenever it is applied to non-spherical cells. There are many different phytoplankton species, which have evolved a range of shapes and have a number of different protuberances, which can add a level of resistance (termed form resistance) and alter the rate of sinking from that predicted by Stokes' Law. Walsby and Xypolyta (1977) for instance, found that the chitan fibres which protrude from each valve of the diatom *Thalassiosira fluviatilis* decreased the sinking velocity by 1.7 times due to an increase in form resistance.

A resistance variable can be added to Equation 1.1 to take into account any form resistance (Φ) while the radius, which is difficult to determine for an odd-shaped cell, can be substituted with the effective radius (r_e), which is the radius of a sphere of an identical volume, where;

$$r_e = (3V/4\pi)^{1/3} \quad \text{(Equation 1.2)}$$

and;

$$\mu = 2gr_e^2 (\rho' - \rho)/9\eta\Phi \quad \text{(Equation 1.3)}$$

Form resistance can be calculated for simple non-spherical shapes, like ellipsoids and cubes but once the shape becomes highly non-uniform, for example through the addition of spines (such as is the case in some diatoms) it becomes impossible to do so. Where this is the case, the velocity must first be found empirically and form resistance calculated by substituting the velocity value into Equation 1.3. Accurate sinking velocity predictions, using odd shaped cells, therefore cannot be made. It is also difficult to use Stokes' Law to make general long-term sinking velocity predictions as we do not know how the biochemistry of phytoplankton cells will change under climate change (e.g. some species may accumulate more lipids) and whether any changes will alter cell density (ρ'). Despite this, Stokes' Law is useful in that it can be applied to validate any method used to measure sinking velocities and because it increases our understanding about what influences sinking, i.e. cell radius, density and any form resistance.

1.4 Will the efficiency of the biological carbon pump change under climate change?

It is unknown whether increased concentrations of CO_2 will impact negatively or positively upon sinking velocities and the efficiency of the biological carbon pump. In a mesocosm study by Riebesell et al. (2007), it was shown that an increase of dissolved CO_2 resulted in an increased rate of inorganic carbon consumption by natural phytoplankton assemblages and a greater loss of organic carbon from surface layers. In a high CO_2 world therefore, the biological carbon pump could increase its working capacity and could act as a negative feedback to rising atmospheric CO_2 concentrations. In some regions however, warming surface waters and increased vertical ocean stratification will reduce the return flow of remineralized carbon and nutrients, including nitrogen (N) and phosphorus, from the deep oceans to the surface waters, which could reduce overall primary production (Beardall et al., 2001, Raven et al., 2005, Riebesell et al., 2007). Furthermore, since many diatoms, in general, have large cells and high nutrient requirements, it is expected that these organisms will be strongly affected by nutrient depletion, while smaller-celled species (including *Prochlorococcus* or eukaryotic nanophytoplankton such as the coccolithophorid *Emiliania huxleyi*), which perform better than large cells under low nutrient concentrations and which sink slower because of their reduced radii, will dominate the nutrient depleted regions (Beardall et al., 2009a, Beardall et al., 2009b). Although larger phytoplankton may be better adapted to variable pH conditions than smaller species (as they themselves generate variable pH conditions during the light:dark cycle), the more extreme future diel pH range may eventually become damaging to these cells also (Flynn et al., 2012).

Alternatively, increased concentrations of CO_2 could enhance the sedimentation rate of organic matter due to a greater rate of marine snow formation. The biological pump is mainly driven by the formation and rapid settlement of marine snow, which is comprised of large aggregations formed

from single organic and inorganic particles (Engel, 2002). Small, individual phytoplankton cells generally sink less than 2 m d^{-1}, whereas sinking velocities of aggregates can range over one order of magnitude from ~5 m d^{-1} to ~ 50 m d^{-1} (De La Rocha and Passow, 2007).

The formation of marine snow is enhanced by the presence of sticky transparent exopolymer particles (TEPs), which form from exopolymer carbohydrates exuded by phytoplankton and bacteria (Alldredge et al., 1993, Alldredge and Silver, 1988, Engel, 2002). The production of TEP by *Emiliania huxleyi* has been found to increase when cells are grown under higher concentrations of CO_2 and, therefore, increased CO_2 concentrations could increase the rate of aggregation and thus marine snow formation (Engel et al., 2004, Raven et al., 2005). TEP production is also influenced by nutrient limitation. For instance populations of a diatom, *Chaetoceros calcitrans*, produced more TEP when grown in a N-limited environment (Corzo et al., 2000). TEP production, therefore, could be greatly enhanced under the high CO_2, low nutrient conditions associated with climate change, which in turn could enhance particle sedimentation rates. TEPs are rich in polysaccharides however, and the degradation of polysaccharides by bacterial extracellular enzymes may be significantly accelerated under ocean acidification due to increased bacterial glucosidase activity (Piontek et al., 2010). This ultimately has the potential to reduce TEP concentrations and thereby decrease carbon export to the deep sea (Piontek et al., 2010).

Aggregates of phytoplankton form faster, have a greater mass and have a higher settling velocity when the phytoplankton cells are calcified (Engel et al., 2009b). Calcifying coccolithophores for instance, produce dense calcium carbonate platelets called coccoliths, which facilitate the sinking of cells, and their carbon content, into deeper waters (Armstrong et al., 2001, Klaas and Archer, 2002, Raven et al., 2005). Calcium carbonate has been found to dissolve however, unless the surrounding seawater has a sufficiently high concentration of carbonate ions. At a certain depth therefore,

where the carbonate ion concentration is sufficiently low, all calcium carbonate structures dissolve. This point is called the saturation horizon and it shifts depending on the temperature, pressure and the saturation state of carbonate ions (Raven et al., 2005). In addition, different forms of calcium carbonate (calcite or aragonite) have different saturation horizons (Refer to figure 1.1.6 of Zeebe and Wolf-Gladrow, 2001).

The composition of inorganic carbon in seawater shifts away from carbonate towards more bicarbonate as the concentration of CO_2 in the water increases and thus pH decreases. The oceans are expected to take up more CO_2 in the future. Therefore, within the surface waters, concentrations of bicarbonate will increase slightly and there will be fewer carbonate ions (Table 1.1). As a result, the saturation horizon could shift closer to the surface and it is likely that there will be a reduced amount of calcium carbonate production and potentially, an increased rate of calcium carbonate dissolution (Raven et al., 2005). Beaufort et al. (2011) quantified the calcite mass of dominant coccolithophores in the present ocean and over the past forty thousand years, and found a marked pattern of decreasing calcification with increasing partial pressure of CO_2 and decreasing concentrations of carbonate ions. A decrease in the amount of calcium carbonate in response to ocean acidification could thus lead to reduced cell densities and a diminished ballast effect, reducing the flux of particulate organic carbon and marine snow to the deep ocean (Barker et al., 2003, Raven et al., 2005).

Questions also arise as to whether the macromolecular composition of algal cells will change in the future and whether any compositional changes will influence sinking rates due to of changes in cell density, radius or form resistance. Shifrin and Chisholm (1981) for instance found that N deprivation resulted in a two to three fold increase in the lipid content of green algae and Parrish and Wangersky (1990) found that higher triglyceride yields were obtained when *Chaetoceros gracilis*

was exposed to low concentrations of N. In addition, Ganf et al. (1986) established that N-limitation resulted in diminished protein levels and enhanced carbohydrate storage in *Scenedesmus quadricauda*. If cellular lipid, carbohydrate or protein concentrations are influenced by the conditions associated with climate change, in particular as a result of nutrient limitations, then the density, and hence the sinking rate of cells, could be affected. A number of authors have suggested that lipid accumulation in *Emiliania huxleyi* will alter cell density and that this will significantly influence the rate of sinking (Fernández et al., 1994, Paasche, 2002). Smayda (1970) however, concluded that lipid accumulation is generally an unimportant suspension mechanism in phytoplankton and that the impacts it has on sinking were deemed to be negligible. Boyd and Gradmann (2002) also considered the role that osmolytes play in sinking. They observed that cells can change their density and buoyancy by altering the concentrations of organic osmolytes and reserves of carbohydrates.

While it is hypothesised that algal cells will store more lipids and carbohydrates and will form marine snow more readily under a high CO_2, low nutrient environment, it is also hypothesised, that the cells will reduce their protein and chlorophyll concentrations and calcifying organisms such as *Emiliania huxleyi* will produce fewer or smaller coccoliths. How these factors influence the cells sinking velocity however remains to be seen.

1.5 Study Aims and Hypothesis

This project aimed to determine whether the sinking velocity of phytoplankton cells will change under some of the conditions associated with climate change, specifically nitrogen limitation and elevated CO_2. Where changes in the sinking velocity are seen, attempts will be made to determine why this may be the case. It was hypothesised that:

- Increases in CO_2 and nitrogen limitation will influence the size and macromolecular composition of phytoplankton cells;
- Changes in macromolecular composition will influence the density and thus the sinking rate of phytoplankton; and
- In accordance with Stokes Law, cell size will be a primary factor that influences the sinking rate.

Chapter 2.0: General Methods

2.1 Species Used

As diatoms and coccolithophores are the principal drivers of biologically induced carbon export to the deep sea (Young and Ziveri, 2000, Riebesell et al., 2007), a diatom species and a coccolithophore were used for the experiments described here.

The chosen species, sourced from the Australian National Algae Culture Collection (ANACC) at the Commonwealth Scientific and Industrial Research Organisation (CSIRO) in Hobart, Tasmania were *Chaetoceros didymus* and *Emiliania huxleyi CS 812*. The strains of these species used were originally isolated originally from waters off the east Australian coast and Tasmania. Furthermore, these species are of different size, shape and mass, which will have an impact on the rate of sinking (Table 2.1).

The chosen strain of the coccolithophore, *E. huxleyi CS 812*, produces heavily calcified coccoliths. *E. huxleyi* is a small species however with a diameter of approximately 5 µm (Carmelo et al., 1997). *C. didymus* is a diatom and is larger than *E. huxleyi.* It is capable of forming chains with individual cells ranging from 10 – 40 µm long. It also has long silica spines (Table 2.1), which could add a level of form resistance to sinking.

Table 2.1: The size ranges and shape of the two phytoplankton species.

Species	**Size range**	
C. didymus	Apical axis 10 – 40 µm	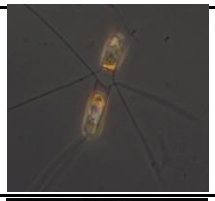
E. huxleyi	Diameter 5 – 10 µm	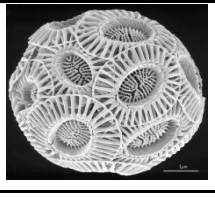

2.2 Growth Conditions – Batch cultures

Preliminary batch culture experiments were carried out for both species in order to determine the concentration of N required to limit growth rates by 50%.

Batch cultures of *C. didymus* and *E. huxleyi* CS 812 were maintained at a constant 18 ^{o}C and photosynthetically active radiation was provided continuously at a photon flux of 80 µmol quanta m^{-2} s^{-1}. *E. huxleyi* batch cultures were exposed to different concentration of N, supplied as $NaNO_3$ plus NH_4Cl, in K medium (Keller et al., 1987).. *C. didymus* cells however, were exposed to differing concentration of $NaNO_3$ in F/2 medium (Jeffrey and LeRoi, 1997). Nitrogen was chosen as the limiting nutrient for this study because it is one of the nutrients most commonly expected to become limiting in the future as a result of ocean stratification and a reduced mixed layer depth (Beardall et al., 2001, Beardall et al., 2009a). There were five different N concentrations, ranging from replete (0.932 mmol.L^{-1} $NaNO_3$ and NH_4Cl combined for the K medium and 0.8825 mmol.L^{-1} $NaNO_3$ for the F/2 medium), down to one twentieth of the replete concentration for each respective medium. The growth rate was determined by daily cell counts using a Neubauer haemocytometer (Boeco, Hamburg, Germany) (Section 2.6).

N stress was also determined by measurements of the maximum quantum efficiency of PSII (F_v/F_m) (Section 2.12). Declines in F_v/F_m can be indicative of N starvation in phytoplankton (Kolber et al. 1998), however they are not a reliable means to determine phosphorus limitation (Beardall et al. 2001), nor are they a reliable determinant of N stress in steady state cultures (Parkhill et al. 2001).

2.3 Growth Conditions – Semi Continuous Cultures

Cells were grown in semi-continuous cultures, either under current day CO_2 concentrations (400 p.p.m.) or that which is the predicted atmospheric CO_2 concentration for the year 2100 (1000 p.p.m.) (Table 2.2).

The cultures grown under current day CO_2 levels (400 p.p.m.) were aerated with ambient air passed through a 0.2 µm PTFE membrane in-line air filter (Pall Corporation, Roseville, USA, ARCO 50 vent device) at a rate of 450 ml min^{-1}. In order to aerate the cells with 1000 p.p.m. CO_2, 5% CO_2 was mixed with ambient air using a 150 mm Two-Tube Gas Blender (Series 150A, Advanced Specialty Gas Equipment, NJ, USA). The CO_2 concentration within cultures was monitored daily through measurements of pH, alkalinity and DIC (Section 2.13). To ensure acclimation, the cells were maintained in a semi-continuous state for a minimum of 7 generations prior to any analysis.

N concentrations were also varied so that the cultures were either grown in N-replete or N-limited conditions (Table 2.2). The limiting concentration of N was determined during the batch culture experiments (Sections 3.2.1 and 5.2.1).

Table 2.2: The experimental growth conditions.

[CO_2]			
400 p.p.m.		1000 p.p.m.	
N-limited	N-replete	N-limited	N-replete

2.4 Measuring the sinking velocity

The cell sinking velocity was measured according to the method of Walsby and Holland (2006) by repeatedly scanning a density-stabilized sedimentation column with a laser beam (wavelength 660 – 680 nm, maximum output, 5 mV) (Figure 2.1). The cells were introduced as a layer at the top of the column and allowed to sink for a minimum of 4 hours. This method recorded the depth of the sinking cells at any given time without perturbing the column (Walsby and Holland, 2006). Light scatter from cells was measured using a light-absorbing diode connected to a digital/analogue interface (LabJack u3-LV, Lakewood, Colorado, USA) and recorded on a PC (LabJack Applications Lakewood, Colorado, USA). The sinking velocity was determined by comparing the distance between the peaks of the scatter vs. position curves through time.

In order to have sufficiently high resolution in sinking measurements, the cells needed to be at a high cell number per unit volume for each run. The cells were therefore concentrated by filtering them onto cellulose nitrate, 3 μm membrane filters (Sartorius, Gottingen, Germany) and gently resuspending them in 1 ml of fresh growth medium.

The density gradient was created using a gradient former (model 385; Bio-Rad, Hercules, California, USA) with 15% Percoll (Sigma, St. Louis, Missouri, USA) and growth medium. Prior to making the gradient, sodium chloride was mixed with the Percoll at 35 g l^{-1} to ensure that it was isotonic with seawater.

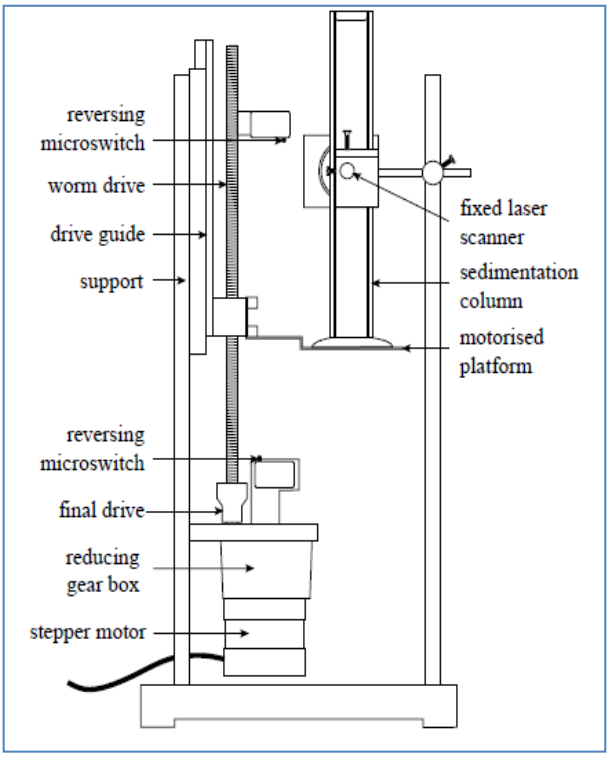

Figure 2.1: A density-stabilized sedimentation column with a laser beam scanning device.

2.5 Cell size and density

Cell diameter was measured in order to understand the role of cell size in sinking velocities. At harvest, photographs of at least 30 unfixed cells were taken using a x100 oil-immersion objective lens on a Zeiss compound microscope (Axio Scope.A1 with AxioCam ICc1 camera Carl Zeiss, Gottingen, Germany). Using the photographs, cell size (µm) was measured using the Axio Vision Release 4.7.1 software (Carl Zeiss, Gottingen, Germany).

Cell density was determined by first creating a density gradient in a 15 ml centrifuge tube (BD Falcon, BD Biosciences, Bedford, USA), as per the method described in section 2.4 using 100% Percoll and medium. Cell suspension (0.5 ml) was carefully pipetted onto the meniscus of the gradient and the tube was centrifuged (Heraeus Multifuge 3ST+ Centrifuge, Thermo Scientific, Brookfield, WI, USA) at 500 g for 10 minutes. During centrifugation, the cells sink as a band until

they reach a density that is equivalent to their own density. Using a needle, a small sample from the band of cells was removed and its density was determined using a refractometer.

Where the cells were too dense and would not remain suspended in the density gradient, the density had to be calculated by substituting the values obtained for cell diameter and sinking velocity into the Stokes' Law equation (Equation 1.1). Attempts were made to increase the density of the density gradient, which would improve suspension of cells, by using solutions such as glucose and sucrose, rather than Percoll. These solutions formed a precipitate when mixed with the seawater based medium however.

2.6 Growth Rates

Growth rates were determined from changes in cell number on a daily basis, using a Neubauer haemocytometer. 10 µL of culture was added to each chamber of the haemocytometer, and the cells were counted. Counts were repeated until a minimum of 100 cells were counted, and the results averaged.

2.7 Chlorophyll concentrations

Chlorophyll *a* and *c* concentrations were measured during the exponential growth phase. 1.5 ml of cells was centrifuged (Heraeus Pico 17 Centrifuge, Thermo Electron Corporation, Brookfield, WI, USA) at 1000 r.p.m for 10 minutes. The supernatant was removed and the pellet was resuspended using 1 ml of 90% acetone. The chlorophyll was then extracted in the dark at 4 ^{o}C for 1 hour.

After 1 hour, the suspension was centrifuged and the absorbance of the supernatant was measured at 630, 647, 664 and 750 nm using a Cary-50 UV-visible spectrophotometer (Bio, Varian, Mulgrave, Australia). The white pellet was retained for protein analysis.

The concentration of chlorophylls *a* and *c* were determined using the equations of Jeffrey & Humphrey (1975).

2.8 Proteins

The pellet obtained following chlorophyll extraction was used for protein analysis. The pellet was re-suspended in 500 µL of a detergent mix comprising 1% sodium dodecyl sulfate (SDS) and 0.1 M NaOH. The concentration of protein in the solution was then determined using a protein assay kit (BioRad DR), which was based on the assay developed by Lowry et al (1951), and measuring the absorbtion at 750 nm using a Cary-50 UV-visible spectrophotometer (Bio, Varian, Mulgrave, Australia).

A standard curve was created using bovine serum albumin (Sigma - Aldrich, St. Louis, Missouri, USA) (2 mg ml^{-1} stock) and the SDS/NaOH detergent according to the concentrations in Table 2.3.

Table 2.3: The preparation of the BSA standard curve for protein analysis.

BSA (µL)	0	25	50	100	150	250
SDS/NaOH detergent (µL)	500	475	450	400	350	250
BSA Final Concentration (mg ml^{-1})	0	0.1	0.2	0.6	1.0	1.6

2.9 Lipids

Lipids were extracted from cells using chloroform/methanol/water technique as developed by Bligh and Dyer (1959) with various modifications. A known number of between 10^8 and 10^9 cells were harvested through centrifugation (Heraeus Multifuge 3ST+ Centrifuge, Thermo Scientific, Brookfield, WI, USA) at 3000 r.p.m for 10 minutes. The wet pellet was then stored at -20 ^{o}C.

The cells were resuspended in 20 ml of 50 mM phosphate buffer (pH 8) in order to preserve the native state of lipids (White et al., 1979, Guckert et al., 1988). Then, to ensure that all cells were broken, the cells were sonicated for 5 minutes. The broken cells were transferred into a separation funnel to which 25 ml of chloroform and 50 ml methanol were added. The funnel was shaken vigorously and the phases were allowed to separate for a minimum of 18 hours. The following day, a further 25 ml chloroform and 25 ml distilled water were added to the funnel. The phases were then allowed to separate out for a further 18 hours.

Once the chloroform and distilled water phases separated, the lower chloroform layer was collected in a pre-weighed round bottom flask and evaporated to dryness using a rotary evaporator (Type W 240; Buchi Flawil, Switzerland) at 50 ^{o}C. The flask was reweighed, and lipids were estimated by difference.

2.10 Carbohydrates

Two types of carbohydrates were extracted from the cells. The first type, β-1,3 glucan, is used as a carbohydrate food reserve and represents the final product of photosynthesis (Kusaikin et al.,

2010). β-1,3 glucan is water soluble and is therefore extracted using dilute sulphuric acid according to the technique developed by Granum and Myklestad (2002). The cells, 10^6 – 10^8, were filtered onto glass fibre filters (Millipore, 25 cm, GF/C) and incubated with 5 ml of 0.05 M H_2SO_4 for 20 minutes at 60 ^oC in a water bath. Following incubation, the mixture was filtered again using a new glass fibre filter. The resulting glucan extract was then analysed using the phenol-sulphuric acid method (DuBois et al., 1956).

The second type of carbohydrates is the cell wall polysaccharides. These are important cell wall constituents and are generally insoluble in water. They are therefore extracted by incubating the cells in 80% sulphuric acid (Granum and Myklestad, 2002). The filters from the last stage of the glucan analysis were washed with dH_20 and dried for 12 hours at 60 ^oC. The filters were then incubated with 0.5 ml 80 % (v/v) H_2SO_4 at 4 ^oC for 20 hours. The resulting hydrolysate was then diluted to 1M H_2SO_4 through the addition of 6 ml H_20 and then filtered through a fresh GF/C filter. The extract was then used for cell wall polysaccharide determination using the phenol-sulphuric acid method by adding 0.5 ml of 3% aqueous phenol and 5 ml of 80% H_2SO_4 to 2 ml of extract. The extracts were then left to stand for 30 minutes and absorbance determined at 485 nm using a Cary-50 UV-visible spectrophotometer (Bio, Varian, Mulgrave, Australia).

A glucose stock solution [0.25 mg ml^{-1}] and dH_2O were used to create a standard curve according to Table 2.4.

Table 2.4: Preparation of the glucose standard curve for carbohydrate analysis.

Glucose Stock (µL)	0	250	500	1000	2000
dH_2O (µL)	4000	3750	3500	3000	2000
Glucose Final Concentration (µg ml^{-1})	0	15.6	31.25	62.5	125

2.11 TEP Concentration

The production of TEP was measured using the methods of Passow and Alldredge (1995). Culture (5 ml) was filtered at a low constant vacuum (at 100 mm Hg) onto 25-mm polycarbonate filters (Millipore Isopore membrane filters, 0.4 µm HTTP). The particles that remained on the filter were stained, for 2 seconds, with 500 µl of a 0.02% aqueous solution of alcian blue (8GX, Sigma - Aldrich, St. Louis, Missouri, USA) in 0.06% acetic acid. Blank filters were also stained using this method. Excess dye was rinsed from the filters using dH_2O. The stained filters were then frozen at -25 ^oC.

The filters were transferred to small glass beakers with 3 ml of 80% H_2SO_4 and allowed to soak for two hours. The beakers were agitated 3 – 5 times during this period. The absorbance of the H_2SO_4 was then measured using a Cary-50 UV-visible spectrophotometer (Bio, Varian, Mulgrave, Australia) at 787 nm. The concentration of TEP (C_{TEP}) was then determined according to equation 2.1.

$$C_{TEP}\ (\mu g\ litre^{-1}) = (E_{787} - C_{787}) \times (V_f)^{-1} \times f_\chi \quad \text{(Equation 2.1)}$$

where E_{787} is the measured absorbance of the sample, C_{787} is the absorbance of the blank, V_f is the volume filtered (in litres) and f_χ is a calibration factor.

f_χ was determined according to equation 2.2.

$$f_\chi\ (\mu g) = W \times [(est_{787} - C_{787}) \times V_{st}^{-1}]^{-1} \quad \text{(Equation 2.2)}$$

Where W is the dry weight of the calibration standard (in µg), est_{787} is the average absorbance of the calibration standard and V_{st} is the volume of calibration standard filtered for staining (in L).

The calibration standard was prepared by mixing 15 mg of gum xanthan (Lotus Foods, Cheltenham, Vic, Australia) into 200 ml of dH_2O. A 3 ml aliquot of the calibration standard then filtered onto pre-weighed filters using the methods described above. The filters were then dried and the dry weight (W) of the calibration standard determined.

A further 3 ml sample of the calibration standard was filtered and stained with alcian blue and the absorbance measured (est_{787}).

As there is a high degree of error with this method, a minimum of 4 filters were prepared for each culture replicate.

2.12 Measuring Photosynthesis

Light energy that is absorbed by chlorophyll is either used to drive photosynthesis (photochemical quenching), is re-emitted as heat (non-photochemical quenching) or is lost as fluorescence. These processes help minimise a build up of energy in the light harvesting apparatus, reducing the rate of cellular damage. If there is an increase in fluorescence, then that may indicate that one or both of the quenching processes has been impaired (Maxwell and Johnson, 2000).

Fluorescence emissions at room temperature are almost entirely due to photosystem II (PSII) activity (Maxwell and Johnson, 2000).

Fluorescence was measured using a pulse amplitude modulated fluorometer (PHYTO-PAM, Heinz Walz GmbH, Effeltrich, Germany). 5 ml of cells were withdrawn from each culture during the

exponential growth phase and dark adapted for 15 minutes. After dark adaption, all PSII reaction centres are open (there are no electrons in the electron transport chain). 3 ml of the dark-adapted cell suspension were then placed in a glass cuvette that had two adjacent mirrored sides and placed into the PHYTO-PAM. A weak measuring beam, which is too weak to promote photosynthesis, was turned on. This light induced minimal florescence (F_o). The cells then received a saturating flash to promote maximum fluorescence (F_m). The difference between F_o and F_m is called the variable fluorescence (F_v). If the reaction centres of PSII are damaged, then F_o will be greater and consequently F_v will be lower. The parameter F_v/F_m, which indicates the maximum quantum efficiency of PSII is then calculated (Equation 2.3). A drop in F_v/F_m indicates the efficiency of PSII has been impaired. The data was recorded and generated using PhytoWIN software.

$$F_v/F_m = [F_m - F_o]/F_m \quad \text{(Equation 2.3)}$$

Subsequently, 16 photosynthetically active radiation (PAR) irradiances, from 16 to 610 µmol photons m^{-2} s^{-1} were each applied for 30 seconds in increasing order. This allowed the light adapted parameter, the effective quantum yield of PSII (ΦPSII), to be calculated at each PAR (Equation 2.4).

$$\Phi\text{PSII} = [F'_m - F'_o] / F'_m \quad \text{(Equation 2.4)}$$

Where F'_o and F'_m are the corresponding light-acclimated minimum and maximum fluorescence values.

The relative electron transport rate (rETR) is an approximation of the rate of electrons pumped through the photosynthetic electron transport chain where rETR = ΦPSII x PAR (Ralph and Gademann, 2005).

A rapid light curve (RLC) measures ΦPSII as a function of irradiance and is generated by plotting the rETR versus PAR (Ralph and Gademann, 2005). RLCs provide additional information about the efficiency and capacity of photosynthesis (Belshe et al., 2007). The initial slope of the RLC is defined by α (alpha), which is a measure of the efficiency of light harvesting. The asymptote of the curve represents $rETR_{max}$ and corresponds to the saturated electron transport rate. The point where α and $rETR_{max}$ intercept is defined as I_k, and represents the photon flux that is required to approach light saturation.

2.13 Measuring the CO_2 System

The partial pressure of CO_2 (pCO_2) in the culture was calculated daily in order to ensure that the cells were growing in the correct conditions. Using measurements of dissolved inorganic carbon (DIC), pH, total alkalinity (TA), salinity and temperature and the known ionic concentrations in the medium, calculations of pCO_2 were completed using the R software package AquaEnv (Hofmann et al., 2010).

The pH was measured using a SensION+ pH meter (PH31, Hach). TA was measured using the Gran titration method described by Denney et al. (1983) using a Titralab Tim854 Titration Manager (Radiometer Analytical, Lyon, France). The volume of 0.1 M HCl used to reduce the pH in a 20 ml medium sample to 4.2, 4.0, 3.9 and 3.7 respectively was recorded. This data was then used to construct Gran plots and linear regression was used to calculate the theoretical alkalinity endpoint volume.

In order to determine the DIC concentration, air, which had been stripped of its CO_2 by passage through soda lime granules (4 – 8 mesh, Ajax Finechem, Taren Point, NSW, Australia), was bubbled

upwards into a sealed glass vessel containing 20 ml 0.1M HCl. To this, 1 ml samples of cell-free medium was added using a syringe. The air collected at the top of the vessel was then passed through the desiccant magnesium perchlorate (Anhydrous ACS, Alfa Aesar, MA, USA) and the CO_2 within the air stream measured continuously using an infra-red gas analyser (IRGA; LICOR LI-840 A) until all CO_2 was stripped out of the medium sample. The CO_2 concentration was recorded using LI-840A software, and the area under the curve of CO_2 vs time plot was compared with that obtained from a standard curve. The DIC standard curve was created by calculating the summed CO_2 from known concentrations of $NaHCO_3$ using the same methods as described above.

Chapter 3.0: Impacts of N-limitation on the Sinking Rate of the Coccolithophorid *E. huxleyi* (Prymnesiophyceae).

Previously published as Pantorno A., Holland D.P. , Stojkovic S and Beardall J. (2013). Impacts of nitrogen limitation on the sinking rate of the coccolithophorid *E. huxleyi* (Prymnesiophyceae). *Phycologia* 52 (3), 288–294

3.1 Introduction

This study focused on the effects of N-limitation, as a consequence of climate change, on the sinking velocity of *E. huxleyi* (Lohmann) Hay & Mohler, a coccolithophore responsible for significant phytoplankton blooms and the biological drawdown of carbon (Young and Ziveri, 2000, Riebesell et al., 2007). N is a critical macronutrient for phytoplankton growth. It is necessary for protein synthesis, including for the maintenance of the proteins associated with the photosynthetic apparatus and PSII repair (Loebl et al., 2010). N starvation influences CO_2 exchange by impairing cellular capacity to make Rubisco and can result in decreased photosynthetic capacity and a marked reduction in chlorophyll *a* and accessory pigments as well as modifying chloroplast thylakoid membranes leading to chlorosis (Osborne and Geider, 1986, Paasche, 2002). N availability therefore, can have a strong influence on phytoplankton, including *E. huxleyi* blooms, development (Dyhrman et al., 2006).

Future N-limitation may also change the macromolecular composition of phytoplankton and, consequently, influence cellular density and sinking velocities. Also, Boyd and Gradmann (2002) observed that cells can change their density, and buoyancy, by altering the concentrations of organic osmolytes and reserves of carbohydrates. A number of authors have also suggested that lipid accumulation in *E. huxleyi* will alter cell density and that this will influence the rate of sinking (Fernández et al., 1994, Paasche, 2002). Smayda (1970) however, concluded that lipid accumulation is generally an unimportant suspension mechanism in phytoplankton and that its impact on sinking is negligible. This chapter therefore empirically tests whether changes in macromolecular composition, focussing on lipids, proteins and carbohydrates, influence cell size and density and what role that may play, if any, in sinking velocity. In addition, the concentrations of TEPs were examined. TEPs form from exopolymer carbohydrates exuded by phytoplankton and bacteria

(Alldredge and Silver, 1988, Alldredge et al., 1993, Engel, 2002). They are sticky, causing cells and debris to aggregate, and as a result, the formation of marine snow, a driver of carbon export, is enhanced by their presence (Engel, 2000, Engel et al., 2004). The production of TEPs by phytoplankton can be influenced by nutrient limitations (Corzo et al., 2000). It was also considered necessary, therefore, to investigate whether N-limitation would influence the production of TEPs and, consequently, influence the sinking velocity of *E. huxleyi*.

3.2 Methods

3.2.1 Batch Culture Experiments

Batch culture experiments were completed for *E. huxleyi*, in order to determine the concentration of N required to limit growth rates by 50% (Section 2.2).

Batch cultures of *E. huxleyi* were established in 60 ml flasks (Nalgene Square Polycarbonate bottles) and were exposed to 5 different concentration of N, using $NaNO_3$ and NH_4Cl in K medium as the N source.

The batch cultures were initially provided with 882.5 µmol l^{-1} $NaNO_3$ and 50 µmol l^{-1} NH_4Cl (N-replete). The N concentrations were reduced in subsequent batch cultures as follows:

- 441.25 µmol l^{-1} $NaNO_3$ and 25 µmol l^{-1} NH_4Cl;
- 220.63 µmol l^{-1} $NaNO_3$ and 12.5 µmol l^{-1} NH_4Cl;
- 88.25 µmol l^{-1} $NaNO_3$ and 5 µmol l^{-1} NH_4Cl; and
- 44.13 µmol l^{-1} $NaNO_3$ and 2.5 µmol l^{-1} NH_4Cl.

3 replicates were maintained at each of the N concentrations. The growth rate was determined daily (Section 2.6).

3.2.2 Semi-Continuous Culture Experiments

E. huxleyi was grown in three independent, semi-continuous cultures (600 ml) in 1-litre glass Erlenmeyer flasks using N-replete K medium (Keller et al., 1987). Cultures were maintained at 18 ± 1

^{o}C with photosynthetically active radiation (PAR; 400 – 700 nm) provided continuously at a photon flux of 80 µmol quanta m^{-2} s^{-1} from fluorescent tubes (Philips TLD 18W/865, cool daylight; Philips, Eindhoven, The Netherlands). Cultures were stirred constantly using a magnetic stirrer at 160 r.p.m and continuously aerated with ambient air passed through a 0.2 µm PTFE membrane in-line air filter (Pall Corporation, Roseville, USA, ARCO 50 vent device) at a rate of 450 ml min^{-1}.

Experimental cultures were grown to 0.7 – 2 X 10^6 cells ml^{-1}. Cells were then maintained in a semi-continuous state by diluting them to approximately 0.5 X 10^{6} cells ml^{-1} daily. The cultures were thus kept in exponential growth phase during this part of the experiment. In the first instance these cultures were maintained in N-replete conditions. After a minimum of 3 steady states in each flask, the replete medium was substituted by N-limited medium and a new semi-continuous steady state developed.

The N-limited medium had 88.25 µmol l^{-1} $NaNO_3$ and 5 µmol l^{-1} NH_4Cl. While this amount of N is high compared to the natural marine environment, it was limiting within these cultures because the concentration of cells was significantly higher than usually found in natural populations.

N-limitation was confirmed prior to any analysis using chlorophyll measurements and measurements of chlorophyll fluorescence-based quantum yield (F_v/F_m), which describes the maximum quantum efficiency of photosystem II. F_v/F_m was measured using the PAM fluorometer (Section 2.12). Cultures with values of F_v/F_m below 0.40 were considered N-limited. Concentrations of chlorophylls *a* and *c* were also measured, during the exponential growth phase (Section 2.7).

The sinking velocity was measured according to the method of Walsby & Holland (2006) (Section 2.4). In order to have sufficiently high resolution, at least 10 million cells in a 1 ml sample were

required for each run. The cells were therefore concentrated by filtering them onto cellulose nitrate, 3 µm membrane filters (Sartorius, Gottingen, Germany) and resuspending them in 1 ml of fresh K medium.

Using the methods described in Section 2.5, cell diameter was measured in order to understand the role of cell size in sinking velocities. Using photographs, cell diameter (µm), both including and excluding the coccosphere, was measured, and the coccosphere thickness was thereby calculated. The density of the cells was then calculated by substituting the values obtained for cell diameter and sinking velocity into the Stokes' Law equation (Equation 1.1).

The concentrations of cell protein, lipid and carbohydrate were examined at each harvest during semi-continuous exponential growth. Protein concentration was measured using a Bio-Rad DR Protein assay kit (Section 2.8). Lipids were extracted from the cells using a modified Bligh & Dyer (1959) technique and the concentration of lipids was determined gravimetrically (Section 2.9). The carbohydrates, β-1,3 glucan and cell wall polysaccharides, were extracted from the cells and the resulting glucan extract and the cell wall hydrolysate were analysed separately using the phenol-sulphuric acid spectrophotometric method (Section 2.10).

3.2.3 Further Batch Culture Experiments – For TEP Analysis

Since the production of TEPs is associated mainly with the stationary and senescent stages of life (Corzo et al., 2000, Hong et al., 1997) a separate batch culture experiment was carried out on cells that were allowed to grow until stationary phase (5 – 7 days), starting with either N-replete or N-limited conditions.

The concentration of TEPs were measured (at both exponential and stationary growth phases) using the methods of Passow and Alldredge (1995) (Section 2.11).

The sinking velocity, diameter and density were also determined for the cells at stationary growth phase.

3.2.4 Statistical Analysis

For statistical analysis, in those cases where two treatments were compared, an unpaired two-tailed t test was performed. When four treatments were compared, analysis of variance was used to establish significance, followed by a post hoc Tukey test to determine which treatments differed significantly. Significance was set at $P < 0.05$. For measurements where only two replicates were taken, the standard deviation of the sample was calculated, and no statistical test was attempted. All statistical analyses were conducted using GraphPad Prism 5 (GraphPad Software Inc., La Jolla, California, USA).

3.3 Results

3.3.1 Initial Batch Culture Experiments to Determine the Limiting Concentration of N

The maximum growth rate of *E. huxleyi* increased as N concentrations increased (Figure 3.1). Growth rates were particularly decreased when N concentration were decreased to one tenth or one twentieth of the replete concentration.

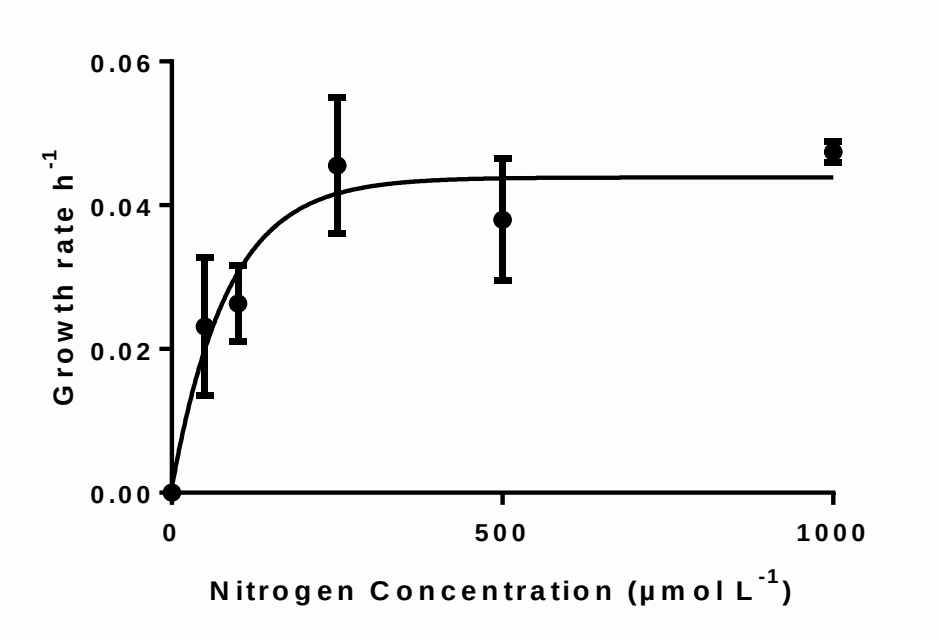

Figure 3.1. The specific growth rate of *E. huxleyi* as a function of N concentration. Data are the mean of three independent cultures and standard error presented as a double sided bar.

3.3.2 Semi-Continuous Culture Experiments and TEP Analysis

The growth rates of *E. huxleyi* were significantly reduced by approximately 50% under N-limitation (Figure 3.2). A decrease of 30% was observed in concentrations of chlorophyll *a* and *c* during the exponential growth under N-limitation (Figure 3.3), which was paralleled by a decrease in F_v/F_m (Table 3.1).

N-replete *E. huxleyi* cells during the exponential growth phase sank approximately 1 µm s^{-1} (23%) faster than the N-limited cells (Figure 3.4). During stationary phase, however, N-limited cells sank with a greater velocity than N-replete cells, though not as fast as the replete, exponential phase cells (Figure 3.4). Overall, those cells in exponential growth in N-replete conditions sank the fastest.

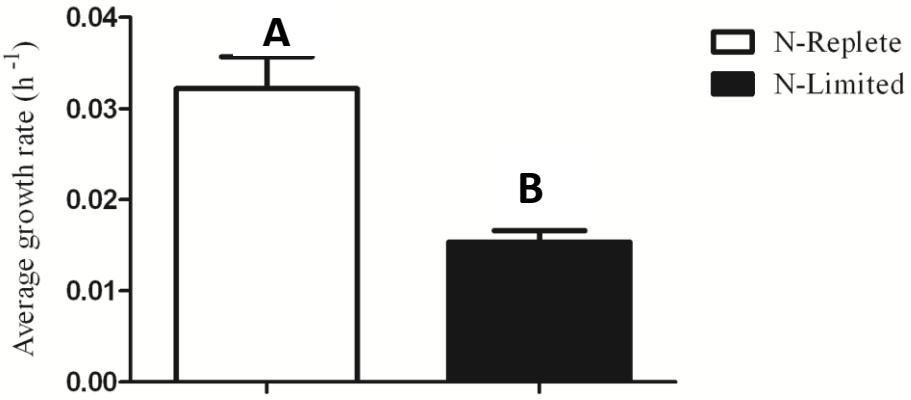

Figure. 3.2. The specific growth rate of *E. huxleyi* when grown in semi-continuous cultures under replete or N-limited conditions. Data are the mean of three independent cultures. Standard error is presented as a single-sided bar. Different letters indicate statistically significant differences among mean values ($p< 0.05$).

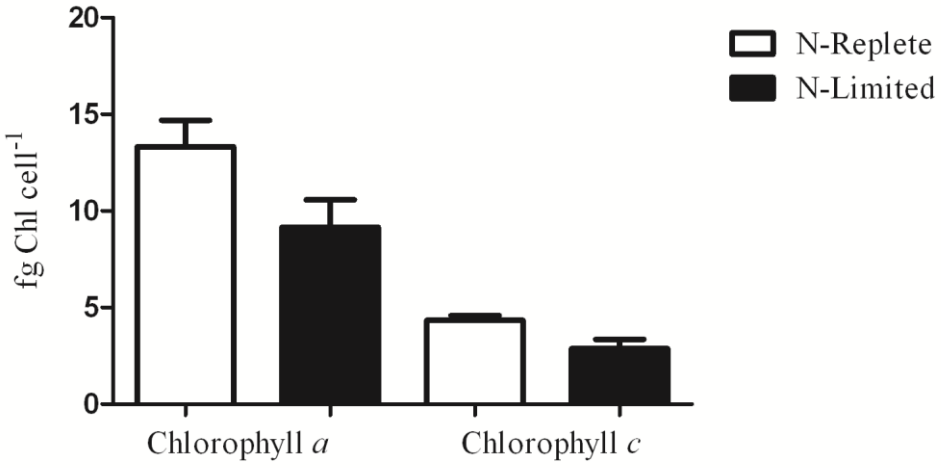

Figure 3.3. Chlorophyll *a* and *c* concentrations (fg Chl $cell^{-1}$) in *E. huxleyi* during the exponential growth phase. Data are the mean of two independent cultures, and standard deviation is presented as a single-sided bar. Statistical significance of differences in the means could not be determined as there were only two replicates under each condition.

Table 3.1. Changes in the macromolecular composition, F_v/F_m and TEP concentrations in *E. huxleyi* under replete or N-limited conditions.[1]

	N-Replete		N-Limited	
	Concentration	Error (±)	Concentration	Error (±)
F_v/F_m*	0.46	0.016	0.32	0.016
Protein (pg cell^{-1})	82.9	6.7 (*SD*)	71	7.4 (*SD*)
Lipids (pg cell^{-1})	11.4	0.009 (*SD*)	69	13.3 (*SD*)
β-1,3 glucan (pg cell^{-1})*	1.86	0.13	2.86	0.32
Cell wall polysaccharides (pg cell^{-1})*	0.98	0.074	1.267	0.13
TEP (fg cell^{-1}) Stationary*	0.00125	0.00028	0.00391	0.00046
TEP (fg cell^{-1}) Exponential	0.00127	0.00016	0.0014	0.00006

[1] F_v/F_m, Protein, lipids, and carbohydrates were measured only during the exponential growth phase. TEPs were measured during the stationary and exponential growth phases. The error is standard error unless stated otherwise**.** *Indicates that there was a statistically significant differences among mean values ($p < 0.05$). Significance could not be determined for proteins and lipids as there were only two replicates for each condition.

Differences in macromolecular composition between the N-replete and N-limited cultures were evident during the exponential stage of growth. N-limited cultures appeared to have slightly lower protein concentrations; whereas, lipid concentrations were sixfold higher than N-replete cultures (Table 3.1). Increases in both β-1,3 glucan levels and cell wall polysaccharides were also observed in the N-limited cells (Table 3.1). In addition, TEPs in N-limited cells were approximately two-thirds higher than in N-replete cells during stationary phase (Table 3.1).

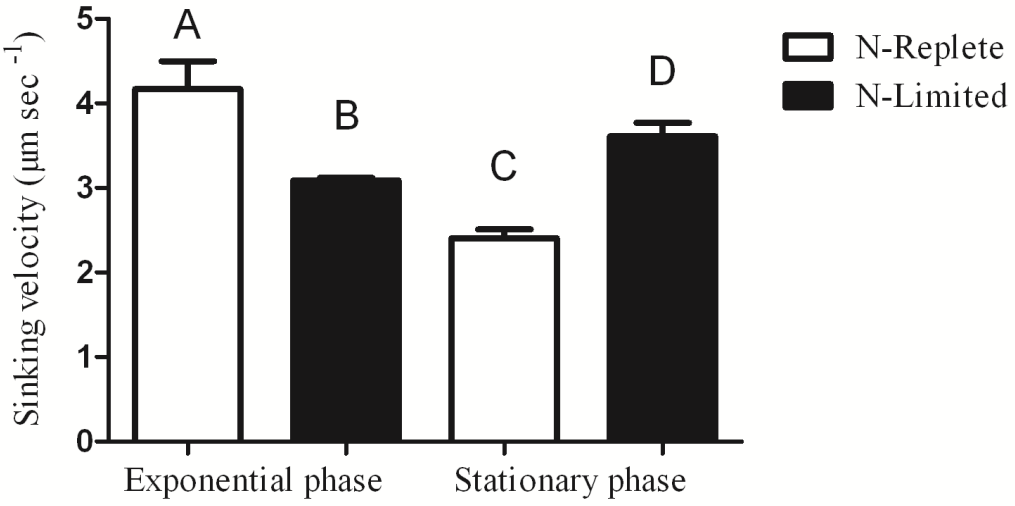

Figure 3.4. The sinking velocity (µm s^{-1}) of *E. huxleyi* under replete or N-limited conditions during two different stages of growth. Data are the mean of three independent cultures, and standard error is presented as a single-sided bar. Different letters indicate statistically significant differences among mean values ($p < 0.05$).

The average diameter of N-replete cells during the exponential growth was approximately 0.65 µm (~10%) greater than in the N-limited cells (Figure 3.5). The reverse was true during stationary phase, when N-limited cells were approximately 0.63 µm (~8.5%) greater in diameter than N-replete cells (Figure 3.5). This size difference in stationary but not exponential phase cells was due largely to an increase in the thickness of the coccosphere layer, from 0.29 µm (± 0.15) in N-replete stationary phase cells to 0.75 µm (± 0.024) in N-limited stationary phase cells (Figure 3.6). The size of the protoplast, however, did not change (Figure 3.7).

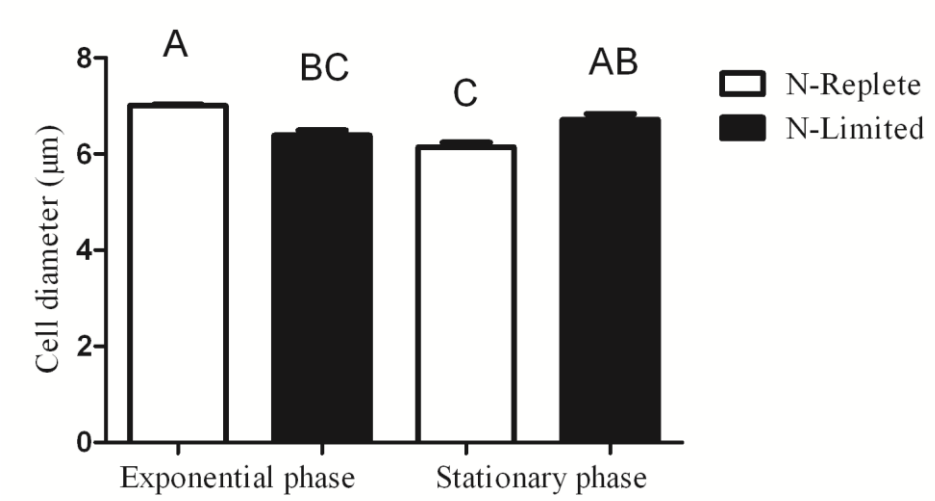

Figure 3.5. The average diameter (µm) of *E. huxleyi* cells under replete or N-limited conditions during two different stages of growth. The coccosphere is included in the measurements. Data are the mean of three independent cultures, and standard error is presented as a single-sided bar. Different letters indicate statistically significant differences among mean values ($p < 0.05$).

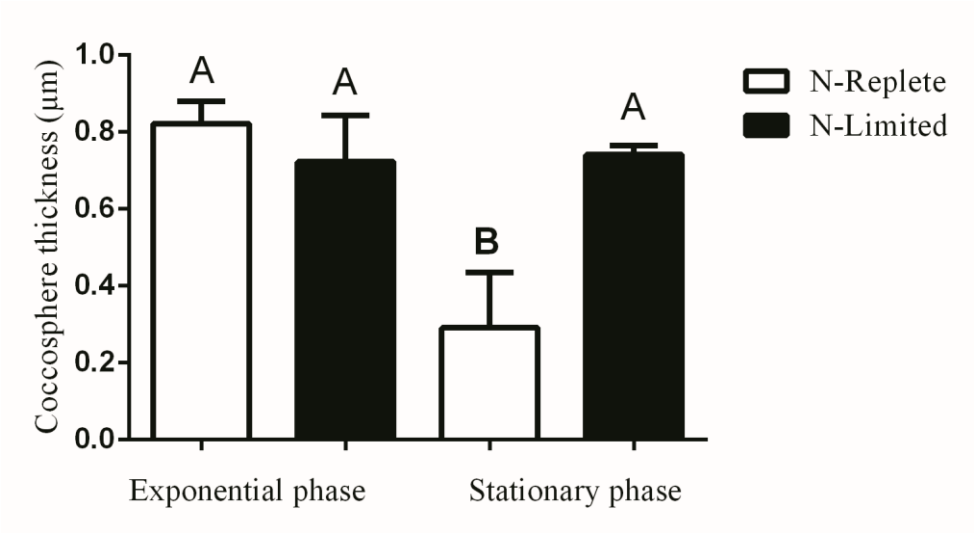

Figure 3.6. The average thickness (µm) of the coccosphere in *E. huxleyi* during the exponential and stationary phases when grown under replete or N-limited conditions. Data are the mean of three independent cultures, and standard error is presented as a single sided bar. Different letters indicate statistically significant differences among mean values ($p < 0.05$).

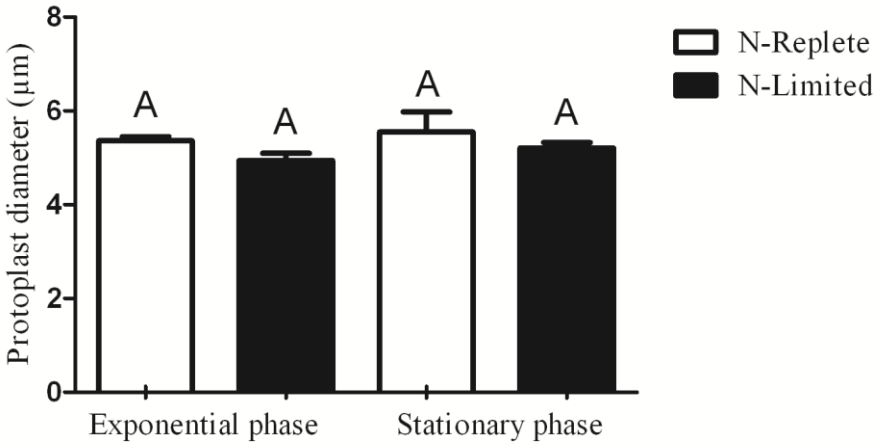

Figure 3.7. The average diameter (µm) of *E. huxleyi* protoplast under replete or N-limited conditions during two different stages of growth. The coccosphere was not included in the measurements. Data are the mean of three independent cultures, and standard error is presented as a single-sided bar. Different letters indicate statistically significant differences among mean values ($p< 0.05$).

The cell density was consistent between treatments and during both exponential and stationary growth (Figure 3.8). With no change in cell density, we assumed that the sinking rate depended on the size of the cell; as expected, as cell size increased, so too did the sinking rate (Figure 3.9).

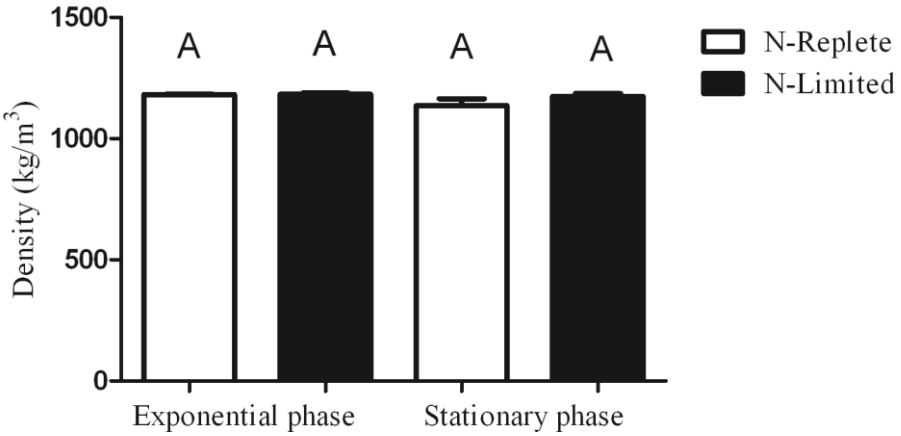

Figure 3.8. The average density (kg m^{-3}) of *E. huxleyi* during the exponential growth phases under replete or N-limited conditions. Data are the mean of three independent cultures, and standard error is presented as a single sided bar. The same letter indicates that there are no statistically significant differences among mean values ($p> 0.05$).

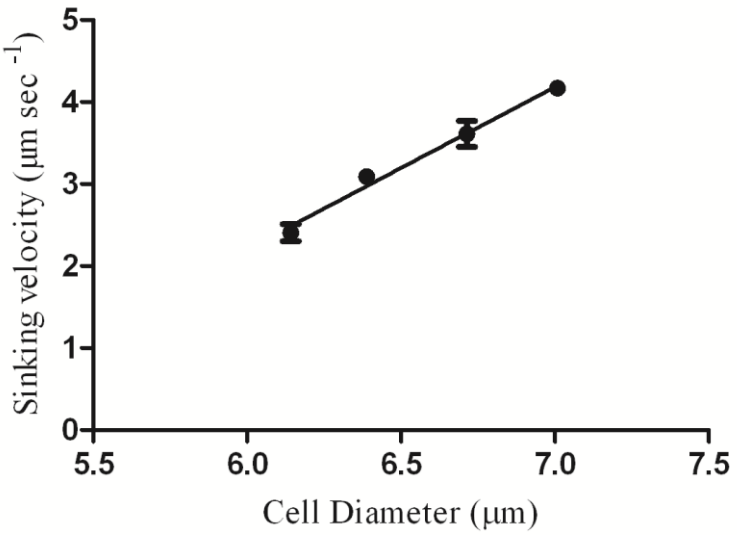

Figure 3.9. Sinking velocity as a function of cell diameter (inclusive of coccosphere) for *E. huxleyi*. Cell diameter varied as a consequence of different growth conditions (Figure 3.4). y = 1.975x – 9.641, r^2 = 0.9877.

3.4 Discussion

The nutrient status of cells influences the capacity for photochemical work (Beardall et al., 2001). When grown in an N-limited environment, F_v/F_m, growth rates and chlorophyll per cell all declined, a set of responses that is characteristic of N-limitation.

During the exponential growth phase, the N-replete cells sank faster. From Stokes' Law we know that cell density and cell size are the two parameters that determine sinking rate. The N-limited cells produced greater concentrations of lipids as a response to the nutrient stress, and as lipids are less dense than water, an accumulation of lipids could reduce the density of the N-limited cells, causing them to sink at a slower rate. Indeed, Fernández et al. (1994) estimated that a lipid content of 60% of the total cellular organic carbon in *E. huxleyi* could reduce the cell density and the sinking velocity by 20%. No change in the overall cellular density was detected in our experiments however. In our experiments therefore, lipid accumulation would appear to be an unimportant factor in determining the sinking velocity. Perhaps we would have seen a physiological response similar to that predicted by Fernández et al. (1994) if we incubated the cells with the same 16 h light, 8 h dark photo period.

There was a general increase in the concentration of β-1,3 glucan carbohydrates and cell wall polysaccharides in the N-limited cells. These carbohydrates were being stored under N-limitation, most likely as reserves to sustain future growth and cellular structure. This is not surprising since β-1,3 glucan can still be produced from photosynthetic CO_2 fixation when N or phosphorus are limiting (Granum et al., 2002) providing the photosynthetic machinery is not entirely compromised. It is possible, therefore, that the overall cellular density of cells did not change because the increase in carbohydrates cancelled out any decrease in density caused by the accumulation of lipid.

Whether or not this is the case, the fact that there were no changes seen in the overall cellular density indicates that these alterations in macromolecular composition were playing no significant role in changing the sinking capacity of the cells.

Given that density was consistent across all treatments, we might assume that cell size is the major driver of changes to the sinking velocity, and we found that the N-limited cells were significantly smaller than the N-replete cells at exponential growth phase. A reduction in size and a consequent increase in surface area to volume ratio is seen as an acclimation to improve nutrient uptake in response to nutrient-limiting conditions (Hein et al., 1995). This decrease in cell size though also caused the N-limited cells to sink more slowly.

During stationary phase, the N-limited cells had a greater sinking velocity than the N-replete cells, the opposite of what was seen during the exponential growth phase. The N-limited cells in stationary phase cultures were larger than their N-replete equivalents. This increase in size was due to the increased layering of coccoliths, which was not seen during the exponential growth phase. Several authors have associated N-limitation and starvation with coccolith production (Linschooten et al., 1991, Lecourt et al., 1996), the production of coccoliths increasing as the N levels decline (Paasche, 1998). In a low-nutrient environment, movement through the water to nutrient-rich waters is essential for survival (Paasche, 2002). It has been suggested, therefore, that *E. huxleyi* cells compensate for their lack of motility by producing coccoliths to facilitate their sinking to nutrient rich deeper waters (Linschooten et al., 1991, Lecourt et al., 1996, Paasche, 2002). Klaas and Archer (2002) also confirmed, through their analysis of sediment trap data, that most of the organic carbon that is transferred to the deep sea is carried in association with calcium carbonate, acting as ballast. It is also interesting to note that calcification in coccolithophores is decreased at low light, reducing the likelihood of cells sinking into lower light conditions (Raven and Waite, 2004). It is

likely therefore, that *E. huxleyi* did alter its coccolith concentration under these conditions in order to facilitate sinking.

The densities of the N-replete and the N-limited cells were not different, however. This suggests that the calcium carbonate coccoliths were not adding significant weight to the cell. Rather, the coccoliths modulated sinking by increasing the size of the cell. Interestingly, however, if not for the coccosphere, the N-replete cells and the N-limited cells would have been the same size and would therefore have more than likely sunk at the same rate.

During stationary phase, the N-limited cells produced significantly more TEPs than did the N-replete cells. This finding is not unexpected, as Corzo et al. (2000) found that populations of a diatom, *Chaetoceros calcitrans* (Paulsen) Takano, produced more TEPs when grown in a N-limited environment. Production of TEPs has been associated with increasing cellular aggregation, marine snow formation and increased sedimentation rates (Alldredge and Silver, 1988, Alldredge et al., 1993, Engel, 2002). We did not specifically observe or attempt to quantify aggregation and marine snow, nor did we attempt to replicate conditions where marine snow might form, but, given that large aggregates of phytoplankton sink orders of magnitude faster than single cells (De La Rocha and Passow, 2007, Biermann and Engel, 2010), the observed increase in TEPs under N-limitation suggests a potential for this to have a major impact on the drawdown of organic carbon.

N-limitation is only one of the likely consequences of global climate change. Increased global temperatures and CO_2 concentrations, ocean acidification and the limitation of other key elements, including phosphorus, are likely to result from climate change, and there will be a combined effect that may alter cell properties and sinking velocities further (Raven et al., 2005). Recent studies have also indicated that N cycles will alter in response to increases in atmospheric CO_2 whereby there

may be an increase in the NH_4^+/NO_3^- ratio and an increase in the use of NH_4^+ by phytoplankton (Beman et al., 2011, Lefebvre et al., 2012). In an increased NH_4^+/NO_3^- environment, Lefebvre et al. (2012) observed a 53% reduction in calcification by *E. huxleyi* (calcifying strain CCMP 371) when grown in conjunction with elevated CO_2 (1000 p.p.m.). De Bodt et al. (2010) also observed a reduction in the mean coccosphere volume of *E. huxleyi* (strain AC481) with increasing CO_2 and temperature, while Müller et al. (2012) observed that *E. huxleyi* (morphotype A) cell diameter increased by 0.05 µm with every 100 µatm *p*CO2 under N-limited conditions. However, Müller et al. (2012) compared batch cultures with continuous cultures, so the differences in volume may have been a reflection of the different culturing methods. It has been suggested that in the future ocean, environmental factors will synergistically affect *E. huxleyi* and cause a reduction in coccolith production and cell size, leading to a reduced flux of particulate organic carbon to the deep ocean (Raven et al., 2005, De Bodt et al., 2010, Lefebvre et al., 2012).

Regardless of the growth conditions, in our experiments the sinking velocity depended solely on the size of the cell. This is not unexpected since Stokes' Law tells us that size is a determining factor in sinking velocity. What is somewhat unexpected, however, is that the data indicate that the density remained constant regardless of growth conditions and regardless of macromolecular change. This is, however, in accordance with the findings of Smayda (1970), who determined that lipid accumulation is generally an unimportant suspension mechanism in phytoplankton.

In some regions of the ocean, where warming surface waters and stratification will reduce the return flow of remineralized carbon and nutrients from the deep oceans to the surface waters, it is expected that overall primary production will decline (Beardall et al., 2001, Raven et al., 2005, Riebesell et al., 2007). In addition, it is expected that larger phytoplankton cells, which have higher nutrient requirements, will be strongly affected by nutrient depletion, allowing smaller-celled

species, with higher surface area to volume ratios, to dominate the nutrient depleted regions (Beardall et al., 2009a, Beardall et al., 2009b). The data reported here support the hypothesis that cell size appears to be the main factor in determining sinking velocity. Consequently, an increase in smaller-celled species that sink at reduced velocities will affect the efficiency of the biological carbon pump, but given the potential increase in marine snow, associated with possible increases in TEP and aggregation of particulate matter, the overall effect could be positive or negative. It is also uncertain whether all species of phytoplankton will behave in the manner that we observed in *E. huxleyi*. Because of its small spherical shape, *E. huxleyi* behaves strongly according to Stokes' Law. Many species are nonspherical or have protuberances that affect their sinking rates (Holland, 2010), and they will not sink according to Stokes' Law. Consequently, it is difficult to make predictions about the sinking behaviour of different species and their impact on the biological carbon pump in the future ocean. However, given that *E. huxleyi* is a numerically important species and a major contributor to the export of carbon to the deep ocean (Zondervan et al., 2001), subtle changes in sinking behaviour exhibited by this species may significantly influence the biological carbon pump.

Chapter 4.0: Impacts of High CO_2 on the Sinking Velocity of *E. huxleyi*

4.1 Introduction

The exchange of CO_2 between the ocean and the atmosphere is in part determined by the conversion of DIC into organic matter through the process of photosynthesis and its subsequent export to the deep ocean (Ziveri et al., 2007). Coccolithophores have a unique dual role however, as they are able to use DIC to not only produce organic matter but also to produce calcium carbonate ($CaCO_3$) platelets called coccoliths which, among other roles, can act as ballast material aiding in the transport of organic matter to the deep sea (Ziveri et al., 2007, Engel et al., 2009b, Hutchins, 2011). Coccolithophores are considered to be the most productive calcifying organisms on earth (Rost and Riebesell, 2004) and *E. huxleyi* is the most abundant of the coccolithophore species, showing the widest global distribution (Westbroek et al., 1993). *E. huxleyi* is also said to be the most abundant eukaryotic marine phytoplankton species globally (Emiliani, 1993). *E.huxleyi* therefore plays a vital role in the global carbon cycle and how it will react to predicted future levels of elevated CO_2 remains an important area of research.

Atmospheric CO_2 that is absorbed by the ocean is partitioned to CO_2, bicarbonate ions (HCO_3^-) and carbonate ions (CO_3^{2-}) and as more atmospheric CO_2 is absorbed by the surface waters as a result of anthropogenic activities, increased dissolved CO_2 leads to increased formation of carbonic acid and decreased pH. The lower pH causes a shift in equilibrium between DIC species resulting in fewer CO_3^{2-} ions and small increases in HCO_3^- (Table 1.1) (Raven et al., 2005, Beaufort et al., 2011). Because of its effect on calcium carbonate saturation state, ocean acidification is a major threat to marine ecosystems and particularly to calcifying organisms such as coral, foraminifera and coccolithophores (Riebesell et al., 2000, Beaufort et al., 2011). Riebesell et al. (2000) for instance, reported that under elevated CO_2, the coccolithophores *E. huxleyi* and *Gephyrocapsa oceanic*a had reduced calcification rates and exhibited an increased proportion of malformed coccoliths. This

reduction in calcification could lead, therefore, to reduced ballast effects in coccolithophores which could ultimately impact on sinking velocities and the efficiency of the biological carbon pump.

Riebesell et al. (2000) also proposed, however, that this reduction in calcification could potentially act as a negative feedback mechanism to rising atmospheric CO_2 levels. While $CaCO_3$ calcification can aid sinking, depending on the $CaCO_3$ rate of production, it can also have a negative influence on atmospheric CO_2 conditions. The production of organic matter through photosynthesis consumes CO_2 thus removing CO_2 from the upper surface waters, and ultimately the atmosphere (Equation 4.1). In contrast, the process that produces $CaCO_3$, releases CO_2 because two HCO_3^- molecules are converted into one $CaCO_3$ molecule as well as one CO_2 molecule (Equation 4.2).

$$CO_2 + H_2O + \text{light} \rightarrow CH_2O + O_2 \quad \text{(Equation 4.1)}$$

$$Ca^{2+} + 2\ HCO_3^- \rightarrow CaCO_3 + CO_2 + H_2O \quad \text{(Equation 4.2)}$$

Therefore the ratio of $CaCO_3$ production to organic matter production and its subsequent sinking (the rain ratio) could influence atmospheric CO_2 concentrations. It should also be noted that the dissolution of DIC and the mineralisation of particulate organic carbon (POC) during sedimentation can also have an influence on the biological carbon pump.

However the findings of Riebesell et al. (2000) have not been consistently repeated across all coccolithophore species or even among *E. huxleyi* strains, leading to a recognition that the likely future outcomes for coccolithophores, in response to increased CO_2 concentrations, will be species and strain specific (Langer et al., 2009). For instance Langer et al. (2006) observed that at 920 p.p.m. CO_2, the coccoliths of *Calcidiscus leptoporus* were severely malformed while the coccoliths of *Coccolithus pelagicus* when grown at 915 p.p.m. CO_2, exhibited no CO_2 sensitivity. Müller et al.

(2010) also observed that the morphology of *E. huxleyi* coccoliths did not display any visible changes when grown at under 1150 µatm CO_2, despite the fact that the ratio of particulate inorganic carbon to particulate organic carbon (PIC:POC) decreased considerably with increased CO_2 concentrations. On the other hand, Iglesias-Rodriguez et al. (2008) observed that cultures of *E. huxleyi* doubled their calcification rate and net primary production when grown under 750 p.p.m. These contradictory results and differences in CO_2 sensitivity among coccolithophore species and strains are likely to have a genetic basis (Langer et al., 2009) and therefore each different species or strain is likely to have a different influence on carbon export and the biological carbon pump.

The majority of the downward vertical flux of organic matter in the sea is caused by the settling of aggregates (Fowler and Knauer, 1986). TEP production, which assists in aggregation, has been observed to be significantly greater in *E. huxleyi* cultures grown in a high CO_2 environment (~713 p.p.m.: Engel et al., 2004). It is thought that this is because *E. huxleyi* primary production is stimulated by elevated pCO_2, and primary production is closely coupled with discharge of the precursors for TEP production (phytoplankton exudation, which is comprised of up to 80% carbohydrates) (Borchard and Engel, 2012). Enhanced TEP production and increased aggregation rates have been associated with increased phytoplankton sinking velocities (Passow et al., 2001, Engel et al., 2009a). Despite this, Biermann and Engel (2010) observed that cultures of *E. huxleyi* (strain PML B92/11) had a significantly reduced sinking velocity when grown under high CO_2 concentrations (750 µatm CO_2) when compared to those cultures grown at ~180 or ~380 µatm CO_2. The authors suggested that this decrease in sinking velocity was due to a decline in the excess density of aggregates as a result of a reduction in PIC:POC caused by ocean acidification. This was despite the fact that aggregates appeared larger. The sinking velocity of *E. huxleyi* could therefore be impaired in those strains that display CO_2 sensitivity even where enhanced rates of TEP formation and aggregation are observed.

Increases in atmospheric CO_2 concentrations could also alter the macromolecular composition of coccolithophores, which could further influence the sinking velocity of cells. Other species of phytoplankton have displayed high lipid productivity in response to increased CO_2 concentrations, including the fresh water species *Chlorella vulgaris* (Widjaja et al., 2009) and the marine diatoms *Nitzschia inconspicua* (Chu et al., 1996) and *Phaeodactylum tricornutum* (Chrismadha and Borowitzka, 1994). As lipids are less dense than water, an increase in lipids in coccolithophores such as *E. huxleyi* could have the consequence of reducing sinking velocities. However, increases in lipid concentrations are often accompanied by increases in cellular carbohydrates, with overall cellular densities remaining constant (Pantorno et al., 2013). Indeed, corresponding increases in carbohydrates have been observed in both *Nitzschia inconspicua* and *Phaeodactylum tricornutum* in response to increasing CO_2 concentrations (Chrismadha and Borowitzka, 1994, Chu et al., 1996*).* It is therefore unknown whether changes in the macromolecular molecular composition, as a result of enhanced CO_2 concentrations, will influence the sinking velocity of coccolithophores and how this will influence the biological carbon pump.

The aim of the experiments reported in this chapter was therefore to determine the effects of high CO_2 conditions on the sinking velocity of the coccolithophore *E. huxleyi* (CS 812). In order to understand any sinking differences observed, changes in coccolith morphology and coccosphere thickness were examined as well as changes in macromolecular composition, cell size and density and TEP concentrations.

4.2 Methods

4.2.1 Semi-Continuous Culture Experiments

E. huxleyi (CS 812) was grown in 3 independent, semi-continuous cultures (1 litre) in 1-litre glass Schott bottle (to minimise the headspace) using F/2 medium. Cultures were maintained at 18 ± 1 ^{o}C with photosynthetically active radiation (PAR; 400 – 700 nm) provided continuously at a photon flux of 80 µmol quanta m^{-2} s^{-1} from fluorescent tubes (Philips TLD 18W/865, cool daylight; Philips, Eindhoven, The Netherlands). Cultures were stirred constantly using a magnetic stirrer at 160 r.p.m. and continuously aerated (See below).

The 3 experimental cultures were grown to 0.5 – 0.8 X 10^6 cells ml $^{-1}$. Cultures were then maintained in a semi-continuous state by diluting them to 0.1 – 0.3 X 10^6 cells ml $^{-1}$ daily. The cells were thus kept in exponential growth phase during this part of the experiment. Growth rates were determined daily (Section 2.6). The general physiological state of cultures was also confirmed prior to any analysis using chlorophyll *a* and *c* measurements (Section 2.7) and by measurements of chlorophyll fluorescence-based quantum yield (F_v/F_m), which describes the maximum quantum efficiency of photosystem II. F_v/F_m was measured using the PAM fluorometer (Section 2.12).

The CO_2 concentration in cultures was varied during these experiments. In the first instance cultures were grown under current day CO_2 levels (400 p.p.m.) by aerating the cells with ambient air passed through a 0.2 µm PTFE membrane in-line air filter (Pall Corporation, Roseville, USA, ARCO 50 vent device) at a rate of 450 ml min^{-1}. The CO_2 concentration was then increased to 1000 p.p.m. by mixing 5% CO_2 with ambient air using a 150 mm Two-Tube Gas Blender (Series 150A, Advanced Specialty Gas Equipment, NJ, USA). The cells were then aerated with the 1000 p.p.m. air. The CO_2 concentration was monitored daily through measurements of pH and DIC (Section 2.13). Alkalinity

could not be recorded as the probe was out of commission at the time these experiments were carried out. To ensure acclimation, the cells were maintained in a semi-continuous state for a minimum of 7 generations prior to any analysis.

The sinking velocity was measured according to the method of Walsby & Holland (2006) (Section 2.4). In order to have sufficiently high resolution, at least 10 million cells in a 1 ml sample were required for each run. The cells were therefore concentrated by filtering them onto cellulose nitrate, 3 µm membrane filters (Sartorius, Gottingen, Germany) and resuspending them in 1 ml of fresh F/2 medium.

The concentrations of cell protein, lipid and carbohydrate were examined at each harvest during semi-continuous exponential growth. Protein concentration was measured using a Bio-Rad DR Protein assay kit (Section 2.8). Lipids were extracted from the cells using a modified Bligh & Dyer (1959) technique and the concentration of lipids was determined gravimetrically (Section 2.9). The carbohydrates, β-1,3 glucan and cell wall polysaccharides, were extracted from the cells (Section 2.10) and the glucan extract and the cell wall hydrolysate were analysed separately using the phenol-sulphuric acid spectrophotometric method (Section 2.10). The photosynthetic parameters (α, I_k and $rETR_{max}$) were also measured using PAM fluorometer based RLCs (Section 2.12).

Cell diameter was measured in order to understand the role of cell size in sinking velocities (Section 2.5). Using photographs, cell diameter (µm), both including and excluding the coccosphere, was measured, and the coccosphere thickness was thereby calculated. The density of the cells was then calculated by substituting the values obtained for cell diameter and sinking velocity into the Stokes' Law equation (Equation 1.1).

The surface area of coccoliths was also calculated by measuring coccolith length and width using scanning electron micrographs. The scanning electron micrographs were generated at the Monash Micro Imaging facility (Monash University) using a Hitachi S570 scanning electron microscope (SEM). *E. huxleyi* cells, taken during the exponential growth phase, were filtered onto an Isopore, 13 mm, 0.22 µm, GTTP membrane filter (Milipore, Billerica, MA, USA). The filters were dried by submerging them, for 5 minutes, into a series of ethanol solutions (75% – 100% dry ethanol), being allowed to dry for 5 minutes in between each ethanol concentration. Finally, the filters were submerged in a series of hexamethyldisilazane (HMDS): ethanol mixtures (5 minutes in each of 1 HMDS: 2 dry ethanol and 2 HMDS: 1 ethanol, followed by two-5 minute submergences in 100% HMDS). The filters were then dried in the fume hood until all HMDS had evaporated. Prior to examination by SEM, the samples were gold plated using a Balzers SCD005 Sputter coater (at 25 mA for 60 seconds).

4.2.2 Batch Culture Experiments - For TEP Analysis

Since the production of TEPs is associated mainly with the stationary and senescent stages of algae (Corzo et al., 2000, Hong et al., 1997) a separate batch culture experiment was carried out on cells that were allowed to grow until stationary phase (5 – 7 days), being bubbled continuously with either 400 or 1000 p.p.m. CO_2. The concentration of TEPs was measured using the methods of Passow & Alldredge (1995) after 5 ml of culture was filtered at a low constant vacuum (at 100 mm Hg) onto 25-mm polycarbonate filters (Isopore membrane filters, 0.4 µm HTTP, Millipore, MA, USA) (Section 2.11).

However, growing cultures of *E. huxleyi* rapidly consume CO_2 and therefore they could not be maintained at equilibrium when at the high cell density characteristic of stationary phase. As a result, rather than being maintained at 400 and 1000 p.p.m. CO_2 during stationary phase, the average measured concentrations of CO_2 in these cultures was 87.56 and 147 p.p.m. CO_2 respectively (Table 4.1). As a result of this, no further experiments, other than TEP analysis, were completed on cultures at stationary phase.

4.2.3 Statistical Analysis

Statistical significance between the two treatments was determined using an unpaired two-tailed t test. Significance was set at $P < 0.05$. All statistical analyses were conducted using GraphPad Prism 5 (GraphPad Software Inc., La Jolla, California, USA).

4.3 Results

4.3.1 Culture Conditions

Measurements of pH, DIC and pCO_2 are presented in Table 4.1. During the exponential growth phase, the pCO_2 increased in those cultures that were aerated with 1000 p.p.m. CO_2 by approximately 49% compared to those aerated with 400 p.p.m. CO_2, maintaining the pCO_2 at approximately 790 p.p.m. Those cultures aerated with 400 p.p.m. CO_2, maintained a CO_2 concentration of approximately 387 p.p.m. CO_2 concentrations of less than equilibrium in these cultures is indicative of C uptake by the cells, despite the relatively low cell number employed. Under elevated CO_2, the pH decreased by an average of 0.27 units over the course of growth while the DIC increased by approximately 2%. At stationary growth phase however, the CO_2 could not be held in equilibrium and despite being aerated with 1000 or 400 p.p.m. CO_2, the pCO_2 in the medium dropped to an average of 147 and 87.56 p.p.m respectively. These resulting CO_2 concentrations were not statistically different from one another. This is reflected in the fact that there were no significant differences seen in pH and DIC concentrations at this stage of growth (Table 4.1).

Table 4.1. Measured concentrations of dissolved inorganic carbon (DIC), pH, and pCO_2 in F/2 medium at each harvest of *E. huxleyi* cells during the exponential and stationary growth phase.[1]

	pCO_2 aim (p.p.m.)	pH	Error (±)	DIC (mmol kg^{-1} SW)	Error (±)	pCO_2 (p.p.m.)	Error (±)
Exponential growth phase	1000	7.82	0.012	1730.83	167.86	790.93	28.57
	400	8.085	0.008	1694.16	91.84	386.89	22.49
Stationary growth phase	1000	7.94	0.082	308.89	103.84	147	60.93
	400	8.016	0.146	269.34	34.26	87.56	19.83

[1] Values are means and the error is the standard error. N = 3.

4.3.2 Semi-Continuous Culture Experiments and TEP Analysis

The specific growth rate of *E. huxleyi* appeared to increase by an average of ~30% when aerated with 1000 p.p.m. CO_2 compared to those cultures aerated with 400 p.p.m. CO_2 (Figure 4.1). However this difference in growth rate was not statistically different. There were no statistically significant changes in chlorophyll *a* and *c* concentrations with an increase in CO_2 (Figure 4.2). Nor were there any observable differences in F_v/F_m, α or I_k (Table 4.2). However, $rETR_{max}$ significantly increased with an increase in CO_2 by an average of ~14% (Table 4.2).

During the exponential growth phase, the *E. huxleyi* cultures aerated with 400 p.p.m. CO_2 sank with an average velocity of 4.9 µm s^{-1}. The average sinking velocity for the *E. huxleyi* cells aerated with 1000 p.p.m. CO_2 was 5.37 µm s^{-1} which was not statistically different (Figure 4.3).

Significant differences in macromolecular composition between the cells aerated with 400 p.p.m. and 1000 p.p.m. CO_2 were evident. Lipid concentrations increased significantly and were on average 3.4 times higher in the cultures aerated with 1000 p.p.m. CO_2 than with those aerated with 400 p.p.m. (Table 4.2). β-1,3 glucan levels also increased by an average of 26%, while cell wall polysaccharides increased significantly by an average of 48% when aerated with 1000 p.p.m. CO_2 (Table 4.2). Protein concentration significantly increased, by an average of 44%, in those cultures aerated with 1000 p.p.m. CO_2 (Table 4.2). At stationary phase there appeared to be a decline in TEP concentrations by approximately 47% when the cultures were aerated with 1000 p.p.m (Table 4.2). The difference in TEP concentrations between those aerated with 400 and 1000 p.p.m. was however not statistically significant due to the large standard error associated with these measurements.

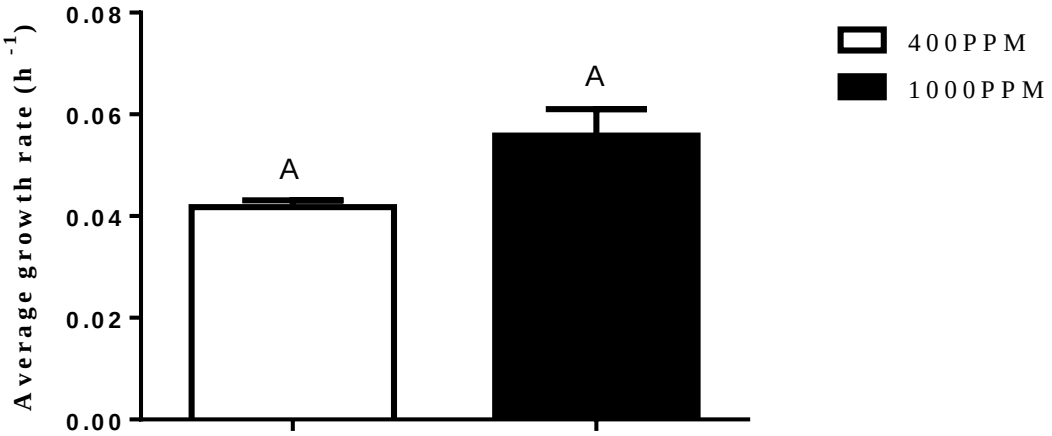

Figure. 4.1. The specific growth rate of *E. huxleyi* when grown in semi-continuous cultures and aerated with 400 or 1000 p.p.m. CO_2. Data are the mean of three independent cultures. Standard error is presented as a single-sided bar. The same letters indicate no statistically significant differences among mean values (p= 0.053).

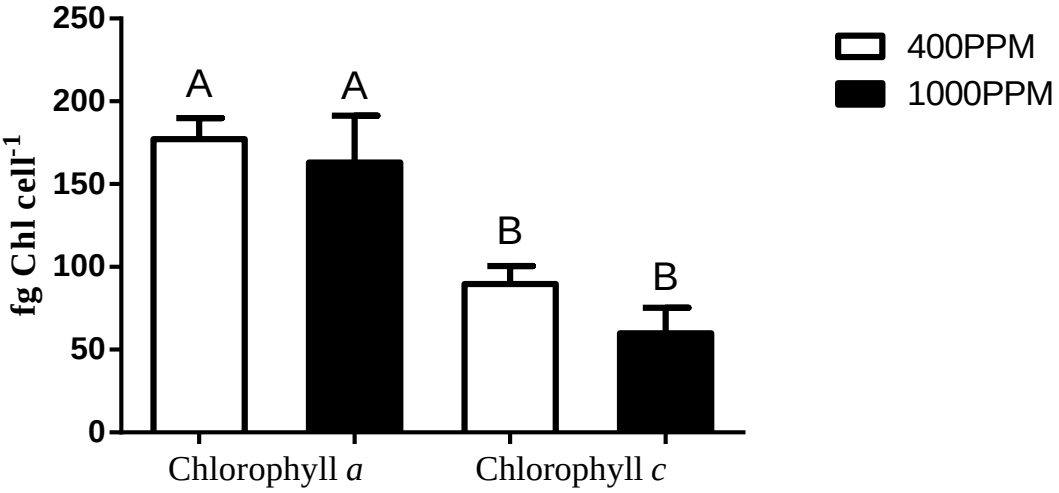

Figure. 4.2. Chlorophyll *a* and *c* concentrations (fg Chl $cell^{-1}$) in *E. huxleyi* during the exponential growth phase and aerated with 400 or 1000 p.p.m. CO_2. Data are the mean of three independent cultures, and standard error is presented as a single-sided bar. Different letters indicate statistically significant differences among mean values (p< 0.05).

Table 4.2. Changes in macromolecular composition, photosynthetic parameters and TEP concentrations in *E. huxleyi* when aerated with 400 p.p.m. or 1000 p.p.m. CO_2.[2]				
	400 p.p.m.		1000 p.p.m.	
	Mean	Error (±)	Mean	Error (±)
F_v/F_m	0.474	0.009	0.48	0.01
α (µmol electrons / µmol photons)	0.184	0.008	0.186	0.004
$rETR_{max}$ (µmol electrons $m^{-1}s^{-1}$)*	21.91	0.53	25.3	0.55
I_k (µmmol photons $m^{-1}s^{-1}$)	121.3	6.8	138.1	5.15
Protein (pg $cell^{-1}$)*	88.3	8.4	158	11.5
Lipids (pg $cell^{-1}$)*	521.85	75.15	1795.186	193.64
β-1,3 glucan (pg $cell^{-1}$)	1.49	0.13	2.02	0.16
Cell wall polysaccharides (pg $cell^{-1}$)*	0.49	0.048	0.94	0.12
TEP (µg $cell^{-1}$) Stationary phase[2]	0.785	0.34	0.417	0.12

[2] TEP was only measured at stationary phase as TEP concentrations during the exponential growth phase are negligible. At stationary phase however, CO_2 concentrations could not be held in equilibrium therefore, these TEP concentrations are representative of 87.56 and 147 p.p.m. CO_2 respectively. . *Indicates that there was a statistically significant difference among mean values ($p < 0.05$).

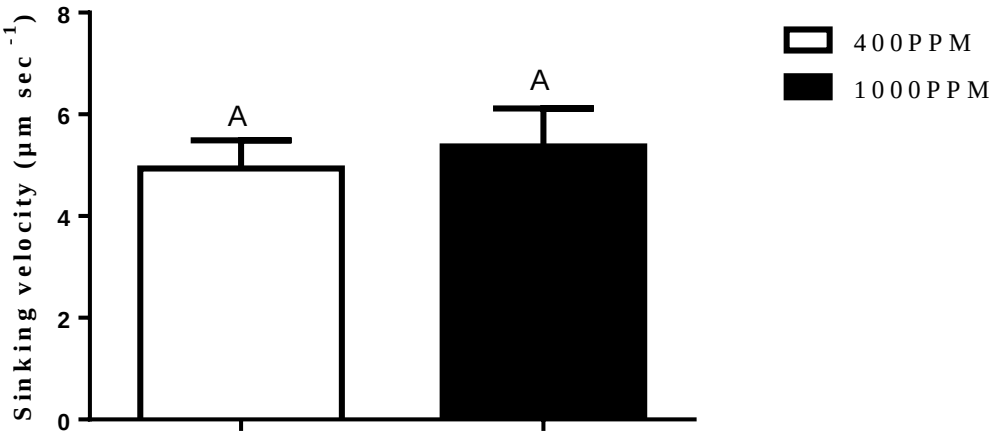

Figure 4.3. The sinking velocity (µm s^{-1}) of *E. huxleyi* during the exponential growth phase and aerated with 400 or 1000 p.p.m. CO_2. Data are the mean of three independent cultures, and standard error is presented as a single-sided bar. The same letters indicate no statistically significant differences among mean values (p= 0.067).

There were no significant differences observed in total cell diameter between the cultures aerated with 400 p.p.m. and those aerated with 1000 p.p.m. (Figure 4.4). The average diameter for individual cells in both growth conditions was approximately 6 µm. The average coccosphere thickness was however, significantly larger (~18%) in those cultures that were aerated with 400 p.p.m. (Figure 4.5), while the protoplast was significantly larger (~5%) in those cells that were aerated with 1000 p.p.m. (Figure 4.6). Despite this, cell density was consistent between treatments and no significant differences in cell density were observed (Figure 4.7).

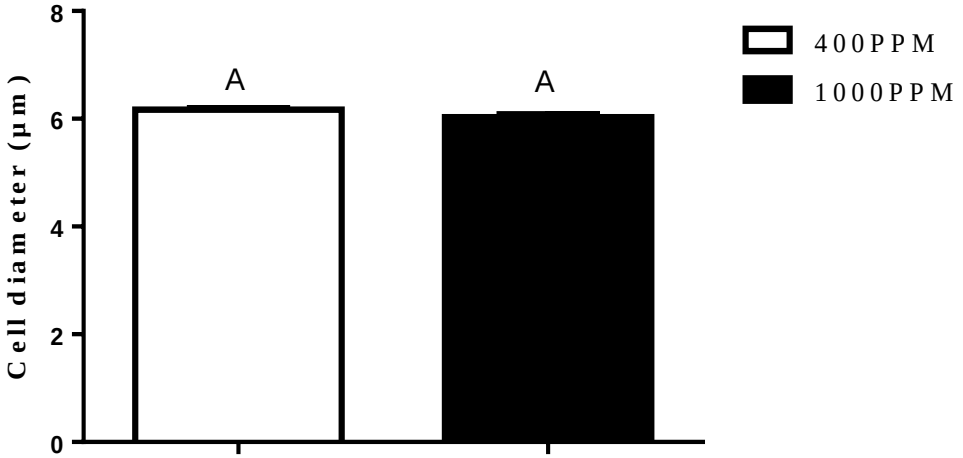

Figure 4.4. The average diameter (µm) of *E. huxleyi* during the exponential growth phase and aerated with 400 or 1000 p.p.m. CO_2. The coccosphere is included in these measurements. Data are the mean of three independent cultures, and standard error is presented as a single-sided bar. The same letters indicate no statistically significant differences among mean values (p= 0.12).

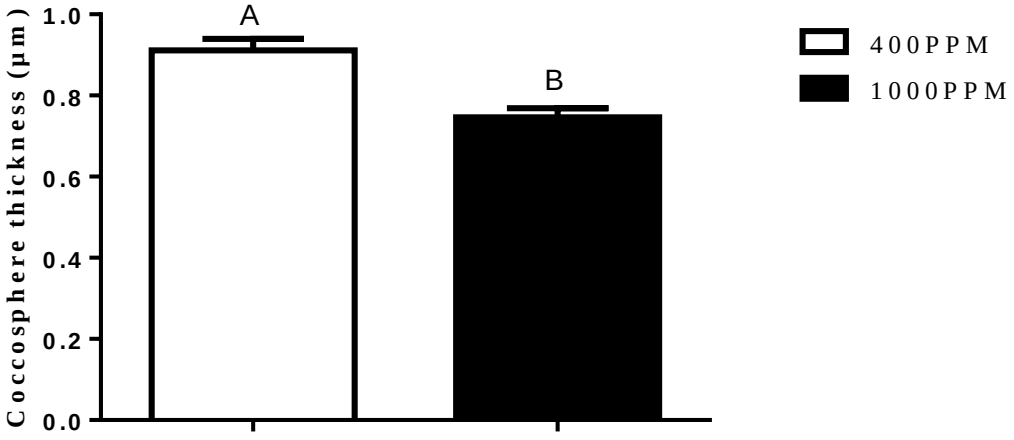

Figure 4.5. The average thickness (µm) of the coccosphere in *E. huxleyi* during the exponential growth phase and aerated with 400 or 1000 p.p.m. CO_2. Data are the mean of three independent cultures, and standard error is presented as a single sided bar. Different letters indicate statistically significant differences among mean values (p= 0.01).

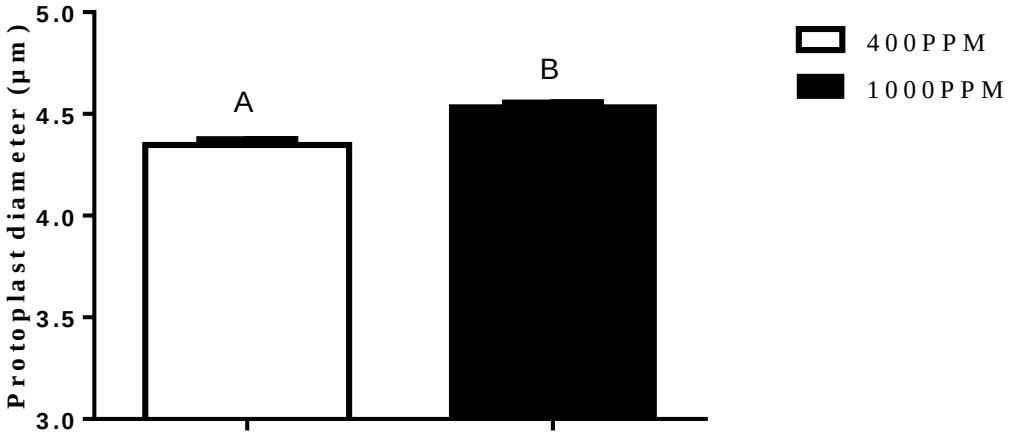

Figure 4.6. The average diameter (µm) of *E. huxleyi* protoplast during the exponential growth phase and aerated with 400 or 1000 p.p.m. CO_2. The coccosphere was not included in these measurements. Data are the mean of three independent cultures, and standard error is presented as a single sided bar. Different letters indicate statistically significant differences among mean values (p= 0.003).

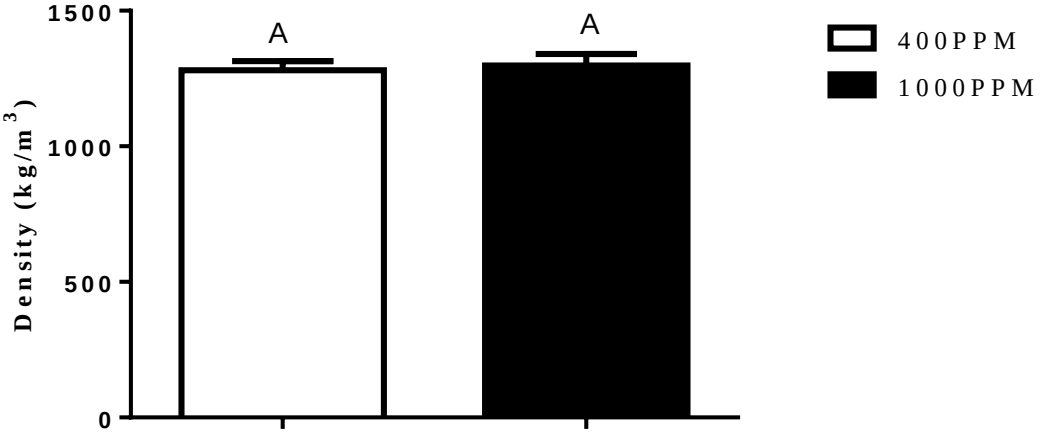

Figure 4.7. The average density (kg m^{-3}) of *E. huxleyi* during the exponential growth phase and aerated with 400 or 1000 p.p.m. CO_2. Data are the mean of three independent cultures, and standard error is presented as a single sided bar. The same letter indicates that there are no statistically significant differences among mean values (p= 0.76).

The average coccolith surface area appeared to be greater in those cultures that were aerated with 400 p.p.m CO_2 but the difference was still not statistically significant ($p = 0.22$, Figure 4.8). The coccoliths of the cultures aerated with 1000 p.p.m. were on average 1.2 μm^2 smaller (~17%) than those aerated with 400 p.p.m CO_2. Despite the apparent smaller size of coccoliths in cultures bubbled with 1000 p.p.m. CO_2, cell SEM micrographs did not reveal any coccolith malformations or dissolution (Figure 4.9).

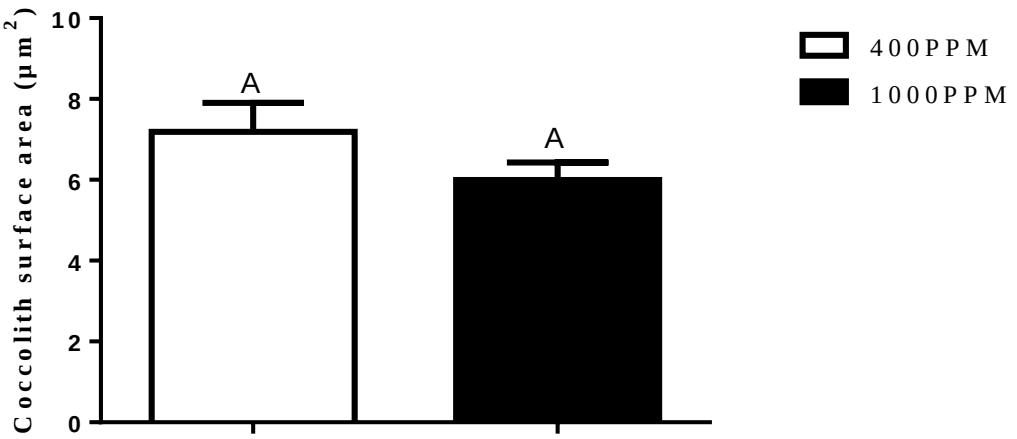

Figure 4.8. The average surface area (μm^2) of individual *E. huxleyi* coccoliths during the exponential growth phase and aerated with 400 or 1000 p.p.m. CO_2. Data are the mean of three independent cultures, and standard error is presented as a single sided bar. The same letter indicates that there are no statistically significant differences among mean values ($p= 0.22$).

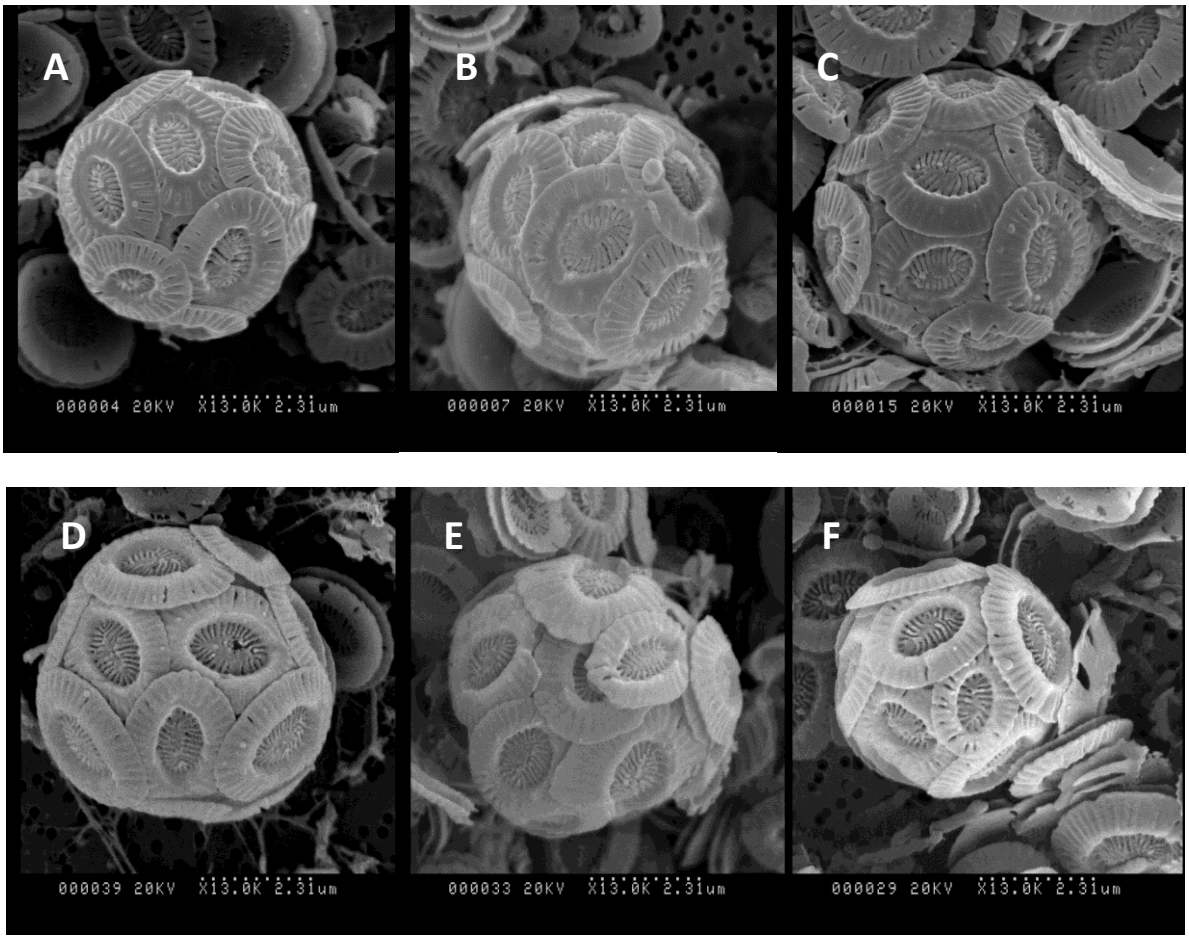

Figure 4.9: Representative SEM images of (A – C) *E. huxleyi* cells aerated with 400 p.p.m. CO_2 and (D – F) *E. huxleyi* cells aerated with 1000 p.p.m. CO_2.

4.4 Discussion

The sinking velocity of *E. huxleyi* was not altered by an increase in CO_2 from 400 p.p.m to 1000 p.p.m. According to the Stokes equation, the sinking velocity of a spherical cell is determined by its density and size (Equation 1.1). The similarity seen in sinking is therefore reflected in the fact that there were no significant changes in the overall cellular density or cell size.

An increase in CO_2 from 400 p.p.m to 1000 p.p.m. did not change the overall cell size. The high CO_2 cells did however result in an increase in the protoplast diameter by approximately 5%. This increase in organic matter with increased CO_2 concentrations is not surprising since numerous authors have made similar findings for *E. huxleyi* (Riebesell et al., 2000, Zondervan et al., 2002, Borchard et al., 2011). For instance, Riebesell et al. (2000) observed an 8.5% increase in POC production in laboratory-cultured *E. huxleyi* cells when grown at 750 p.p.m.v. CO_2. It is thought that this is possibly due to a decrease in the net diffusive efflux of CO_2 because of an increase in CO_2 in the surrounding environment and thus a reduction in the energy needed to maintain high CO_2 inside the cell and additional energy therefore being available for organic carbon fixation (Barcelos e Ramos et al., 2010). Regardless, this increase in protoplast diameter allowed the cells to maintain their size and their sinking velocity in the high CO_2 environment.

E. huxleyi CS 812 is believed to show CCM activity (Rost et al., 2006, Stojkovic et al., 2013). An increase in CO_2 could therefore lead to a down-regulation of CCMs, and the energy normally used to transport CO_2 into the cell could also be used for calcification (Stojkovic et al., 2013). During this study however, while the protoplast increased in size, the width of the coccosphere of those cells that were aerated with 1000 p.p.m. CO_2, was significantly smaller than those cells that were aerated with 400 p.p.m CO_2 (~18%). This may be due to a decrease in the rate of calcification.

Several authors have suggested that under elevated CO_2 and ocean acidification, *E. huxleyi* will reduce its rate of calcification (Riebesell et al., 2000, Zondervan et al., 2001, Müller et al., 2010) and as a result, Lecourt et al. (1996) hypothesised that the sinking rate of coccolithophore-derived particulate material may decline. Lecourt et al. (1996) failed to consider that organic matter production may also be affected with CO_2 increases and this could influence particle sinking rates due to an increase in cell size (Zondervan et al., 2001). Therefore, even where *E. huxleyi* calcification rates do decline as a result of increased CO_2, where there is an increase in organic matter production, as was the findings in this study, the sinking velocity may be maintained and the biological carbon pump may be unaffected. Furthermore, since the production of organic matter through photosynthesis consumes CO_2 while the production of $CaCO_3$ releases CO_2 (Equations 4.1 and 4.2), this observed increase in organic matter and decline in $CaCO_3$, could potentially alter the rain ratio and act as a negative feedback mechanism to rising atmospheric CO_2 levels (Riebesell et al., 2000, Zondervan et al., 2001).

As a consequence of a decrease in calcification, Rokitta et al. (2012) proposed that in a high CO_2 environment, inorganic carbon would be channelled away from calcification and into the Calvin Cycle, stimulating the activity of the pentose phosphate pathway (PPP), an alternate pathway for the production of NADPH. This would lead to increased levels of NADPH being generated which could then be used to produce storage compounds like carbohydrates and lipids. In the present study, a significant increase in the concentration of lipids and carbohydrates was observed in those cells aerated with 1000 p.p.m. CO_2. The PPP therefore, may have been stimulated and the increased amounts of lipids and carbohydrates may have provided a means for the storage of excess carbon (Gordillo et al., 1998, Rokitta et al., 2012). The idea of using oxidative PPP to produce NADPH is debatable however, as it is an energy-costly process and NAPDA can be produced directly through photoproduction (John A Raven, University of Dundee, personal communication).

Despite these changes in macromolecular composition, there were no differences observed in density, possibly because any changes in cellular density due to the increases in lipids was counteracted by increases in carbohydrates (Pantorno et al., 2013).

The increase in macromolecule concentrations and protoplast diameter also corresponds with an increase in the specific growth rate of *E. huxleyi*. Those cultures aerated with 1000 p.p.m. CO_2 increased their average specific growth rate by approximately 30% over those cells that were aerated with 400 p.p.m. CO_2. Despite this increase being marginally insignificant ($p = 0.053$), we regard it to be a biologically significant phenomenon. As stated above, *E. huxleyi* CS 812 is believed to show CCM activity. Therefore it may be expected that *E. huxleyi* will exhibit increased growth rates at higher CO_2 concentrations if CCMs are down-regulated and more energy is available for growth (Wu et al., 2008). Numerous authors have however, reported a decrease in the growth rate of *E. huxleyi* as a response to increasing concentrations of CO_2 (Langer et al., 2009, Barcelos e Ramos et al., 2010, Müller et al., 2010). Müller et al. (2010) for example, observed a 9% decrease in the growth rate of *E. huxleyi* with increasing CO_2 from 260 to 1150 µatm. Likewise, Langer et al. (2009) observed a 35% decrease in growth rate of *E. huxleyi* strain RCC1256 with varying CO_2 from 399 µatm to 915 µatm. These different responses in terms of growth rate appear to be strain specific, with some strains displaying heightened sensitivities (Langer et al., 2009), perhaps due to changes in the pH which can affect cell division (Hansen et al., 2007, Barcelos e Ramos et al., 2010). As *E. huxleyi* CS 812 did not decrease its growth rate and up-regulated protein production in the high CO_2 environment, it may be suggested that this specific strain is insensitive to changes in pH and CO_2 over the range tested. Furthermore, the increase in CO_2 did not negatively affect chlorophyll concentrations, F_v/F_m, $rETR_{max}$, α or I_k, the cells remaining photosynthetically healthy throughout. This further suggests that the CO_2 and pH conditions were within the tolerance levels of *E. huxleyi* CS 812.

Riebesell et al. (2000) reported that under elevated CO_2, the coccolithophore *E. huxleyi* exhibited an increased proportion of malformed coccoliths. During the present study however, despite an observed decrease in pH, there appeared to be no malformations of coccoliths when the cells were aerated with 1000 p.p.m. CO_2. Furthermore, the surface area of individual *E. huxleyi* coccoliths did not significantly change with an increase in CO_2. This is similar to the findings of Young et al. (2014) who observed that *E. huxleyi* coccolith morphology was not significantly affected by the changing CO_2 conditions even under 1000 µatm CO_2. Iglesias-Rodriguez et al. (2008) also found no degradation of calcification. Rather cultures of *E. huxleyi* doubled their calcification rate when grown under 750 p.p.m CO_2. This may be because these studies, including the present study, used heavily calcified morphotypes of *E. huxleyi* (Type A and R), which are generally regarded to be less delicate than the type B morphotype (Henderiks et al., 2012, Patil et al., 2014). Langer et al. (2009) however observed that morphotype did not influence the response that *E. huxleyi* had to changing seawater carbonate chemistry, rather any susceptibility to acidification was connected to genotype. In that study, Langer (2009) observed that two type A strains of *E. huxleyi* exhibited both the weakest and the strongest responses to high CO_2, while the intermediate responses were displayed by the type R and type B strains.

TEP are mainly carbohydrates and thus are relatively rich in carbon (Passow, 2002, Engel et al., 2004). It has been hypothesised therefore that TEP production is a process by which algal cells dispose of excess carbon whenever biomass production is affected by nutrient limitations (Engel et al., 2004). In fact, the relationship between relative TEP production and CO_2 uptake has been found to be highly significant, implying that there is a direct relationship between inorganic carbon acquisition and organic carbon exudation (Engel, 2002). During these experiments however, the concentration of TEP in the cells aerated with 1000 p.p.m. CO_2 was not statistically different from

those that were aerated with 400 p.p.m. CO_2. However, it could not be said that the cells aerated with 1000 p.p.m. CO_2 were growing in a high CO_2 environment. The growing cultures of *E. huxleyi* consumed CO_2 rapidly and therefore could not be maintained at equilibrium when cell numbers were high during stationary phase. As a result, the average measured concentration of CO_2 in both cultures was low. It is not surprising therefore that TEP concentrations were not statistically different from one another. While this finding sheds no light on the association between sinking velocity and TEP formation, it does further highlight the positive relationship between CO_2 concentrations and TEP.

The data here suggest that under increased concentrations of CO_2, up to 1000 p.p.m., the coccolithophore, *E. huxleyi* CS 812 will not change its sinking velocity. The enhancment of organic matter production, including the production of carbohydrates, seems to enable the cells to make up for any reduction in size or density that may have been caused by the loss of coccoliths or an increase in lipids. This ability to maintain sinking velocity while calcification decreases could potentially alter the rain ratio and act as a negative feedback mechanism to rising atmospheric CO_2 levels (Riebesell et al., 2000, Zondervan et al., 2001). In some regions of the ocean however, an increase in the vertical stratification of the water column will lead to a decrease in the mixing between the surface ocean and the deeper layers and this will cause a decrease in the supply of nutrients and an increase in the temperature and at the surface ocean (Bopp et al., 2001, De Bodt et al., 2010).

The variability of environmental factors, including nutrients, temperature and CO_2 could all influence the size, density and ultimately, the sinking velocity of *E. huxleyi* cells. For instance, Sciandra et al. (2003) observed that N limited *E. huxleyi* cells decreased their size of by ~13% with and an increase in CO_2 from 400 to 700 p.p.m. CO_2. While De Bodt et al. (2010) observed that

increasing the temperature by 5 ^{o}C, decreased calcification in *E. huxleyi* by a further 11% when grown at 750 p.p.m. CO_2 as compared to ambient CO_2 conditions. Furthermore, Feng et al. (2008) observed that cellular PIC content in *E. huxleyi* decreased by 66% when the irradiance, temperature and pCO_2 were increased to mimic greenhouse conditions (400 µmol m^{-1} s^{-1}, 24 ^{o}C and 750 p.p.m. CO_2). If cell size and density are affected as a result of these cellular changes, the sinking velocity of *E. huxleyi* could also be altered and therefore, these other environmental factors must be taken into account when making any conclusions about the sinking vulnerability of *E. huxleyi* in the future ocean.

Chapter 5.0: Impacts of N-limitation and High CO_2 on the Sinking Velocity of the Diatom *Chaetoceros didymus*

5.1 Introduction

Diatoms are a major component of the oceanic phytoplankton, accounting for 40% of the total primary production in the ocean (Smetacek, 2000, Sarthou et al., 2005). Diatom species cover a range of sizes, from 5 μm to 5 mm in diameter or length (Smetacek, 2000). The smaller diatoms, those ranging from 5 – 50 μm, have high rates of growth and accumulate biomass rapidly following the stabilisation and warming of nutrient-rich surface waters (Smetacek, 2000). When the nutrients run out, these cells tend to aggregate and sink quickly, fuelling carbon drawdown and the biological carbon pump, making them one of the main players in the biogeochemical cycling of carbon (Smetacek, 2000, Sarthou et al., 2005). Indeed, diatoms may be the predominant producers of phytoplankton aggregates, as they are capable of voluminous production of the TEP that drives the aggregation process (De La Rocha and Passow, 2007).

Aquatic primary productivity, especially in surface waters, is frequently limited by the availability of nutrients (Beardall et al., 2001). Intensified ocean stratification, caused by warming surface waters, could further decrease marine nutrient availability and uptake rates in phytoplankton in some regions of the ocean (Li et al., 2012). This is particularly true for N availability which is seen as a major limiting factor for algal growth in the oceans due to the fact that approximately 50% of the N mineralized in sediments is lost via denitrification (Caraco et al., 1990, Li et al., 2012) and nitrogen fixation by prokaryotes does not compensate for this denitrification (Sohm et al., 2011).

In marine phytoplankton, N-limitation has been found to affect photosynthesis by reducing the efficiency of energy collection due to loss of chlorophyll *a* and increases in non-photochemically active carotenoid pigments (Berges et al., 1996). N deficiencies have also been shown to decrease protein synthesis, in particular the synthesis of the proteins associated with PSI and PSII reaction

centres (Falkowski et al., 1989, Berges et al., 1996, Li et al., 2012). However Berges et al. (1996) observed that only PSII reactions centres were severely affected by N-starvation in diatoms and there were no apparent impacts on PSI. Furthermore, activity of Ribulose 1,5-bisphosphate carboxylase oxygenase (Rubisco), the enzyme responsible for CO_2 fixation in photosynthesis, is also markedly reduced under N-limited conditions, further impairing photosynthetic performance (Beardall et al., 1991, Plumley and Schmidt, 1989).

N deficiencies can also be associated with the storage of carbohydrates and lipids and an increased rate of TEP formation, factors which could potentially influence cell density and sinking capacity (Ganf et al., 1986, Parrish and Wangersky, 1990, Corzo et al., 2000). Several studies have also found that N deficiency is an important factor in the formation of resting spores in marine diatoms (Sugie et al., 2010). Diatom resting spores generally sink faster than vegetative cells (Davis et al., 1980, McQuoid and Hobson, 1996). This may be due to diatom resting spores often differing in appearance from vegetative cells, having thicker and heavier frustules, a rounder shape and less elaborate surficial patterns (McQuoid and Hobson, 1996). The spines found on some diatom spores may also become entangled, encouraging the formation of aggregates and marine snow (McQuoid and Hobson, 1996). Alldredge et al. (1995) observed that *Chaetoceros* resting spores can represent a significant proportion (up to 18%) of cells in a diatom aggregate. Furthermore, diatom resting spores can account for a large fraction (> 50%) of the opaline sediment component in coastal regions, partly due to their abundance but also due to their heavily silicified walls, which give them increased resistance to dissolution and grazing (McQuoid and Hobson, 1996, Abelmann et al., 2006).

As stated previously in this thesis, since the onset of the industrial revolution atmospheric CO_2 concentrations have risen from 280 p.p.m. to 400 p.p.m. and are predicted to rise as high as 1000

p.p.m. by the end of the century (Meehl et al., 2007). This elevation of atmospheric CO_2 will cause a measurable decrease in seawater pH and carbonate saturation (Riebesell et al., 2007), and the impacts of this on phytoplankton growth and photosynthesis will vary according to species. For instance, those species lacking carbon concentrating mechanisms (CCMs) which acquire CO_2 by diffusive uptake, may be potentially carbon-limited under present-day CO_2 levels and therefore it may be expected that these species might show enhanced growth rates as atmospheric CO_2 levels increase (Beardall et al., 2009b).

Diatoms do operate CCMs and many diatoms are at or close to CO_2 saturation at present day CO_2 levels, therefore an increase in CO_2 may confer no benefits in terms of growth (Riebesell, 2004, Hopkinson et al., 2011). The type of CCM can vary from species to species however, with *Thalassiosira weissflogii* possibly operating a single C_4-type CCM or arguably operating C3-C4 intermediate C fixation (Reinfelder et al., 2000, Roberts et al., 2007), while most other species examined rely on active transport of HCO_3^- into the chloroplast, an energy consuming process (Hopkinson et al., 2011). With an increase of CO_2, species will be able to down-regulate the use of their CCMs while maintaining C acquisition rates and in some instances therefore, cells will have more energy available for growth. For instance, Tortell et al. (2008) observed that elevated CO_2 led to a measurable increase in the abundance of the large chain-forming *Chaetoceros* spp. In contrast though, Burkhardt et al. (1999) reported that elevated CO_2 had very little effect on growth in four marine diatoms.

Increases in atmospheric CO_2 concentrations could also further alter the macromolecular composition and TEP concentrations of diatom cells. For instance, Chu et al. (1996) observed that cultures of *Nitzschia inconspicua* increased their concentrations of lipids and carbohydrates when aerated with 5% $C0_2$. The concentration of proteins however declined compared to that of the

control. In contrast, Chrismadha and Borowitzka (1994) observed that growth at 5% CO_2 resulted in a significant increase in cell protein per cell as well as increases in carbohydrates and lipids in *Phaeodactylum tricornutum*. Silica concentrations per cell have also been known to change with increasing CO_2. Milligan (2004) observed that the silica quota in *Thalassiosira weissflogii* was higher in cells grown at 100 p.p.m. CO_2 compared with cells grown at 750 p.p.m., the latter showing a significantly increased rate of silica dissolution. Furthermore, high CO_2 concentrations can be associated with increased concentrations of TEP, Engel (2002) having observed that the relationship between relative TEP production and CO_2 uptake in natural phytoplankton assemblages is highly significant. These factors could influence the density and aggregation rates of algal cells and this is turn, could influence their sinking velocity.

The aim of the experiments reported in this chapter was to determine the effects on sinking velocity of the marine diatom *C. didymus* when grown under N-limitation in conjunction with high CO_2. Changes in macromolecular composition, cell size and density and TEP concentrations were also examined in order to understand any sinking differences observed.

5.2 Methods

5.2.1 Batch Culture Experiments

Batch culture experiments were initially carried out for *C. didymus*, in order to determine the concentration of N required to limit growth rates by 50%. The batch cultures were established in 60 ml flasks (Nalgene Square Polycarbonate bottles) and were exposed to 5 different concentration of N, using $NaNO_3$ in F/2 medium as the N source.

The batch cultures were initially provided with 882.5 µmol l^{-1} $NaNO_3$ (N-replete). The $NaNO_3$ concentrations were reduced in the subsequent batch cultures to:

- 44.13 µmol l^{-1};
- 88.25 µmol l^{-1};
- 220.63 µmol l-1; and
- 441.25 µmol l^{-1}.

3 replicate cultures were grown at each of the N concentrations. The growth rate was determined daily by cell counts using a Neubauer haemocytometer (Section 2.6).

5.2.2 Semi-Continuous Culture Experiments

C. didymus was grown in three independent, semi-continuous cultures (1 litre) in 1-litre glass Schott bottle (to minimise headspace) using N-replete F/2 medium. Cultures were maintained at 18 ± 1 ^{o}C with photosynthetically active radiation (PAR; 400 – 700 nm) provided continuously at a photon flux of 80 µmol quanta m^{-2} s^{-1} from fluorescent tubes (Philips TLD 18W/865, cool daylight; Philips, Eindhoven, The Netherlands). Cultures were stirred constantly using a magnetic stirrer at 160 r.p.m.

and continuously aerated with either ambient air or ambient air mixed with 5% CO_2 as described in previously (Section 2.3).

Experimental cultures were grown to 0.2 – 0.5 X 10^6 cells ml $^{-1}$. Cells were then maintained in a semi-continuous state by diluting them to approximately 0.1 – 0.2 X 10^6 cells ml $^{-1}$ daily. The cultures were thus kept in exponential growth phase during this part of the experiment. In the first instance these cultures were maintained in N-replete conditions. After a minimum of three steady states in each flask, the replete medium was substituted by N-limited medium and a new semi-continuous steady state developed.

The N-limited medium had 88.25 µmol l^{-1} $NaNO_3$. This concentration was used because it was shown in the preliminary batch culture experiment to limit cell growth rate by approximately 50%.

N-limitation was established prior to any analysis using chlorophyll measurements and measurements of F_v/F_m. F_v/F_m measurements were performed using the PAM fluorometer (Section 2.12). Cultures with values of F_v/F_m below 0.40 were considered N-limited. Chlorophyll *a* and *c* concentrations were measured during the exponential growth phase (Section 2.7). To confirm N-limitation, NOx concentrations were then measured. Samples (10 – 15 ml) of filtered media (obtained using a 25 mm syringe filter unit fitted with 0.2 µm, hydrophilic, cellulose acetate filters, Advantec, Japan) were taken in 15 ml centrifuge tubes (BD Falcon, BD Biosciences, Bedford, USA), and frozen at -25 ^oC. The samples were then analysed in a NATA accredited analytical laboratory using standard methods and quality control procedures (AMHA-AWWA-WPCF, 1998).

The CO_2 concentration in cultures was also altered in combination with N. Initially the cells were grown under current day CO_2 levels (400 p.p.m.) by aerating the cells with ambient air passed

through a 0.2 μm PTFE membrane in-line air filter (Pall Corporation, Roseville, USA, ARCO 50 vent device) at a rate of 450 ml min^{-1}. The CO_2 concentration was then increased to 1000 p.p.m. by mixing 5% CO_2 with ambient air using 150 mm Two-Tube Gas Blenders (Series 150A, Advanced Specialty Gas Equipment, NJ, USA). The CO_2 concentration was monitored daily (Section 2.13).

The sinking velocity was measured according to the method of Walsby & Holland (2006) (Section 2.4). In order to have sufficiently high resolution, at least 1 million cells in a 1 ml sample were required for each run. The cells were therefore concentrated by filtering them onto a 3 μm membrane filter (Sartorius, Gottingen, Germany) and resuspending them in 1 ml of fresh F/2 medium.

In order to understand the role that cell size plays in sinking velocities, the volume (in μm^3) was calculated for individual cells as well as for the chains of cells according to Equation 5.1;

$$Volume = \pi r^2 h \quad \text{(Equation 5.1)}$$

Where r is cell radius (in μm) and h is cell height (in μm).

Using photographs the cell dimensions were measured (Section 2.5) and the volume calculated.

The density of the cells was also determined by pipetting 0.5 ml of concentrated cells onto the meniscus of a density gradient and allowing the band of cell to sink to their own density level as described in Section 2.5. Form resistance (Φ) was also calculated by substituting the sinking velocity (in metres s-1), the effective radius (r_e in metres: Equation 1.2) and density into the modified Stokes' equation (Equation 1.3).

The concentrations of cell protein, lipid and carbohydrate were examined at each harvest during semi-continuous exponential growth. Protein concentration was measured using a Bio-Rad DR Protein assay kit (Section 2.8). Lipids were extracted from the cells using a modified Bligh & Dyer (1959) technique and the concentration of lipids was determined gravimetrically (Section 2.9). The carbohydrates, β-1,3 glucan and cell wall polysaccharides, were extracted from the cells (Section 2.10) and the glucan extract and the cell wall hydrolysate were analysed separately using the phenol-sulphuric acid spectrophotometric method (Section 2.10). The photosynthetic parameters (α, I_k and $rETR_{max}$) were also measured using PAM fluorometer based RLCs (Section 2.12).

5.2.3 Additional Batch Culture Experiments - For TEP Analysis

Since the production of TEPs is associated mainly with the stationary and senescent stages of life (Corzo et al., 2000, Hong et al., 1997) a separate batch culture experiment was carried out on cells that were allowed to grow until stationary phase (5 – 7 days), starting with either N-replete or N-limited conditions in combination with 400 or 1000 p.p.m. CO_2.

The concentration of TEPs were measured (at stationary growth phases only) using the methods of Passow & Alldredge (1995) after 5 ml of culture was filtered at a low constant vacuum (at 100 mm Hg) onto 25-mm polycarbonate filters (Isopore membrane filters, 0.4 μm HTTP, Millipore, MA, USA) (Section 2.11).

The sinking velocity, cell volume, density and form resistance were also determined for the cells at stationary growth phase.

5.2.4 Statistical Analysis

Statistical significance between the four treatments was determined using a two – way analysis of variance followed by a post hoc Tukey test. Significance was set at $P < 0.05$. All statistical analyses were conducted using GraphPad Prism 5 (GraphPad Software Inc., La Jolla, California, USA).

5.3 Results

5.3.1 Initial Batch Culture Experiments to Determine the Limiting Concentration of N

The maximum growth rate of *C. didymus* increased as N concentrations increased (Figure 5.1). Growth rates were particularly decreased when N concentrations were reduced to one tenth or one twentieth of the replete concentration.

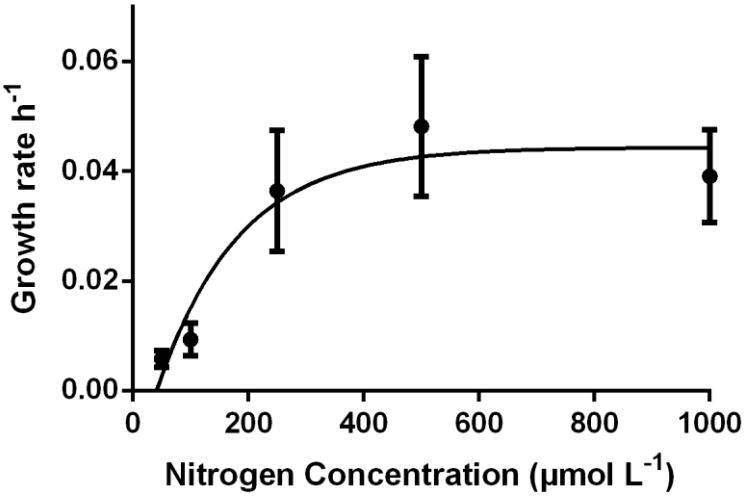

Figure 5.1. The specific growth rate of *C. didymus* as a function of N concentration. Data are the mean of three independent cultures and standard error presented as a double sided bar. Note. It is not clear whether the x-axis intercept represents a true nitrogen compensation concentration or if it is an artefact of fitting the curve.

5.3.2 Culture Conditions

Measurements of NO_X, pH, DIC, TA and pCO_2 are presented in Table 5.1. At exponential growth phase, the pCO_2 increased in those cultures that were aerated with 1000 p.p.m. CO_2 by approximately 66% compared to those aerated with 400 p.p.m. CO_2, maintaining the pCO_2 at approximately 1000 p.p.m. The pCO_2 values reflect the fact that under elevated CO_2 the pH decreased by an average of 0.37 units while the DIC and the TA increased by approximately 10%

and 4% respectively. At stationary growth phase the pH dropped by 0.43 units under high CO_2. The DIC and TA however decreased by an average of approximately 8% and 16% respectively. The pCO_2 increased by approximately 62% and was maintained at concentrations close to or above 1000p.p.m. The pCO_2 of those cultures aerated with 400 p.p.m. CO_2, were maintained at approximately 400 p.p.m. during both stationary and exponential growth phases.

Those cultures that were supplied with reduced amounts of $NaNO_3$ at inoculation had significantly reduced concentrations of NO_X, suggesting that these cells were growing in a N-limited environment (Table 5.1).

5.3.3 Semi-Continuous Culture Experiments and TEP Analysis

Nitrogen had a significant impact on growth rates. The growth rates of *C. didymus* were significantly reduced by ~65% under N-limitation at 400 p.p.m. CO_2 compared to the N-replete cultures grown at 400 p.p.m. or 1000 p.p.m. CO_2 (Figure 5.2). The N-limited culture grown at 1000 p.p.m. CO_2 however, did not show a statistically significant decrease in growth rate compared to the N-replete culture (Figure 5.2). Nitrogen limitation and high CO_2 did not have a significant interactive impact on growth. There was an interactive effect of Nitrogen and high CO_2 on chlorophyll concentrations however. The N-limited cultures at 1000 p.p.m. showed a significant decrease in chlorophyll *a* concentrations (~86%) compared to the N-replete culture at 400 p.p.m CO_2 ($p = 0.004$) (Figure 5.3). An average decrease of approximately 45% was also observed in chlorophyll *a* concentrations under N-limitation at 400 p.p.m. when compared to the two N-replete cultures, although this decrease was not statistically significant (Figure 5.3). The same significant interaction was also observed in regards to chlorophyll *c*, where the N-limited cultures at 1000 p.p.m. showed a significant decrease in chlorophyll *c* concentrations (~77%) compared to the N-replete culture at 400 p.p.m CO_2 ($p = 0.02$) (Figure 5.4). These decreases in chlorophyll *a* and *c* were paralleled by

decreases in F_v/F_m and α for the N-limited cells (Table 5.2). $rETR_{max}$ declined significantly under N-limitation while values for I_k generally increased with high CO_2 (Table 5.2).

Table 5.1. Mean measured concentrations of nitrogen (NO_X), dissolved inorganic carbon (DIC), pH, total alkalinity (TA) and pCO_2 in F/2 medium at each harvest of *C. didymus* cells during the exponential and stationary growth phase.[1]

	Nitrogen aim	pCO_2 aim (p.p.m.)	NO_X (mg l^{-1})	Error (±)	pH	Error (±)	DIC (mmol kg^{-1} SW)	Error (±)	TA (mmol kg^{-1} SW)	Error (±)	pCO_2 (p.p.m.)	Error (±)
Exponential growth phase	N-replete	1000	7.43	0.59	7.97	0.036	2746.2	55.23	3037.58	40	904.55	71.33
	N-limited	1000	0.007	0.003	7.86	0.037	2605	28.6	2761	30 ***SD***	1079.55	92.46
	N-replete	400	8.25	0.454	8.33	0.06	2523.7	139.12	2924.88	150.27	332.4	47.04
	N-limited	400	0.006	0.001	8.24	0.04	2257.2	82.29	2646.5	129.15	345.95	31.59
Stationary growth phase	N-replete	1000	NM		7.80	0.025	3037.4	121.31	3469.33	239.29	1423.6	107.68
	N-limited	1000	NM		7.86	0.029	2727.17	80.27	2917.67	99.69	1076	98.26
	N-replete	400	NM		8.35	0.043	3369.33	134.56	4230	169 ***SD***	416	71.13
	N-limited	400	NM		8.16	0.046	2898.33	255.8	3348		544	75.63

[1] Values are means and the error is the standard error unless stated otherwise. No error is given when only one measurement was made. NM means not measured.

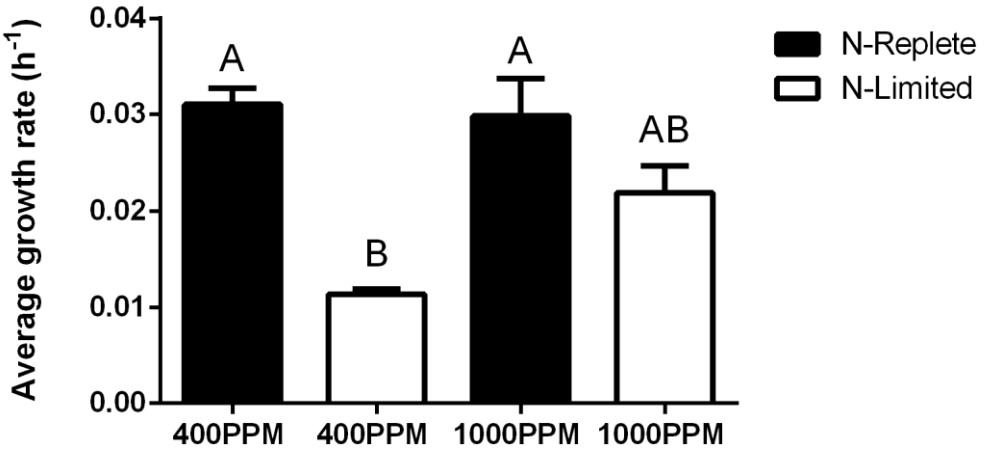

Figure 5.2. Growth rate (h^{-1}) of *C. didymus* during the exponential growth phase under replete or nitrogen limited conditions at approximately 400 p.p.m. and 1000 p.p.m. CO_2. Data are the mean of three independent cultures. Standard error is presented as a single sided bar. Standard error as a single sided bar. Different letters indicate statistically significant differences among the mean values ($p < 0.05$)

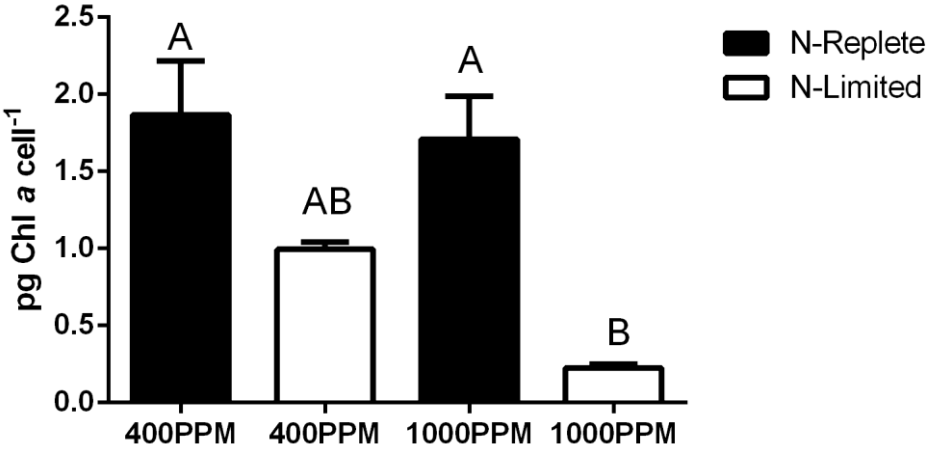

Figure 5.3. Chlorophyll *a* concentrations (pg Chl *a* $cell^{-1}$) in *C. didymus* in the exponential growth phase under replete and nitrogen limited conditions at 400 p.p.m. or 1000 p.p.m. CO_2. Data are the mean of three independent cultures and standard error is presented as a single sided bar. Different letters indicate statistically significant differences among the mean values ($p < 0.05$).

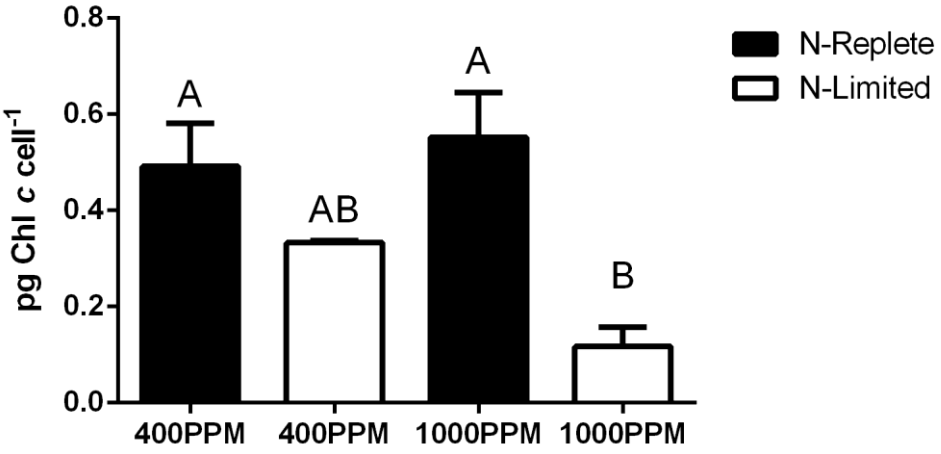

Figure 5.4. Chlorophyll *c* concentrations (pg cell^{-1}) in *C. didymus* in the exponential growth phase under replete and nitrogen limited conditions at 400 p.p.m. or 1000 p.p.m. CO_2. Data are the mean of three independent cultures and standard error is presented as a single sided bar. Different letters indicate statistically significant differences among the mean values ($p < 0.05$).

Table 5.2. Changes in the macromolecular composition, TEP concentrations and photosynthetic parameters in *C. didymus* under N-replete or N-limited conditions at 400 p.p.m. or 1000 p.p.m. CO_2.[2]

	400 p.p.m.				1000 p.p.m.			
	N-Replete		N-Limited		N-Replete		N-Limited	
	Mean	Error (±)	Mean	Error (±)	Mean	Error (±)	Mean	Error (±)
F_v/F_m	0.53	0.011	0.35	0.012	0.56	0.01	0.43	0.004
α (µmol electrons / µmol photons)	0.22	0.009	0.16	0.006	0.23	0.007	0.186	0.003
$rETR_{max}$ (µmol electrons $m^{-1}s^{-1}$)	25.7	2.8	12.88	1.64	38.15	2.18	25.3	0.795
I_k (µmmol photons $m^{-1}s^{-1}$)	106.8	7.44	80.52	10.10	166.25	13.37	134.3	2.92
Protein (pg $cell^{-1}$)	0.328	0.046	0.273	0.017	0.456	0.014	0.174	0.014
Lipids (pg $cell^{-1}$)	301.1	9.815	469	104.6	1937.8	21.57	2155.5	607.2
β-1,3 glucan (pg $cell^{-1}$)	6.876	1.408	6.083	1.656	35.99	4.282	44.354	4.134
Cell wall polysaccharides (pg $cell^{-1}$)	5.076	0.636	6.557	0.848	48.726	6.278	57.727	8.555
TEP (fg $cell^{-1}$) Stationary phase	0.00056	0.00011	0.00058	0.00025	0.00129	0.00028	0.00295	0.00063

[2]Photosynthetic parameters, protein, lipids, and carbohydrates were measured only during the exponential growth phase. TEPs were measured during the stationary growth phases. The error is the standard error.

The results from the two-way analysis of variance suggest that during the exponential growth phase, nitrogen limitation in conjunction with high CO_2 did have an interactive impact on the sinking rate ($p < 0.001$). The N-limited *C. didymus* cells grown at 400 p.p.m. sank approximately 4.4 μm s^{-1} (50%) faster than the N-replete cells grown at 400 p.p.m. (Figure 5.5). While the N-limited cells grown at 1000 p.p.m. sank approximately 5.9 μm s^{-1} (49%) faster than N-replete cells grown at 1000 p.p.m. (Figure 5.5). Overall, those cells grown at 1000 p.p.m. in N-limited conditions sank with the greatest velocity and the cells grown at 400 p.p.m. in the N-replete conditions sank the slowest.

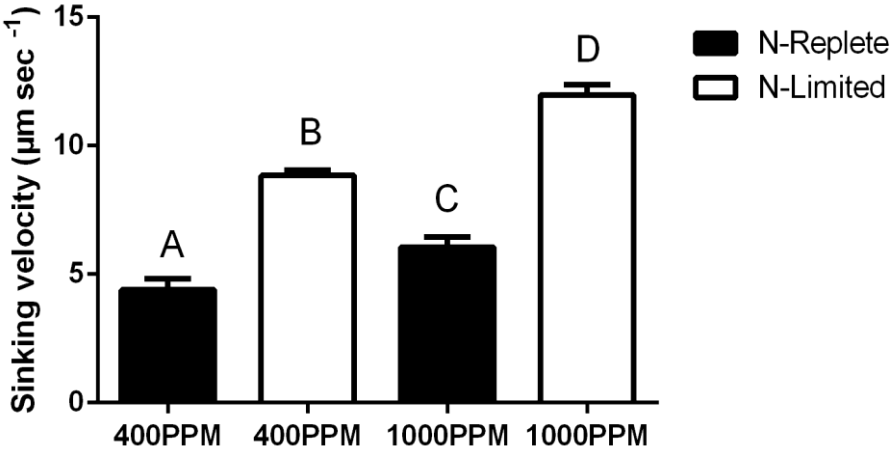

Figure 5.5. The sinking velocity (μm sec^{-1}) of *C. didymus* during the exponential growth phase under replete or nitrogen limited conditions at 400 p.p.m. or 1000 p.p.m. CO_2. Data are a mean of three independent cultures. Standard error is shown as a single sided bar. Different letters indicate statistically significant differences among the mean values ($p < 0.05$).

Differences in macromolecular composition between the cells grown at 400 p.p.m. and 1000 p.p.m. were evident during the exponential stage of growth. Lipid concentrations were 5-fold higher in the cells grow at 1000 p.p.m. than in those grown at 400 p.p.m. (Table 5.2).

An approximate 6-fold increase in β-1,3 glucan levels and an 8-fold increase in cell wall polysaccharides was observed in the cells grown at 1000 p.p.m. over those grown at 400 p.p.m. (Table 5.2).

Under N-replete conditions, protein concentration increased significantly with increasing CO_2 but the protein concentration declined significantly under N-limitation and high CO_2 (Table 5.2). There was no significant difference in protein concentration between the two cultures grown at 400 p.p.m., although the N-limited culture exhibited a decreasing trend.

In most respects, the volume of individual cells did not significantly vary among the groups. However, the N-limited cells grown at 1000 p.p.m. were on average, significantly smaller (~27%) than the cells grown at 400 p.p.m. CO_2 under N-limitation ($p = 0.02$) (Figure 5.6). When considering volume taking into account chains as well as individual cells (taken as mean volume of chains and single cells), there were no significant differences in volume between any of the groups (Figure 5.7). This increase in volume in the 1000 p.p.m., N-limited cells when chains are considered, can be explained by the fact that these cells formed longer chains more readily, appearing as single cells only 64% of the time, whereas the N-replete cells grown at 400 p.p.m. existed as single cells approximately 77% of the time (Figure 5.8).

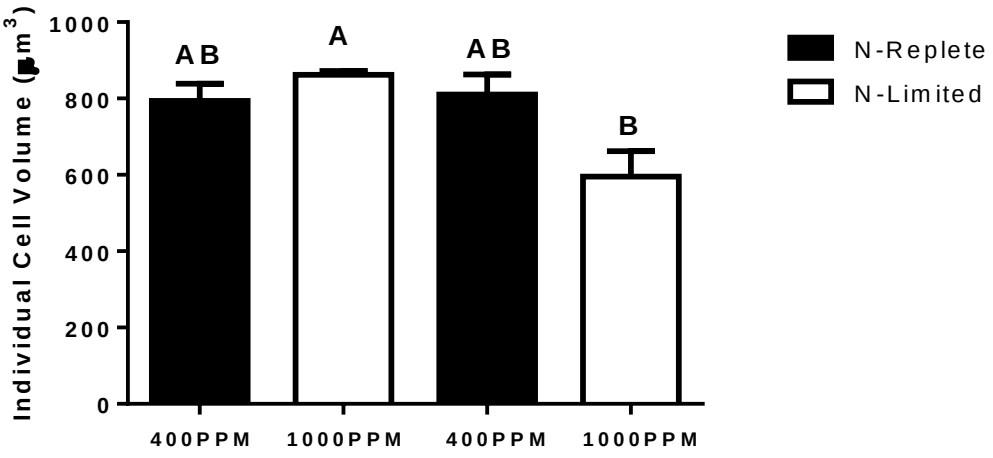

Figure 5.6. The volume (μm^3) of individual *C. didymus* cells during the exponential growth phase under replete or nitrogen limited conditions at 400 p.p.m. or 1000 p.p.m. CO_2. Data are a mean of three independent cultures. Standard error is shown as a single sided bar. Different letters indicate statistically significant differences among the mean values ($p < 0.05$).

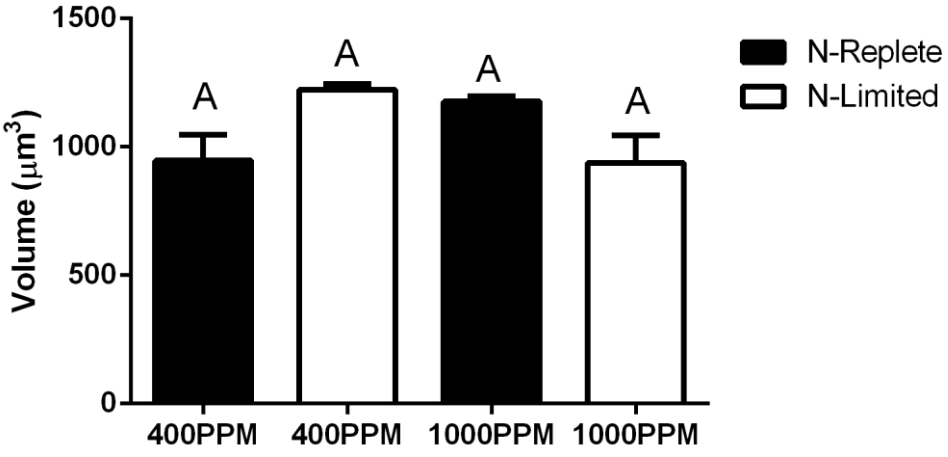

Figure 5.7. The volume (μm^3) of *C. didymus* (taken as the mean volume of individual cells and chains) during the exponential growth phase under replete or nitrogen limited conditions at 400 p.p.m. or 1000 p.p.m. CO_2. Data are a mean of three independent cultures. Standard error is shown as a single sided bar. The same letters indicate no statistically significant differences among the mean values ($p > 0.05$).

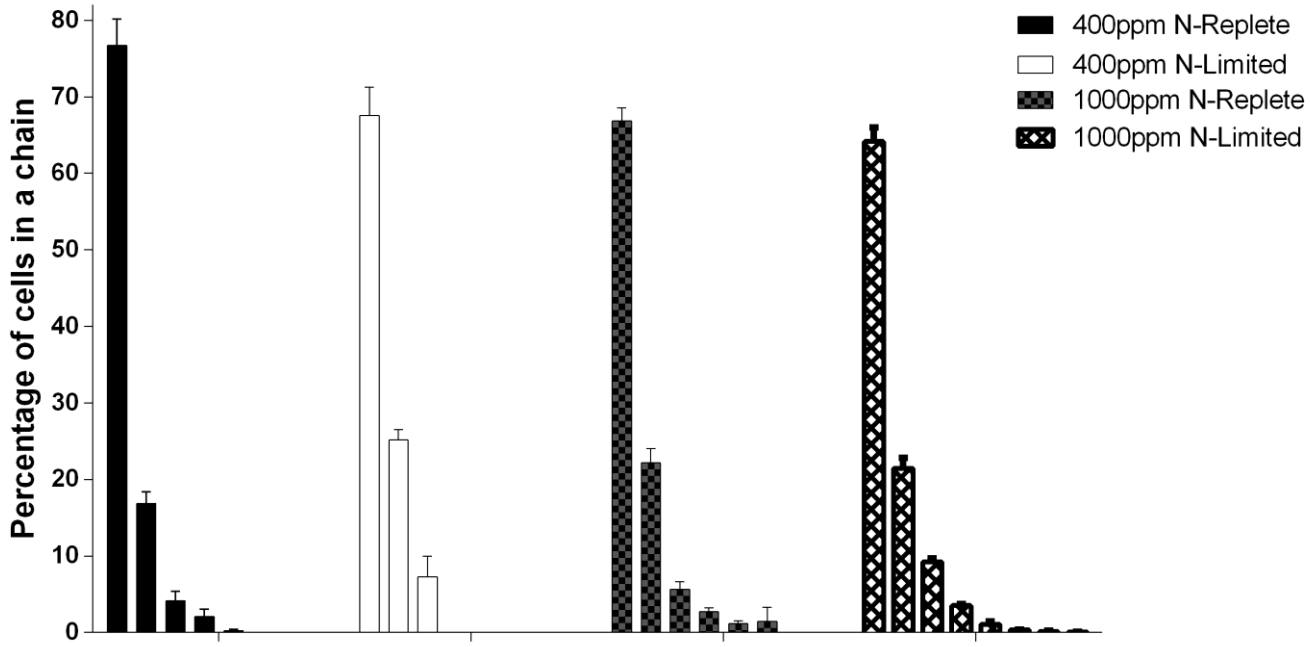

Figure 5.8. The proportion of *C. didymus* cells in a chain. The bars on the far left of each group indicate the percentage of cells that appear as single cells. The second bar of each group indicates the proportion of doubles and so on.

The combination of nitrogen limitation and high CO_2 did not appear to have an interactive impact on density. However, the N-limited cells grown at 1000 p.p.m. had a statistically significantly greater density (2%) than the N-replete cells grown at 1000 p.p.m ($p = 0.03$). The densities of these two groups were not significantly different from those of the cells grown at 400 p.p.m. (Figure 5.9).

At exponential growth phase, N-limitation significantly impact form resistance. The cells grown under N-replete conditions at 400 p.p.m. had a significantly smaller form resistance than those grown under N-limitation at both CO_2 concentrations (Figure 5.10). However, values for the N-replete cells grown at 1000 p.p.m. were not significantly different from those of the N-limited cells grown at either CO_2 concentration. A quadratic relationship did however, appear to exist between the sinking velocity and the form resistance because the sinking velocity increased with the level of form resistance (Figure 5.11).

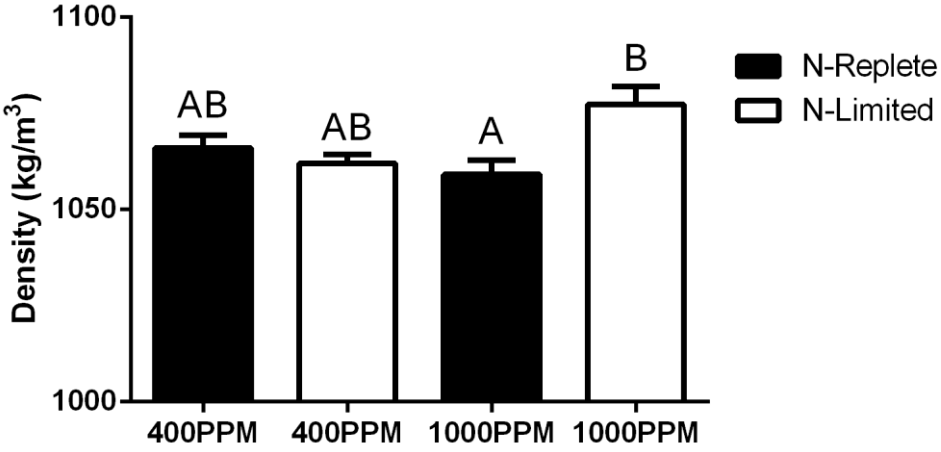

Figure 5.9. The density (kg/m^3) of *C. didymus* during the exponential growth phase under replete or nitrogen limited conditions at 400 p.p.m. or 1000 p.p.m. CO_2. Data are a mean of three independent cultures. Standard error is shown as a single sided bar. Different letters indicate statistically significant differences among the mean values ($p < 0.05$).

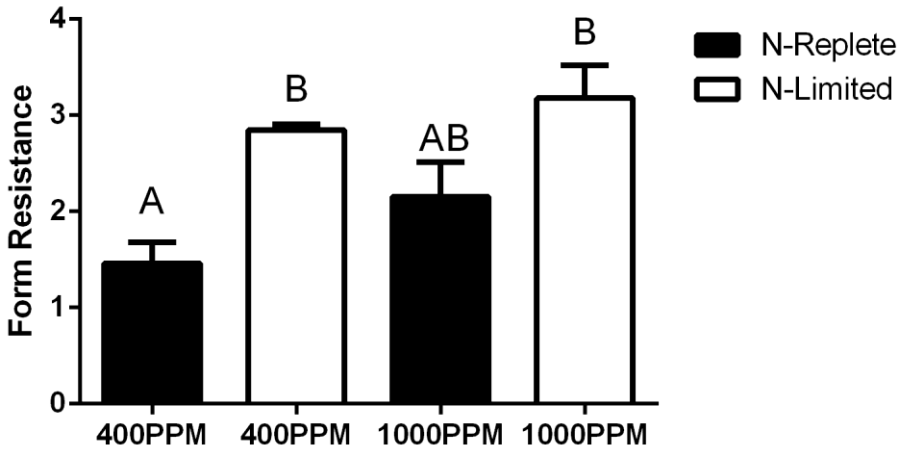

Figure 5.10. The form resistance of *C. didymus* during the exponential growth phase under replete or nitrogen limited conditions at 400 p.p.m. or 1000 p.p.m. CO_2. Data are a mean of three independent cultures. Standard error is shown as a single sided bar. Different letters indicate statistically significant differences among the mean values ($p < 0.05$).

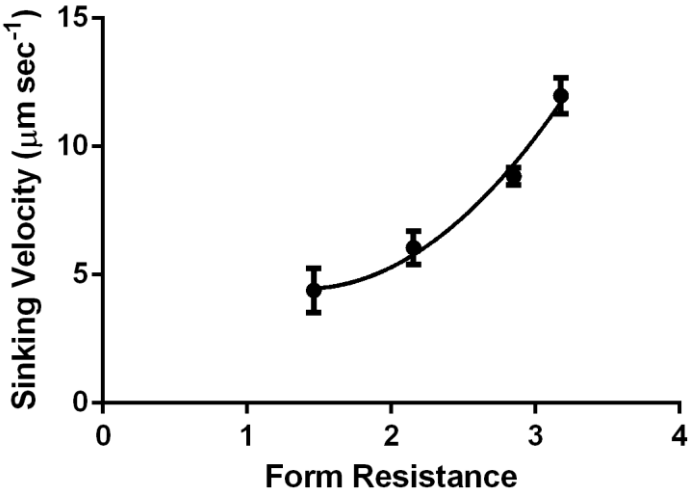

Figure 5.11. Sinking velocity as a function of form resistance for *C. didymus*. y =2.30x^2 – 6.46x + 901, r^2 = 0.99.

The results from the two-way analysis of variance suggest that during stationary growth phase, N-limitation significantly influenced the sinking velocity (p = 0.001) but there was no interactive affects. The N-limited *C. didymus* cells grown at 400 p.p.m. sank approximately 6 μm s^{-1} (45%) faster than the N-replete cells grown at 400 p.p.m. or 1000 p.p.m. (Figure 5.12). The N-limited cells grown at 1000 p.p.m. also sank faster than N-replete cells grown at 1000 p.p.m., although this did not appear to be significant (Figure 5.12). There was no significant difference in sinking velocity between the N-limited cultures grown at the two CO_2 concentrations

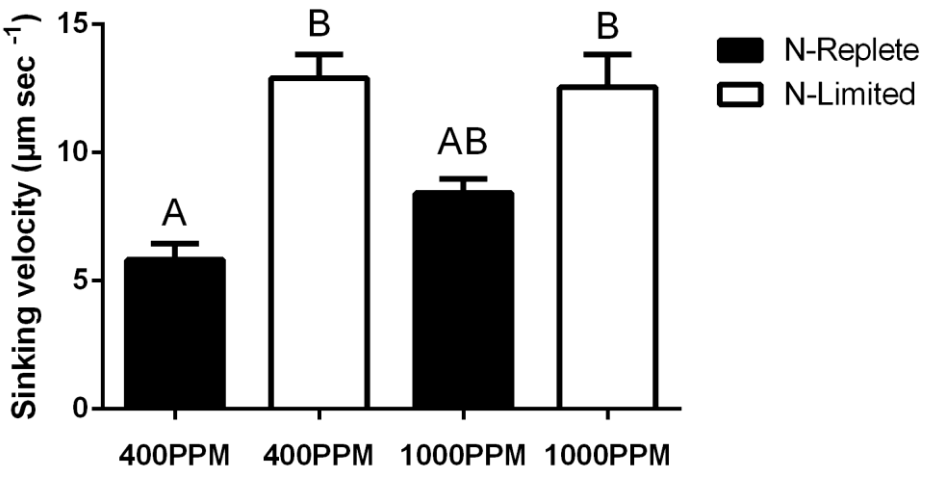

Figure 5.12. The sinking velocity (µm sec^{-1}) of *C. didymus* under replete or nitrogen limited conditions at 400 p.p.m. or 1000 p.p.m. CO_2 during stationary phase. Data are the mean of a minimum of three independent cultures. Standard error is shown as a single sided bar. Different letters indicate significant differences among mean values ($P < 0.05$).

The N-limited cells grown at 400 p.p.m. were on average significantly larger (~39%) than the cells in the N-replete cultures grown at both of the CO_2 concentrations when volume is taken as the mean volume of individual cells and chains (Figure 5.13). These cells also appeared to be larger (~30%) than the N-limited cells grown at 1000 p.p.m., however this difference was not statistically significant (Figure 5.13). The results from the two-way analysis of variance also suggest that the nitrogen and CO_2 did not have an interactive effect on the volume ($p = 0.1$). There were also no significant differences in individual cell volume between any of the groups (Figure 5.14). The increase in mean volume seen when individual cells plus chains are considered in the 400 p.p.m., N-limited cells, despite the lack of increase in individual cell volume, can therefore be explained by the fact that these cells formed longer chains most readily. They appeared as single cells 68.5% of the time, whereas the N-replete cells grown at 400 p.p.m. existed as single cells approximately 90.2% of the time (Figure 5.15).

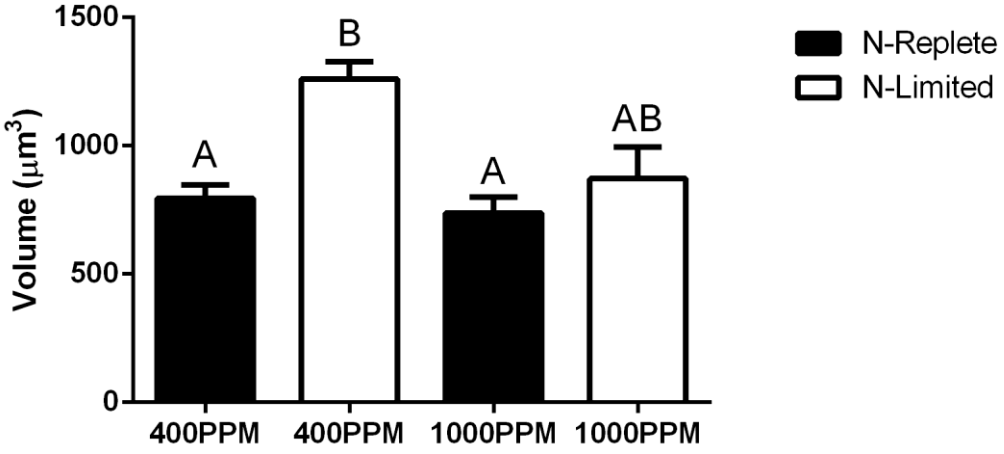

Figure 5.13. The volume (μm^3) of *C. didymus* (taken as the mean volume of individual cells and chains) during stationary growth phase under replete or nitrogen limited conditions at 400 p.p.m. or 1000 p.p.m. CO_2. Data are a mean of three independent cultures. Standard error is shown as a single sided bar. The same letters indicate no statistically significant differences among the mean values ($p > 0.05$).

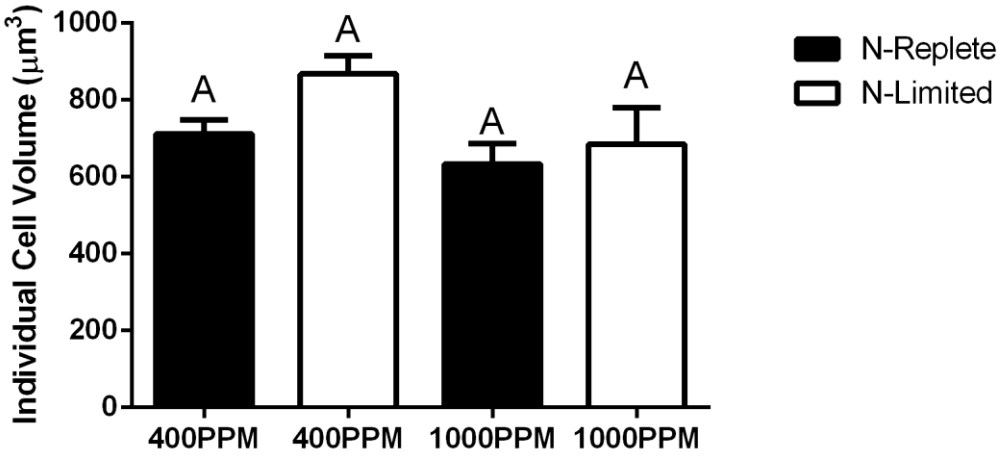

Figure 5.14. The volume (μm^3) of individual *C. didymus* cells during stationary growth phase under replete or nitrogen limited conditions at 400 p.p.m. or 1000 p.p.m. CO_2. Data are a mean of three independent cultures. Standard error is shown as a single sided bar. The same letters indicate no statistically significant differences among the mean values ($p > 0.05$).

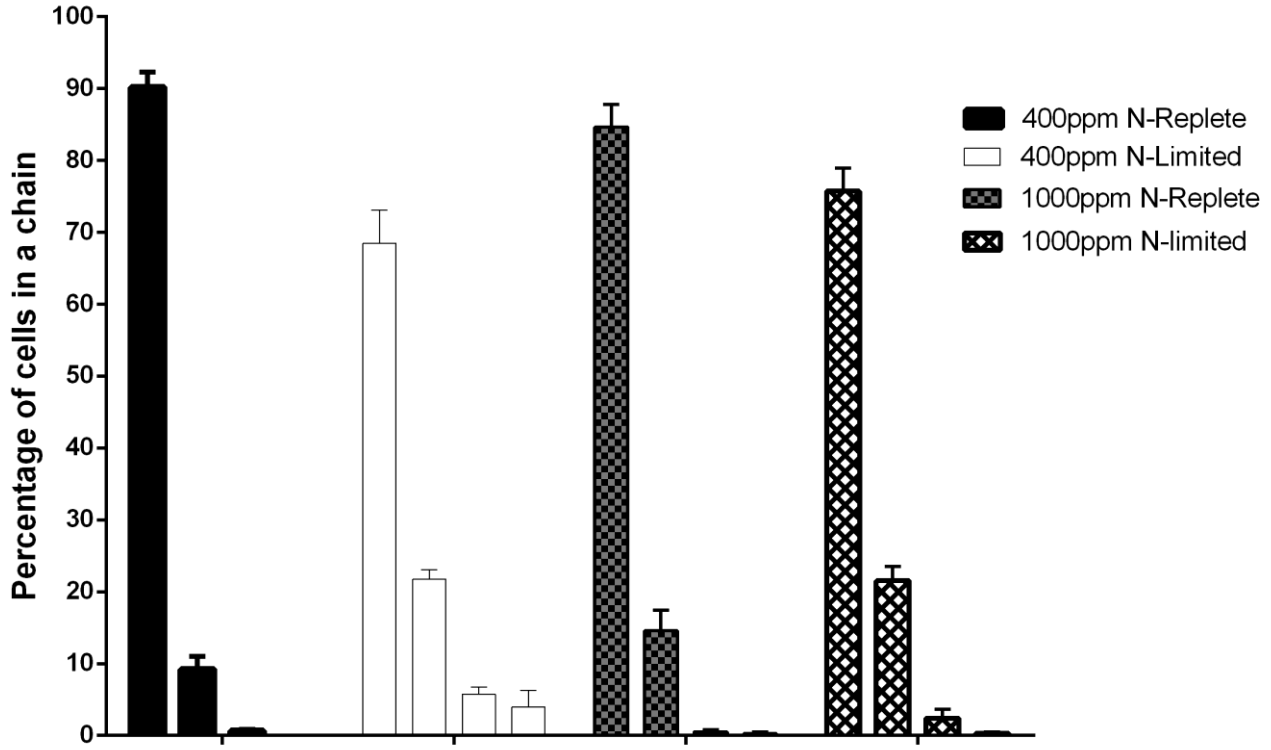

Figure 5.15. The proportion of *C. didymus* cells in a chain at stationary phase. The bars on the far left indicate the percentage of cells that appear as single cells. The second bar indicates the proportion of doubles and so on.

The results from the two-way analysis of variance suggested that the nitrogen and CO_2 did have an interactive affect on density ($p = 0.003$). The N-limited cells grown at 1000 p.p.m. had a statistically significantly greater density than those grown under any other of the conditions (Figure 5.16). The lowest density was seen in the N-replete cells under both CO_2 conditions, which were on average 2.3% less dense the N-limited cells grown at 1000 p.p.m. (Figure 5.16). The N-replete cells grown at 1000 p.p.m. also had a significantly larger form resistance than the other groups (~54%), which were not significantly different from one another (Figure 5.17).

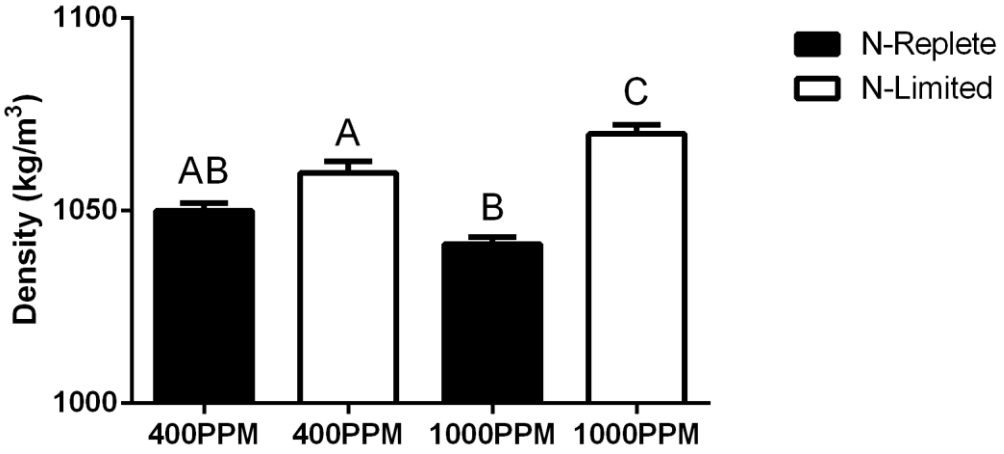

Figure 5.16. The density (kg/m^3) of *C. didymus* during stationary growth phase under replete or nitrogen limited conditions at 400 p.p.m. or 1000 p.p.m. CO_2. Data are a mean of three independent cultures. Standard error is shown as a single sided bar. Different letters indicate statistically significant differences among the mean values ($p < 0.05$).

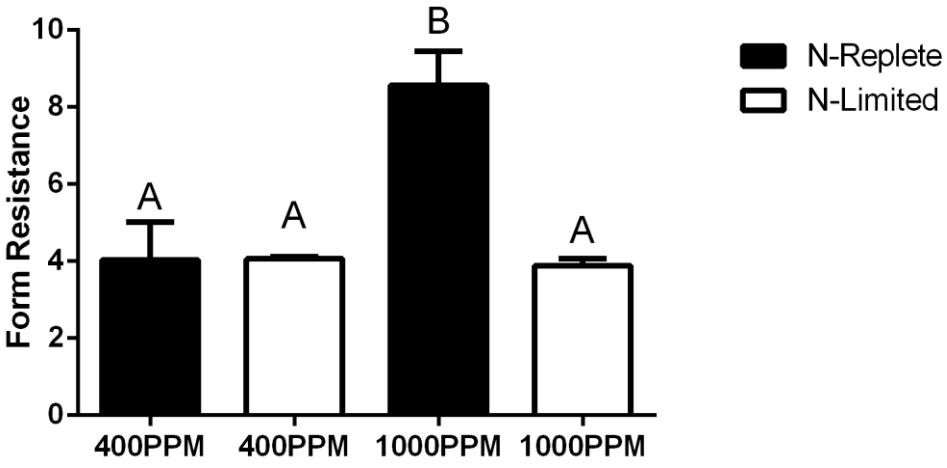

Figure 5.17. The form resistance of *C. didymus* during stationary growth phase under replete or nitrogen limited conditions at 400 p.p.m. or 1000 p.p.m. CO_2. Data are a mean of three independent cultures. Standard error is shown as a single sided bar. Different letters indicate statistically significant differences among the mean values ($p < 0.05$).

5.4 Discussion

The nutrient status of cells influences their capacity for photochemical work (Beardall et al., 2001). When *C. didymus* was grown in an N-limited environment, F_v/F_m, growth rates and chlorophyll per cell all declined, and such changes in cell parameters are generally characteristic of N-limitation in microalgae (Beardall et al., 2001). An increase in the partial pressure of CO_2 conferred no benefits in terms of growth or photosynthetic 'health' however, as there was no significant change in F_v/F_m or the growth rate when cells were grown in a high CO_2 environment. This suggests that *C. didymus* operates a CCM and that the cells were growing at their maximum rate in the lower CO_2 environment. The small recovery in growth and F_v/F_m in N-limited cells when exposed to high CO_2 may be explained in terms of a small down-regulation of CCM activity and CCM-related proteins as a result of a freeing-up of energy and materials for growth and photosynthetic work (Tortell et al., 2000, Wu et al., 2010). The concurrent significant reduction in cellular protein concentrations could suggest that this is the case (Ramanan et al., 2012).

In exponential growth phase, the sinking velocity was seen to increase when the cells were exposed to N-limitation. It has previously been observed that vigorously growing cells will maintain themselves close to neutral buoyancy but when under N depletion, the sinking velocity can dramatically increase (Smetacek, 1985). The results seen here therefore are not surprising as they have a precedent in the literature. The question remains however, why would this occur? Furthermore, why was the sinking velocity further enhanced under high CO_2?

From Stokes' Law we know that cell density and cell size are the two parameters that determine sinking rate. The cells grown in the high CO_2 environment produced a significantly higher concentration of lipids than air-grown cells, and produced still more when the high CO_2 treatment

was combined with N-limitation. Under high CO_2 conditions, carbon incorporation is favoured but because of the nitrogen deficiency, the carbon skeletons are not incorporated into proteins for cell growth, rather enhanced lipid synthesis acts as a carbon sink, as described by Gordillo et al. (1998) for *Dunaliella viridis*. As lipids are less dense than water, an accumulation of lipids could reduce the density of the N-limited cells, causing them to sink at a slower rate (Fernández et al., 1994). There was, however, no change in the cellular density detected from that of the two 400 p.p.m. cultures, therefore lipid accumulation, in accordance with the findings of Smayda (1970), would appear to be an unimportant factor in determining the sinking rate.

There was a significant increase in the concentration of β-1,3 glucan carbohydrates and cell wall polysaccharides when the cells were grown in the high CO_2 environment. This could be because the cells channelled the excess carbon into carbohydrate production, most likely because carbon fixation rates exceeded the intake of essential nutrients required for growth (Hessen and Anderson, 2008). It is possible therefore, that the overall cellular density of cells did not change because the increase in carbohydrates cancelled out any decrease in density caused by the accumulation of lipid (Anderson et al., 1985). Whether or not this is the case, the fact that there was no change seen in the overall cellular density indicates that these alterations in macromolecular composition were playing no significant role in changing the sinking capacity of the cells.

Diatom spores are commonly found in nutrient deficient waters and many authors have found nitrogen depletion to be the most important variable causing sporulation in marine diatoms (McQuoid and Hobson, 1996, Peters and Thomas, 1996). Despite the smaller cell volume of diatom spores, they have thicker and heavier frustules which increase cell density and allow them to sink at a faster rate (Sugie and Kuma, 2008). This mechanism allows cells to survive long adverse growth conditions by reducing cellular metabolism to negligible rates (Peters and Thomas, 1996). The

individual cells grown at 1000 p.p.m. under N-limitation were on average smaller than the individual cells found in the other groups. This reduction in cell volume may be due an increasing presence of spores and this could be another explanation for the increased sinking velocities seen in this group. However, spores were not identified during these experiments and therefore spore concentrations were not measured so it is difficult confirm that spore formation was the cause of the increased sinking velocity. Furthermore, there were no significant differences seen in cell densities among the groups so it is difficult to conclude that the variation in sinking velocity was due to increased spore formation.

During the exponential growth phase, when individual cells and chains are considered, there were also no significant differences seen in cell volume. The changes in sinking velocity therefore, cannot be explained by the given results for cell volume. It is possible however that cell volume was underestimated due to the presence of siliceous spines which extend from each corner of the cell and further increase the effective cell size (Riebesell, 1991). Although silicification was not measured during these experiments, it generally increases as the growth rate is decreased by environmental conditions (Raven and Waite, 2004). Claquin et al. (2002) observed that a decrease in growth rate associated with N-limitation was linked with an elongation of the G2+M phase during the cell life cycle, which allowed for an increase in cell silicification. If increased silicification did occur due to N-limitation, then the spines that protrude from each cell may have been longer as spine growth appears to be as a result of the silicified wall growing forward (Pickett-Heaps et al., 1994). Furthermore, those cells that formed chains more readily would have had more spines present, effectively increasing the cell size further and, depending on the cell configuration in the diatom chain, the effective size may have been much larger than the sum of the cell volumes (Riebesell, 1991). Correct estimates for the effective chain size are extremely difficult to obtain, even if cell size and chain length are carefully measured (Riebesell, 1991). Therefore, cell volume

may have actually been much larger and could have accounted for the increase in sinking velocity seen among the N-limited cells.

Increasing the length of spines or the length of chains generally results in a greater surface area to volume ratio and in the species *Skeletonema costatum*, this has been associated with decreased sinking velocities due to increased form resistance and increasing viscous drag (Smayda and Boleyn, 1966a, Takabayashi et al., 2006). It has also been observed that the sinking velocity of phytoplankton cells (including diatoms) is decreased the further their shape departs from the spherical, including through the production of silicaceous setae or chitinous spines, and it is thought that this allow the cells to remain in euphotic zone when nutrient concentrations are high due to upwelling (Smayda and Boleyn, 1966a, Smayda, 1970, Takabayashi et al., 2006). Then, as nutrients are depleted, the populations shift towards shorter or solitary cells to allow sinking to the nutrient rich ocean depths. The results here however, show that more solitary cells existed among those cells that were grown in the N-replete conditions at 400 p.p.m., which also sank with the slowest velocity. Those cells that sank with the greatest velocity, formed chains more frequently, and were grown under the N-limited and high CO_2 conditions. This may suggest that for *C. didymus*, longer chains assist in nutrient acquisition and also enhance the cells sinking velocity.

Smayda and Boleyn (1966b) did observe this same relationship for the diatoms *Chaetoceros lauderi* and *Bacteriastrum hyalinum,* where an increase in the number of cells per chain was accompanied by an increase in the sinking velocity. They suggested that this may have been due to a decrease in surface area to volume ratio and also due to physiological reasons. Physiologically stressed cells tend to sink faster as they no longer maintain the low density of their protoplasts (Raven and Waite, 2004). For instance, diatoms grown under N-limitation have been found to replace quaternary ammonium compounds with dimethylsulfoniopropionate, a denser compound, which

serves as an osmolyte and an anantioxidant under light or nutrient stress and assists in sinking to nutrient rich waters (Sunda et al., 2002, Raven and Waite, 2004). The N-limited cells were stressed during these experiments, as reflected by the reduced growth rates, chlorophyll concentrations and values for F_v/F_m, but the density of cells did not change significantly. It is difficult to conclude therefore that the changes in sinking velocities were due to physiological changes.

It is more likely that the changes seen in sinking velocity were due to changes in cell physical size, either through increasing chain or spine length. An increase in chain or spine length can increase the sinking velocity of cells if the extra ornamentation increases the density to a point where it exceeds any corresponding increase in viscous drag (Anderson et al., 1985). Furthermore, when two cells are joined to form a chain, the surface area where they touch is no longer available to viscous drag by the suspending medium and the result can be such that a chain will sink faster than an individual cell (Booker and Walsby, 1979).

Increasing chain and spine length could also assist cells to acquire nutrients. In between each cell in a *C. didymus* chain, large gaps are present. It has been observed that chains with large gaps can achieve a significantly greater nutrient supply than compact chains and solitary cells because the gaps work to increase cell surface area to volume ratio, improving the diffusive transport of nutrients to each cell (Pahlow et al., 1998). Musielak et al. (2009) also observed that diatom chains allow the cells to maintain larger effective size and encounter a greater number of resources. As a result of this, the nutrient concentration gradient around each cell increases allowing for greater nutrient uptake. Furthermore, small-scale turbulence, which disrupts the boundary layer surrounding each cell, can increase the advective transport of nutrients to cells if their size approach the Kolmogorov scale (the smallest scales of turbulence), the critical cell size for a 50% increase in the flux being in the range of 63 – 100 μm (Karp-Boss et al., 1996). This is because larger

cells are expected to experience enhanced relative motion (Karp-Boss et al., 1996). Increased spine length may also assist in nutrient acquisition through advection as the various projections are thought to ensure the twisting and rotation of the cells as they are dragged along by water movements. It is thought that this would enhance the exchange of water at the cell surface and allow for the capture of rare nutrients (van den Hoek at al., 1995).

During this study however, there was positive relationship seen between form resistance and the sinking velocity. As the sinking velocity increased, so did the form resistance. This is counter-intuitive as those cells that sink at the fastest rate should have had the lowest resistance to sinking. The form resistance is a function of both cell volume and cell density. If the cell size was underestimated by failing to measure spine length, then the form resistance would have been over-estimated. If higher cell volumes are used to calculate the form resistance in conjunction with the determined cell densities, the form resistance declines. Booker and Walsby (1979) observed that for the chain forming blue-green alga *Anabaena flos-aquae,* the surface area to mass ratio continued to decrease as the chain length increased, while at the same time, the form resistance also approached a minimum value. Although an increase in the length to width ratio has been observed to result in increased levels of form resistance (Davey and Walsby, 1985), colony elongation will ultimately result in increased sinking rates rather than aiding flotation (Bentley, 2006).

While spine length and the rate of silicification was not measured during this study, the rate of chain formation was and it is likely that the increase in mean sinking velocity seen among the N-limited cells grown under high CO_2 was influenced by the longer chains. While *C. didymus* displayed an increase in chain formation under high CO_2, Hoogstraten et al. (2012) observed that at CO_2 concentrations of 598 p.p.m., the diatom *Proboscia alata* was damaged and failed to form chains. It

was suggested that the decrease in pH, resulting from elevated CO_2, damaged the silica cell wall. *Proboscia alata* cell walls are thin and weakly siliceous however and this may be the reason why deterioration was seen under those growth conditions (Al-Kandari et al., 2009). On the other hand, Barcelos e Ramos et al. (2014) observed that under 3400 µatm CO_2, the diatom *Asterionellopis glacialis* increased the number of chains with 7 to 18 cells and reduced the number of chains comprised of 1 to 6 cells. The authors suggested that the creation of longer, spiralled chains could be a strategy to increase the pH in the centre of the colonies. This would only be the case while in the light however. It could also be possible that *C. didymus* implements the same strategy and creates a microclimate in the spaces between the cells, altering the pH to preferable conditions while in the light.

In stationary phase the two N-limited cultures again displayed the greatest sinking velocity while the slowest sinking velocity was also seen in the cells that were grown at 400 p.p.m. in N-replete conditions. However, unlike in exponential growth, it seems that in stationary phase, it is clearer as to why the differences in sinking rates were observed.

N-limited cultures grown at 400 p.p.m. CO_2 had significantly increased cell volumes. When chain formation was taken into account, these cells/cell chains were significantly larger than in the N-replete cultures. There was, however, no difference seen in volume when only individual cells were considered. The increase in cell volume therefore, must be due to increased rates of chain formation. This is confirmed by the observation that there were a lower percentage of solitary cells in this culture. It has generally been observed however that there is a decrease in chain formation and a movement towards solitary cells as cultures approach senescence (Smayda and Boleyn, 1965, Smayda and Boleyn, 1966a, Waite et al., 1992). During this study, most of the cultures also displayed a general decrease in chain formation at stationary growth phase. The N-limited cultures

grown at 400 p.p.m. CO_2 however, maintained their relatively low percentage of solitary cells across exponential and into stationary growth. This further suggests that for *C. didymus*, chain formation is an adaptation to allow the cells to acquire nutrients from the surrounding medium and to accelerate the sinking to nutrient rich waters.

Despite their equally fast sinking velocity, the N-limited cells grown at 1000 p.p.m. CO_2 failed to maintain their relatively low percentage of solitary cells across the different growth phases. This is perhaps due to the cells being suspended in a lower pH environment for a prolonged length of time and the dissolution of the silica spines that link the cells (Hoogstraten et al., 2012). These cells did however display a significant increase in cell density, which appeared to be influencing the rate of sinking. This could suggest that the cells implemented some physiological changes under the high CO_2 and N-limited conditions. For instance, the cells may have continued to accumulate β-1,3 glucan which is a common reserve polysaccharide in diatoms (Myklestad, 1974). This was the case for the diatom *Skeletonema costatum* where the content of β-1,3 glucan at stationary phase accounted for 81% of the organic dry matter (Myklestad, 1974). Buoyancy control could also be in part be due to the exchange of heavier ions for lighter ions in the vacuole (Sarthou et al., 2005). For example, Anderson and Sweeney (1978) observed that *Ditylum brightwelli* regulated its density by active ion selectivity accompanied by trans-vacuolar water movement. It was observed that ion changes during the light period increased cell density by 3.4 mg ml^{-1}.

The sinking velocity of diatoms embedded in marine snow (>500 μm) is generally faster than that of individually sinking cells and the formation of marine snow is generally enhanced by the presence of TEP which are sticky and aggregate particles such as bacteria, phytoplankton, molts, mineral clays and detritus (Alldredge et al., 1993, Engel, 2000, Azetsu-Scott and Passow, 2004). The concentration of TEP increased significantly in this study when the cells were bubbled with 1000

p.p.m. CO_2 and increased by 5 times when the high CO_2 was combined with N-limitation. The N-limitation alone did not seem to have any influence over TEP concentration. Engel (2002) observed that under conditions of nutrient shortage, TEP production increased with pCO_2. This was most likely due to TEP production being linked to cellular carbon overflow whenever nutrient acquisition limited biomass production but not photosynthesis (Engel, 2002). Likewise, the high CO_2 cultures may have been forced to channel the excess carbon into TEP production because the lack of N inhibited cell growth. At stationary phase, the N-replete, 1000 p.p.m. cultures may have also become N limited so they may have also channelled the excess carbon into TEP production, explaining the high concentrations.

If the enhanced concentrations of TEPs influence aggregation and the formation of marine snow then this could explain the increased sinking velocity seen in the high CO_2 N-limited cultures. There was no evidence to suggest that there was an increased aggregation in these cultures however. Furthermore, the N-replete cells grown at 1000 p.p.m. CO_2, which also displayed relatively high TEP concentrations, did not have a sinking velocity that was significantly different from that of the N-replete, 400 p.p.m. CO_2 cultures. It is difficult to conclude therefore, that the increased sinking rate seen in the N-limited high CO_2 cultures was due to the increased presence of TEP.

The formation of marine snow will depend on the presence of solid particles in the medium as well as mechanisms which allow the suspended particles to collide, including Brownian motion, differential settling rates and turbulent fluid shear (Kiørboe et al., 1998, Simon et al., 2002). In the present study there was a lack of clay particles and detritus. Furthermore, the conditions may not have been satisfactory to ensure collision. In fact, Engel et al. (2009a) added mineral particles to cultures of *E. huxleyi* and incubated them using a roller table to promote rapid aggregation. Failing to include solid particles in the present study may have resulted in a reduced rate of aggregation

and hindered the formation of marine snow. It is possible therefore, that in a natural setting, under the conditions associated with climate change, TEP increases as seen here, would have lead to the formation of large particles of marine snow, enhancing sinking velocities further.

In these high CO_2 cultures, there was a high ratio of TEPs to solid particles. Azetsu-Scott and Passow (2004) observed that this can retard sinking, even causing particles to ascend, because TEPs add low density mass. Unless the density of an aggregate or cell colony outweighs the positive buoyancy caused by the TEPs, the cells will not sink (Azetsu-Scott and Passow, 2004). The N-limited, high CO_2 cultures in this study displayed a relatively high density and therefore the cells sank rapidly, despite the high presence of TEPs and the lack of observed aggregation. On the other hand, the N-replete, high CO_2 cultures displayed a relatively low density. The combination of the reduced density and the high TEP concentration may have been responsible for the reduced sinking velocity seen in these cultures and would also explain why a significantly high form resistance was observed.

The data here suggest that under increased concentrations of CO_2 and N-limitation, the chain forming diatom, *C. didymus* will sink at a faster rate. The ability to form long chains, to implement physiological changes, to potentially increase rates of silification and to also form large aggregations, seem to allow the cells to reduce their positive buoyancy and may facilitate their sinking to deeper and nutrient rich waters. In some regions of the ocean however, where warming surface waters and stratification will reduce the return flow of remineralized carbon and nutrients to the surface waters, it is expected that overall primary production will decline (Beardall et al., 2001, Raven et al., 2005, Riebesell et al., 2007). In addition, it is expected that larger phytoplankton cells, which have higher nutrient requirements, will be more strongly affected by nutrient depletion than small cells (Beardall et al., 2009a, Beardall et al., 2009b). Indeed, the data reported here suggest that *C. didymus* will be affected by N-limitation in terms of growth and photosynthesis and

that increased concentrations of CO_2 will confer little advantage. Smaller celled species, that sink at reduced velocities and that do not operate CCMs could therefore become more dominant in the oceans. Given that diatoms like *C. didymus* are currently numerically important and major contributors to carbon export to the deep sea (Smetacek, 2000, Sarthou et al., 2005), this could affect the efficiency of the biological carbon pump.

Chapter 6.0: General Conclusions

6.1 General Conclusion

Approximately 1-3% of the yearly 50–60 Pg C of marine primary production currently settles in the deep ocean, due in part, to the activity of the biological carbon pump (Falkowski et al., 1998, Passow and De La Rocha, 2006). Central to the strength of the biological carbon pump is sinking of phytoplankton cells. In order for accurate predictions to be made about the likely extent of future climate change, it is important to know whether the biological carbon pump will continue to operate at its existing capacity or whether it will change its drawdown capabilities as a consequence of anthropogenic activities. Therefore, it is important to understand whether the sinking velocity of phytoplankton cells will change in the future with changing environmental conditions. In the future, phytoplankton cells in the open ocean are not only predicted to be exposed to higher concentrations of CO_2, but they are also predicted to be subject to nutrient limitation due to enhanced stratification reducing the upwelling of nutrients. Given that growth conditions can result in changes in cell size and macromolecular composition of phytoplankton, it might be expected that such changes could cause alterations in sinking velocity and carbon drawdown via the biological carbon pump.

The aim of this project was therefore to determine whether the sinking velocity of two algal species, *Emiliania huxleyi* and *Chaetoceros didymus*, would change under some of the conditions associated with climate change, those being nitrogen limitation and elevated concentrations of CO_2. In addition, this project aimed to determine why any changes in sinking velocity may or may not have occurred by examining changes in cell size and density. These factors were examined both during the exponential and stationary growth phase. Changes in macromolecular composition and the concentration of TEPs were also examined, as these factors can potentially alter cell size and density.

It was hypothesised that increases in CO_2 or N limitation would alter the size and the macromolecular composition of cells. Based on the data presented here, this was shown to be the case. Both species altered their size and macromolecular composition in response to the environmental changes. This hypothesis was therefore supported.

It was also hypothesised that changes in macromolecular composition would influence the sinking velocity of cells. This generally was not found to be the case. Density was not significantly influenced by the changes in macromolecular composition and as a result, sinking was not altered. This hypothesis was refuted.

Finally, it was hypothesised that cell size would be an important factor when determining the sinking velocity. Cell size did significantly influence the sinking velocity of cells and therefore this hypothesis was also supported.

E. huxleyi N-limited cells in the exponential growth phase sank more slowly than the N-replete cells. Cells in stationary phase showed the reverse trend with N-limited cells sinking faster, although not as fast as N-replete cells in exponential phase. However, under high CO_2, no significant difference in sinking velocity was observed for *E. huxleyi* when cells were in exponential growth phase. It is unknown whether high CO_2 would have altered this sinking velocity during stationary phase because the growing cells rapidly consumed the CO_2 and a high carbon environment could not be maintained under the resulting high cell numbers. *C. didymus* on the other hand, increased its sinking velocity significantly when the cells were exposed to high CO_2 but the sinking velocity was further enhanced under N-limitation during the exponential growth phase. Likewise, during stationary growth phase, the sinking velocity of *C. didymus* was greatest in the two N-limited groups, the concentration of CO_2 making no difference. The data suggest therefore, that N-

limitation plays a more important role in altering the sinking velocity for *E. huxleyi* and *C. didymus* than does CO_2.

During the exponential growth phase, changes in macromolecular composition were detected as a result of N-limitation and high CO_2. Cultures of *E. huxleyi* had slightly lower protein concentrations under N-limitation, whereas lipid and carbohydrate concentrations increased. High CO_2 caused the *E. huxleyi* cells to increase their concentrations of lipids, carbohydrates and proteins. For *C. didymus* there were also significant increases in lipid concentrations when the cells were exposed to high CO_2. N-limitation in combination with high CO_2 further promoted lipid accumulation in *C. didymus*. The same trends were seen in relation to carbohydrates, with the highest concentrations of β-1,3 glucan and cell wall polysaccharides being observed when high CO_2 was combined with N-limitation. Despite these increases in macromolecules, cell densities (specific gravity) during the exponential growth phase remained similar to that of the control group for *E. huxleyi* and *C. didymus*. A number of authors have suggested that lipid accumulation in phytoplankton will alter cell densities and that this will significantly influence the rate of sinking (Fernández et al., 1994, Paasche, 2002). As there were no significant changes in density, this data is in agreement with Smayda (1970) who concluded that lipid accumulation is generally an unimportant suspension mechanism in phytoplankton and that the impacts it has on sinking are negligible.

The sinking velocity of *E. huxleyi* was significantly influenced by cell size. During the exponential growth phase, the N-replete *E. huxleyi* cells, which sank the fastest, had the greatest diameter, while during stationary phase the N-limited *E. huxleyi* cells had the greatest diameter and sank the fastest. The size difference at stationary phase was due largely to an increase in the thickness of the coccosphere layer. Coccolith production has been associated N-limitation and starvation (Linschooten et al., 1991, Lecourt et al., 1996). It has been suggested that in a low-nutrient

environment, movement through the water to nutrient-rich deeper waters is essential for survival so *E. huxleyi* cells produce coccoliths to facilitate their sinking (Linschooten et al., 1991, Lecourt et al., 1996, Paasche, 2002). The results here suggest that coccolith production does facilitate sinking but not because of an increase in density, rather due to an increase in overall cell size.

When grown in the high CO_2 environment, there was no difference seen in the overall average size of *E. huxleyi* cells. There was also no difference seen in the sinking velocity, further suggesting that size does play an important role in the sinking of this species. While there was no difference in the cell size overall, the cells exposed to high CO_2 did reduce the width of their coccosphere. The reduction in the width of the coccosphere may have been due to a decrease in the rate of calcification and it has been hypothesised, that a reduction in calcification could lead to a decrease in sinking velocity (Lecourt et al. 1996, Riebesell et al., 2000, Zondervan et al., 2001, Müller et al., 2010). In the high CO_2 environment however, the *E. huxleyi* cells also increased the size of their protoplast, maintaining an average size overall, and as a result, there was no variation in sinking velocity observed. It is thought that an increase in CO_2 in the surrounding environment suppresses CCM activity which in turn, frees up energy that can be used to support growth and organic carbon fixation (Barcelos e Ramos et al., 2010).

During both exponential and stationary growth phases, the cells of the chain forming *C. didymus,* when grown under N-limitation and present-day CO_2 concentrations, were significantly larger than cells grown under N-replete conditions. This increase in volume could be explained by the fact that these cells formed longer chains more readily. This increase in chain formation may also explain the increase seen in sinking among these cells. An increase in chain length has been observed to increase the sinking velocity of cells if the extra ornamentation increases the density to a point where it exceeds any corresponding increase in viscous drag (Anderson et al., 1985). Furthermore,

when two cells are joined to form a chain, the surface area where they touch is no longer available to viscous drag by the suspending medium and the result can be such that a chain will sink faster than an individual cell (Booker and Walsby, 1979).

Increasing chain length may also assist cells to acquire nutrients so it would make sense that these cells would form chains more readily in the N-limited environment. In between each cell in a *C. didymus* chain, large gaps are present. It has been observed that chains with large gaps achieve a significantly greater nutrient supply than compact chains and solitary cells because the gaps work to increase cell surface area to volume ratio, improving the diffusive transport of nutrients to each cell (Pahlow et al., 1998). Musielak et al. (2009) also observed that diatom chains allow the cells to encounter a greater number of resources, increasing the nutrient concentration gradient around each cell, allowing for greater nutrient uptake. Chain formation therefore, appears to be an adaptation to allow the cells to acquire nutrients from the surrounding medium and to also accelerate the sinking to nutrient rich waters.

Despite their equally fast sinking velocity, the N-limited *C. didymus* cells grown at 1000 p.p.m. CO_2 failed to display a high proportion of chains across the different growth phases. This is perhaps due to the cells being suspended in a lower pH environment for a prolonged length of time and the dissolution of the silica spines that link the cells (Hoogstraten et al., 2012). These cells did however display a significant increase in cell density, which appeared to be increasing the rate of sinking. This may suggest that the cells implemented some physiological changes under the high CO_2 and N-limited conditions, although it is not clear what this change was.

The sinking velocity of diatoms embedded in marine snow is generally faster than that of individually sinking cells and the formation of marine snow is generally enhanced by the presence

of TEP which are sticky and aggregate particles such phytoplankton cells (Alldredge et al., 1993, Engel, 2000, Azetsu-Scott and Passow, 2004). The concentration of TEP increased significantly during this study when the cells were exposed to N-limitation or bubbled with 1000 p.p.m. CO_2 during stationary growth phase. In the case of *C. didymus*, the TEP concentration increased 5 times when high CO_2 and N-limitation were combined. Engel (2002) observed that under conditions of nutrient shortage, TEP production increased with pCO_2. This was most likely due to TEP production being linked to cellular carbon overflow whenever nutrient acquisition limited biomass production but not photosynthesis (Engel, 2002). During these experiments however, there was no evidence to suggest that there was an increased rate of aggregation in the cultures.

The formation of marine snow will depend on the presence of solid particles in the medium as well as mechanisms which allow the suspended particles to collide (Kiørboe et al., 1998, Simon et al., 2002). In the present study there was a lack of clay particles and detritus. Furthermore, the conditions may not have been satisfactory to ensure appropriate collision. In fact, Engel et al. (2009a) added mineral particles to cultures of *E. huxleyi* and incubated them using a roller table to promote rapid aggregation. Failing to include additional solid particles in the present study may have resulted in a reduced rate of aggregation and hindered the formation of marine snow. It is possible therefore, that in a natural setting, under the conditions associated with climate change, TEP increases as seen here could have led to the formation of large particles of marine snow, enhancing sinking velocities.

Owing to its larger size and density, *C. didymus*, generally sank faster than *E. huxleyi* regardless of life stage or growth condition. Since approximately 40% of marine productivity is contributed by diatoms generally, this suggests that large diatoms could play a particularly important role in the drawdown of CO_2 from the atmosphere. While an increase in the sinking velocity of *C. didymus* was

observed under these conditions, the high CO_2 in conjunction with N-limitation also saw a reduction in growth rates, chlorophyll concentrations and the photosynthetic efficiency parameters (F_v/F_m and α). This suggests that this species, and potentially larger diatoms, which have higher nutrient requirements, could perform poorly in the future ocean. As a result, smaller species, which have lower nutrient requirements, may become more dominant in the water column and will make a greater contribution to the biological carbon pump. The overall efficiency of the biological carbon pump could therefore decline as the smaller celled species will sink more slowly. It is however unclear from the results presented here whether the smaller celled *E. huxleyi* will perform any better than *C. didymus*. Further research is required to determine whether the same reductions in growth and photosynthesis will occur in *E. huxleyi* when N-limitation and high CO_2 are combined. Future studies should also be broadened to cover mixed populations so that it can be determined whether smaller species are favoured as CO_2 concentrations and nutrient limitations increase. It may also be beneficial to examine the impact that high CO_2 has on sinking velocities in different strains of *E. huxleyi* since its growth response to high CO_2 is strain specific (Langer et al., 2009).

Using the methods of Engel et al., (2009b), it would also be useful to create an experimental environment that encourages the formation of marine snow so that it can be determined whether increased TEP formation does influence the sinking velocity and the biological carbon pump. Cell size was found to be an important factor during this study. Therefore, cell aggregation is also likely to be an important factor when considering the sinking velocity. Future studies should therefore consider whether changes in the environmental parameters will influence the likelihood of cell aggregation and how this will influence the sinking velocity.

This field of study is critically important and further investments should be made in this area. We must be able to determine whether the biological carbon pump will continue to drawdown CO_2 at

its existing capacity so that accurate predictions about the likely extent of climate change can be made. It is through these means that we may be able to fundamentally change minds and influence governments to create meaningful climate policies in the future.

References

ABELMANN, A., GERSONDE, R., CORTESE, G., KUHN, G. & SMETACEK, V. 2006. Extensive phytoplankton blooms in the Atlantic sector of the glacial Southern Ocean. *Paleoceanography,* 21**,** PA1013.

AL-KANDARI, M., AL-YAMANI, F. & AL-RIFAIE, K. 2009. *Marine Phytoplankton Atlas of Kuwait's Waters,* Kuwait, Kuwait Institute for Scientific Research.

ALLDREDGE, A. L., GOTSCHALK, C., PASSOW, U. & RIEBESELL, U. 1995. Mass aggregation of diatom blooms: Insights from a mesocosm study. *Deep Sea Research Part II: Topical Studies in Oceanography,* 42**,** 9-27.

ALLDREDGE, A. L., PASSOW, U. & LOGAN, B. E. 1993. The abundance and significance of a class of large transparent organic particles in the ocean. *Deep-Sea Research Part I-Oceanographic Research Papers,* 40**,** 1131-1140.

ALLDREDGE, A. L. & SILVER, M. W. 1988. Characteristics, dynamics and significance of marine snow. *Progress in oceanography,* 20**,** 41-82.

AMHA-AWWA-WPCF 1998. *Standard methods for the examination of water and wastewater,* Washington, D.C.

ANDERSON, D. M., LIVELY, J. J., REARDON, E. M. & PRICE, C. A. 1985. Sinking characteristics of dinoflagellate cysts. *Limnology & Oceanography,* 30**,** 1000-1009.

ANDERSON, L. W. J. & SWEENEY, B. M. 1978. Role of inorganic ions in controlling sedimentation of a marine centric diatom *Ditylum Brightwellii*. *Journal of Phycology,* 14**,** 204-214.

ARMSTRONG, R. A., LEE, C., HEDGES, J. I., HONJO, S. & WAKEHAM, S. G. 2001. A new, mechanistic model for organic carbon fluxes in the ocean based on the quantitative association of POC with ballast minerals. *Deep Sea Research Part II: Topical Studies in Oceanography,* 49**,** 219-236.

AZETSU-SCOTT, K. & PASSOW, U. 2004. Ascending marine particles: Significance of transparent exopolymer particles (TEP) in the upper ocean. *Limnology and oceanography:,* 49**,** 741-748.

BARCELOS E RAMOS, J., MÜLLER, M. & RIEBESELL, U. 2010. Short-term response of the coccolithophore *Emiliania huxleyi* to an abrupt change in seawater carbon dioxide concentrations. *Biogeosciences,* 7**,** 177-186.

BARCELOS E RAMOS, J., SCHULZ, K. G., BROWNLEE, C., SETT, S. & AZEVEDO, E. B. 2014. Effects of Increasing Seawater Carbon Dioxide Concentrations on Chain Formation of the Diatom *Asterionellopsis glacialis*. *Plos One,* 9**,** e90749.

BARKER, S., HIGGINS, J. A. & ELDERFIELD, H. 2003. The Future of the Carbon Cycle: Review, Calcification Response, Ballast and Feedback on Atmospheric CO_2. *Philosophical Transactions: Mathematical, Physical and Engineering Sciences,* 361**,** 1977-1999.

BEARDALL, J., ROBERTS, S. & MILLHOUSE, J. 1991. Effects of nitrogen limitation on uptake of inorganic carbon and specific activity of ribulose-1,5-bisphosphate carboxylase/oxygenase in green microalgae. *Canadian Journal of Botany,* 69**,** 1146-1150.

BEARDALL, J., SOBRINO, C. & STOJKOVIC, S. 2009a. Interactions between the impacts of ultraviolet radiation, elevated CO_2, and nutrient limitation on marine primary producers. *Photochemical and Photobiological Sciences,* 8**,** 1257-1265.

BEARDALL, J., STOJKOVIC, S. & LARSEN, S. 2009b. Living in a high CO_2 world: impacts of global climate change on marine phytoplankton. *Plant Ecology & Diversity,* 2**,** 191-205.

BEARDALL, J., YOUNG, E. & ROBERTS, S. 2001. Approaches for determining phytoplankton nutrient limitation. *Aquatic Sciences,* 63**,** 44-69.

BEAUFORT, L., PROBERT, I., DE GARIDEL-THORON, T., BENDIF, E. M., RUIZ-PINO, D., METZL, N., GOYET, C., BUCHET, N., COUPEL, P., GRELAUD, M., ROST, B., RICKABY, R. E. M. & DE VARGAS, C. 2011. Sensitivity of coccolithophores to carbonate chemistry and ocean acidification. *Nature,* 476**,** 80-83.

BELSHE, E. F., DURAKO, M. J. & BLUM, J. E. 2007. Photosynthetic rapid light curves (RLC) of *Thalassia testudinum* exhibit diurnal variation. *Journal of Experimental Marine Biology and Ecology,* 342**,** 253-268.

BEMAN, J. M., CHOW, C.-E., KING, A. L., FENG, Y., FUHRMAN, J. A., ANDERSSON, A., BATES, N. R., POPP, B. N. & HUTCHINS, D. A. 2011. Global declines in oceanic nitrification rates as a consequence of ocean acidification. *Proceedings of the National Academy of Sciences,* 108**,** 208-213.

BENTLEY, K. A. 2006. *Adaptive behaviour through morphological plasticity in natural and artificial systems,* London, University of London.

BERGES, J. A., CHARLEBOIS, D. O., MAUZERALL, D. C. & FALKOWSKI, P. G. 1996. Differential Effects of Nitrogen Limitation on Photosynthetic Efficiency of Photosystems I and II in Microalgae. *Plant Physiology,* 110**,** 689-696.

BIERMANN, A. & ENGEL, A. 2010. Effect of CO_2 on the properties and sinking velocity of aggregates of the coccolithophore *Emiliania huxleyi*. *Biogeosciences,* 7**,** 1017-1029.

BLIGH, E. G. & DYER, W. J. 1959. A rapid method of total lipid extraction and purification. *Canadian journal of biochemistry and physiology,* 37**,** 911-917.

BOOKER, M. J. & WALSBY, A. E. 1979. The relative form resistance of straight and helical blue-green algal filaments. *British Phycological Journal,* 14**,** 141-150.

BOPP, L., MONFRAY, P., AUMONT, O., DUFRESNE, J.-L., LE TREUT, H., MADEC, G., TERRAY, L. & ORR, J. C. 2001. Potential impact of climate change on marine export production. *Global Biogeochemical Cycles,* 15**,** 81-99.

BORCHARD, C., BORGES, A. V., HÄNDEL, N. & ENGEL, A. 2011. Biogeochemical response of *Emiliania huxleyi* (PML B92/11) to elevated CO_2 and temperature under phosphorous limitation: A chemostat study. *Journal of Experimental Marine Biology and Ecology,* 410**,** 61-71.

BORCHARD, C. & ENGEL, A. 2012. Organic matter exudation by *Emiliania huxleyi* under simulated future ocean conditions. *Biogeosciences,* 9**,** 3405-3423.

BOYD, C. & GRADMANN, D. 2002. Impact of osmolytes on buoyancy of marine phytoplankton. *Marine Biology,* 141**,** 605-618.

BURKHARDT, S., RIEBESELL, U. & ZONDERVAN, I. 1999. Effects of growth rate, CO_2 concentration, and cell size on the stable carbon isotope fractionation in marine phytoplankton. *Geochimica et Cosmochimica Acta,* 63**,** 3729-3741.

CALDEIRA, K. & WICKETT, M. E. 2003. Oceanography: Anthropogenic carbon and ocean pH. *Nature,* 425**,** 365-365.

CARACO, N., COLE, J. & LIKENS, G. E. 1990. A Comparison of Phosphorus Immobilization in Sediments of Freshwater and Coastal Marine Systems. *Biogeochemistry,* 9**,** 277-290.

CARMELO, T. R., HASLE, G. R., SYVERTSON, E. E., STEIDINGER, K. A., TANGEN, K., THRONDSEN, J. & HEIMDAL, B. R. (eds.) 1997. *Identifying Marine Phytoplankton,* San Diego, Academic Press.

CHRISMADHA, T. & BOROWITZKA, M. 1994. Effect of cell density and irradiance on growth, proximate composition and eicosapentaenoic acid production of *Phaeodactylum tricornutum* grown in a tubular photobioreactor. *Journal of applied phycology,* 6**,** 67-74.

CHU, W.-L., PHANG, S.-M. & GOH, S.-H. 1996. Environmental effects on growth and biochemical composition of *Nitzschia inconspicua* Grunow. *Journal of applied phycology,* 8**,** 389-396.

CLAQUIN, P., MARTIN-JÉZÉQUEL, V., KROMKAMP, J. C., VELDHUIS, M. J. W. & KRAAY, G. W. 2002. Uncoupling of silicon compared with carbon and nitrogen metabolism and the role of the cell cycle in continuous cultures of *Thalassiosira Pseudonana* (Bacillariophyceae) under light, nitrogen and phosphorus control. *Journal of Phycology,* 38**,** 922-930.

CORZO, A., MORILLO, J. A. & RODRÍGUEZ, S. 2000. Production of transparent exopolymer particles (TEP) in cultures of *Chaetoceros calcitrans* under nitrogen limitation. *Aquatic Microbial Ecology,* 23**,** 63-72.

DAVEY, M. C. & WALSBY, A. E. 1985. The form resistance of sinking algal chains. *British Phycological Journal,* 20**,** 243-248.

DAVIS, C. O., HOLLIBAUGH, J. T., SEIBERT, D. L. R., THOMAS, W. H. & HARRISON, P. J. 1980. Formation of resting spores by *Leptocylindrus Danicus* (Bacillariophyceae) in a controlled experimental ecosystem. *Journal of Phycology,* 16**,** 296-302.

DE BODT, C., VAN OOSTENDE, N., HARLAY, J., SABBE, K. & CHOU, L. 2010. Individual and interacting effects of pCO_2 and temperature on *Emiliania huxleyi* calcification: study of the calcite production, the coccolith morphology and the coccosphere size. *Biogeosciences,* 7**,** 1401-1412.

DE LA ROCHA, C. L. & PASSOW, U. 2007. Factors influencing the sinking of POC and the efficiency of the biological carbon pump. *Deep Sea Research Part II: Topical Studies in Oceanography,* 54**,** 639-658.

DONEY, S. C. 2006. The dangers of ocean acidification. *Scientific American,* 294**,** 58-65.

DUBOIS, M., GILLES, K. A., HAMILTON, J. K., REBERS, P. A. & SMITH, F. 1956. Colorimetric Method for Determination of Sugars and Related Substances. *Analytical Chemistry,* 28**,** 350-356.

DYHRMAN, S. T., HALEY, S. T., BIRKELAND, S. R., WURCH, L. L., CIPRIANO, M. J. & MCARTHUR, A. G. 2006. Long serial analysis of gene expression for gene discovery and transcriptome profiling in the widespread marine coccolithophore *Emiliania huxleyi*. *Applied and Environmental Microbiology,* 72**,** 252-260.

EMILIANI, C. 1993. Viral extinctions in deep-sea species. *Nature,* 366**,** 217-218.

ENGEL, A. 2000. The role of transparent exopolymer particles (TEP) in the increase in apparent particle stickiness (α) during the decline of a diatom bloom. *Journal of Plankton Research,* 22**,** 485-497.

ENGEL, A. 2002. Direct relationship between CO_2 uptake and transparent exopolymer particles production in natural phytoplankton. *Journal of Plankton Research,* 24**,** 49-53.

ENGEL, A., ABRAMSON, L., SZLOSEK, J., LIU, Z. F., STEWART, G., HIRSCHBERG, D. & LEE, C. 2009a. Investigating the effect of ballasting by $CaCO_3$ in *Emiliania huxleyi*, II: Decomposition of particulate organic matter. *Deep-Sea Research Part Ii-Topical Studies in Oceanography,* 56**,** 1408-1419.

ENGEL, A., DELILLE, B., JACQUET, S., RIEBESELL, U., ROCHELLE-NEWALL, E., TERBRUGGEN, A. & ZONDERVAN, I. 2004. Transparent exopolymer particles and dissolved organic carbon production by *Emiliania huxleyi* exposed to different CO_2 concentrations: a mesocosm experiment. *Aquatic Microbial Ecology,* 34**,** 93-104.

ENGEL, A., SZLOSEK, J., ABRAMSON, L., LIU, Z. & LEE, C. 2009b. Investigating the effect of ballasting by $CaCO_3$ in *Emiliania huxleyi*: I. Formation, settling velocities and physical properties of aggregates. *Deep Sea Research Part II: Topical Studies in Oceanography,* 56**,** 1396-1407.

FALKOWSKI, P. G., BARBER, R. T. & SMETACEK, V. 1998. Biogeochemical controls and feedbacks on ocean primary production. (Special Section: Chemistry and Biology of the Oceans). *Science,* 281**,** 200-206.

FALKOWSKI, P. G., SUKENIK, A. & HERZIG, R. 1989. Nitrogen Limitation in *Isochrysis Galbana* (Haptophyceae). II. Relative Abundance of Chloroplast Proteins. *Journal of Phycology,* 25**,** 471-478.

FENG, Y., WARNER, M. E., ZHANG, Y., SUN, J., FU, F.-X., ROSE, J. M. & HUTCHINS, D. A. 2008. Interactive effects of increased pCO_2, temperature and irradiance on the marine coccolithophore *Emiliania huxleyi* (Prymnesiophyceae). *European Journal of Phycology,* 43**,** 87-98.

FERNÁNDEZ, E., BALCH, W. M., HOLLIGAN, P. M. & MARAÑÓN, E. 1994. High rates of lipid biosynthesis in cultured, mesocosm and coastal populations of the coccolithophore *Emiliania huxleyi*. *Marine Ecology Progress Series,* 22**,** 13-22.

FLYNN, K. J., BLACKFORD, J. C., BAIRD, M. E., RAVEN, J. A., CLARK, D. R., BEARDALL, J., BROWNLEE, C., FABIAN, H. & WHEELER, G. L. 2012. Changes in pH at the exterior surface of plankton with ocean acidification. *Nature Climate Change,* 2**,** 510-513.

FOWLER, S. W. & KNAUER, G. A. 1986. Role of large particles in the transport of elements and organic compounds through the oceanic water column. *Progress in oceanography,* 16**,** 147-194.

GANF, G. G., STONE, S. J. L. & OLIVER, R. L. 1986. Use of protein to carbohydrate ratios to analyse for nutrient deficiency in phytoplankton. *Australian Journal of Marine & Freshwater Research,* 37**,** 183-197.

GORDILLO, F. J. L., GOUTX, M., FIGUEROA, F. L. & NIELL, F. X. 1998. Effects of light intensity, CO_2 and nitrogen supply on lipid class composition of *Dunaliella viridis*. *Journal of applied phycology,* 10**,** 135-144.

GRANUM, E., KIRKVOLD, S. & MYKLESTAD, S. M. 2002. Cellular and extracellular production of carbohydrates and amino acids by the marine diatom *Skeletonema costatum*: Diel variations and effects of N depletion. *Marine Ecology Progress Series,* 242**,** 83-94.

GRANUM, E. & MYKLESTAD, S. M. 2002. A simple combined method for determination of β-1,3-glucan and cell wall polysaccharides in diatoms. *Hydrobiologia,* 477**,** 155-161.

GUCKERT, J. B., COOKSEY, K. E. & JACKSON, L. L. 1988. Lipid sovent systems are not equivalent for analysis of lipid classes in the microeukaryotic green alga, *Chlorella*. *Journal of Microbiological Methods,* 8**,** 139-149.

HANSEN, P. J., LUNDHOLM, N. & ROST, B. 2007. Growth limitation in marine red-tide dinoflagellates: effects of pH versus inorganic carbon availability. *Marine Ecology Progress Series,* 334**,** 63-71.

HEIN, M., PEDERSEN, M. F. & SAND JENSEN, K. 1995. Size-dependent nitrogen uptake in micro- and macroalgae. *Marine Ecology Progress Series,* 118**,** 247-254.

HENDERIKS, J., WINTER, A., ELBRAECHTER, M., FEISTEL, R., VAN DER PLAS, A., NAUSCH, G. & BARLOW, R. 2012. Environmental controls on *Emiliania huxleyi* morphotypes in the Benguela coastal upwelling system (SE Atlantic). *Marine Ecology Progress Series,* 448**,** 51-66.

HESSEN, D. O. & ANDERSON, T. R. 2008. Excess carbon in aquatic organisms and ecosystems: physiological, ecological, and evolutionary implications. *Limnology and Oceanography,* 53**,** 1685-1696.

HOLLAND, D. P. 2010. Sinking rates of phytoplankton filaments orientated at different angles: Theory and physical model. *Journal of Plankton Research,* 32**,** 1327-1336.

HONG, Y., SMITH, W. O. & WHITE, A. M. 1997. Studies on Transparent Exopolymer Particles (TEP) Produced in the Ross Sea (Antarctica) and by *Phaeocystis antarctica* (Prymnesiophyceae). *Journal of Phycology,* 33**,** 368-376.

HONJO, S., EGLINTON, T. I., TAYLOR, C. D., ULMER, K. M., SIEVERT, S. M., BRACHER, A., GERMAN, C. R., EDGCOMB, V., FRANCOIS, R. & INGLESIAS-RODRIGUEZ, M. D. 2014. Understanding the role of the Biological Pump in the Global Carbon Cycle: An imperative for Ocean Science. *Oceanography,* 27**,** 10-16.

HOOGSTRATEN, A., TIMMERMANS, K. R. & DE BAAR, H. J. W. 2012. Morphological and physiological effects in *Proboscia Alata* (Bacillariophyceae) grown under different light and CO_2 conditions of the modern Southern Ocean. *Journal of Phycology***,** 48, 559-568.

HOPKINSON, B. M., DUPONT, C. L., ALLEN, A. E. & MOREL, F. M. M. 2011. Efficiency of the CO_2-concentrating mechanism of diatoms. *Proceedings of the National Academy of Sciences*, 108, 3830-3837.

HUTCHINS, D. A. 2011. Oceanography: Forecasting the rain ratio. *Nature,* 476**,** 41-42.

IGLESIAS-RODRIGUEZ, M. D., HALLORAN, P. R., RICKABY, R. E. M., HALL, I. R., COLMENERO-HIDALGO, E., GITTINS, J. R., GREEN, D. R. H., TYRRELL, T., GIBBS, S. J., VON DASSOW, P., REHM, E., ARMBRUST, E. V. & BOESSENKOOL, K. P. 2008. Phytoplankton Calcification in a High-CO_2 World. *Science,* 320**,** 336-340.

JEFFREY, S. & LEROI, J. 1997. *Simple procedures for growing SCOR reference microalgal cultures*, France, UNESCO Publishing.

JEFFREY, S. W. & HUMPHREY, G. F. 1975. New spectrophotometric equations for determining chlorophylls *a*, *b*, c_1 and c_2 in higher plants, algae and natural phytoplankton. *Biochemie und Physiologie der Pflanzen,* 167**,** 191–194.

KARP-BOSS, L., BOSS, E. & JUMARS, P. 1996. Nutrient fluxes to planktonic osmotrophs in the presence of fluid motion. *Oceanography and Marine Biology,* 34**,** 71-108.

KELLER, M. D., SELVIN, R. C., CLAUS, W. & GUILLARD, R. R. L. 1987. Media for the Culture of Oceanic Ultraphytoplankton. *Journal of Phycology,* 23**,** 633-638.

KIØRBOE, T., TISELIUS, P., MITCHELL-INNES, B., HANSEN, J. L. S., VISSER, A. W. & MARI, X. 1998. Intensive aggregate formation with low vertical flux during an upwelling-induced diatom bloom. *Limnology and Oceanography,* 43**,** 104-116.

KLAAS, C. & ARCHER, D. E. 2002. Association of sinking organic matter with various types of mineral ballast in the deep sea: Implications for the rain ratio. *Global Biogeochem. Cycles,* 16.

KOLBER, Z., ZEHR, J. & FALKOWSKI, P. 1988. Effects of growth irradiance and nitrogen limitation on photosynthetic energy conversion in photosystem II. *Plant Physiology,* 88**,** 923-929.

KUSAIKIN, M., ERMAKOVA, S., SHEVCHENKO, N., ISAKOV, V., GORSHKOV, A., VERESHCHAGIN, A., GRACHEV, M. & ZVYAGINTSEVA, T. 2010. Structural characteristics and antitumor activity of a new chrysolaminaran from the diatom alga *Synedra acus*. *Chemistry of Natural Compounds,* 46**,** 1-4.

LANGER, G., GEISEN, M., BAUMANN, K.-H., KLÄS, J., RIEBESELL, U., THOMS, S. & YOUNG, J. R. 2006. Species-specific responses of calcifying algae to changing seawater carbonate chemistry. *Geochemistry, Geophysics, Geosystems,* 7.

LANGER, G., NEHRKE, G., PROBERT, I., LY, J. & ZIVERI, P. 2009. Strain-specific responses of *Emiliania huxleyi* to changing seawater carbonate chemistry. *Biogeosciences,* 6**,** 2637-2646.

LECOURT, M., MUGGLI, D. L. & HARRISON, P. J. 1996. Comparison of growth and sinking rates of non-coccolith and coccolith-forming strains of *Emiliania huxleyi* (Prymnesiophyceae) grown under different irradiances and nitrogen sources. *Journal of Phycology,* 32**,** 17-21.

LEFEBVRE, S. C., BENNER, I., STILLMAN, J. H., PARKER, A. E., DRAKE, M. K., ROSSIGNOL, P. E., OKIMURA, K. M., KOMADA, T. & CARPENTER, E. J. 2012. Nitrogen source and pCO_2 synergistically affect carbon allocation, growth and morphology of the coccolithophore *Emiliania huxleyi*: potential implications of ocean acidification for the carbon cycle. *Global Change Biology,* 18**,** 493-503.

LI, W., GAO, K. & BEARDALL, J. 2012. Interactive effects of ocean acidification and nitrogen-limitation on the diatom *Phaeodactylum tricornutum*. *Plos One,* 7**,** e51590.

LINSCHOOTEN, C., VAN BLEJSWIJK, J. D. L., VAN EMBURG, P. R., DE VRIND, J. P. M., KEMPERS, E. S., WESTBROEK, P. & DE VRIND-DE JONG, E. W. 1991. Role of the light-dark cycle and medium composition on the production of coccoliths by *Emiliania huxleyi* (Haptophyceae). *Journal of Phycology,* 27**,** 82-86.

LOEBL, M., COCKSHUTT, A. M., CAMPBELL, D. A. & FINKEL, Z. V. 2010. Physiological basis for high resistance to photoinhibition under nitrogen depletion in *Emiliania huxleyi*. *Limnology and Oceanography,* 55**,** 2150-2160.

LOWRY, O. H., ROSEBROUGH, N. J., FARR, A. L. & RANDALL, R. J. 1951. Protein measurement with the Folin phenol reagent. *The Journal of biological chemistry,* 193**,** 265-275.

MAXWELL, K. & JOHNSON, G. N. 2000. Chlorophyll fluorescence—a practical guide. *Journal of Experimental Botany,* 51**,** 659-668.

MCQUOID, M. R. & HOBSON, L. A. 1996. Diatom resting stages. *Journal of Phycology,* 32**,** 889-902.

MEEHL, G. A., STOCKER, T. F., COLLINS, W. D., FRIEDLINGSTEIN, P., GAYE, A. T., GREGORY, J. M., KITOH, A., KNUTTI, R., MURPHY, J. M., NODA, A., RAPER, S. C. B., WATTERSON, I. G., A.J., W. & Z.-C., Z. (eds.) 2007. *Global climate projections. Climate Change 2007: The Physical Science Basis. Contribution of Working Group I to the Fourth Assessment Report of the Intergovernmental Panel on Climate Change,* Cambridge, Cambridge University Press.

MILLIGAN, A. J., VARELA, D. E., BRZEZINSKI, M. A. & MOREL, F. M. M. 2004. Dynamics of silicon metabolism and silicon isotopic discrimination in a marine diatom as a function of pCO_2. *Limnology and Oceanography,* 49**,** 322-329.

MÜLLER, M., SCHULZ, K. & RIEBESELL, U. 2010. Effects of long-term high CO_2 exposure on two species of coccolithophores. *Biogeosciences (BG),* 7**,** 1109-1116.

MÜLLER, M. N., BEAUFORT, L., BERNARD, O., PEDROTTI, M. L., TALEC, A. & SCIANDRA, A. 2012. Influence of CO_2 and nitrogen limitation on the coccolith volume of *Emiliania huxleyi (*Haptophyta). *Biogeosciences,* 9**,** 4155-4167.

MUSIELAK, M. M., KARP-BOSS, L., JUMARS, P. A. & FAUCI, L. J. 2009. Nutrient transport and acquisition by diatom chains in a moving fluid. *Journal of Fluid Mechanics,* 638**,** 401-421.

MYKLESTAD, S. 1974. Production of carbohydrates by marine planktonic diatoms. I. Comparison of nine different species in culture. *Journal of Experimental Marine Biology and Ecology,* 15**,** 261-274.

OSBORNE, B. A. & GEIDER, R. J. 1986. Effect of nitrate-nitrogen limitation on photosynthesis of the diatom *Phaeodactylum tricornutum* Bohlin (Bacillariophyceae). *Plant, Cell & Environment,* 9**,** 617-625.

PAASCHE, E. 1998. Roles of nitrogen and phosphorus in coccolith formation in *Emiliania huxleyi (*Prymnesiophyceae). *European Journal of Phycology,* 33**,** 33-42.

PAASCHE, E. 2002. A review of the coccolithophorid *Emiliania huxleyi* (Prymnesiophyceae), with particular reference to growth, coccolith formation, and calcification-photosynthesis interactions. *Phycologia,* 40**,** 503-529.

PAHLOW, M., RIEBESELL, U. & WOLF-GLADROW, D. A. 1998. Impact of cell shape and chain formation on nutrient acquisition by marine diatoms. *Limnology and Oceanography,* 42**,** 1660-1672.

PANTORNO, A., HOLLAND, D. P., STOJKOVIC, S. & BEARDALL, J. 2013. Impacts of nitrogen limitation on the sinking rate of the coccolithophorid *Emiliania huxleyi* (Prymnesiophyceae). *Phycologia,* 52**,** 288-294.

PARKHILL, J. P., MAILLET, G. & CULLEN, J. J. 2001. Fluorescence-based maximal quantum yield for PSII as a diagnostic of nutrient stress. *Journal of Phycology,* 37**,** 517-529.

PARRISH, C. C. & WANGERSKY, P. J. 1990. Growth and lipid class composition of the marine diatom, *Chaetoceros gracilis*, in laboratory and mass culture turbidostats. *Journal of Plankton Research,* 12**,** 1011-1021.

PASSOW, U. 2002. Transparent exopolymer particles (TEP) in aquatic environments. *Progress in oceanography,* 55**,** 287-333.

PASSOW, U. & ALLDREDGE, A. L. 1995. A dye-binding assay for the spectrophotometric measurement of transparent exopolymer particles (TEP). *Limnology and Oceanography,* 40**,** 1326-1335.

PASSOW, U. & DE LA ROCHA, C. L. 2006. Accumulation of mineral ballast on organic aggregates. *Global Biogeochem. Cycles,* 20**,** GB1013.

PASSOW, U., SHIPE, R. F., MURRAY, A., PAK, D. K., BRZEZINSKI, M. A. & ALLDREDGE, A. L. 2001. The origin of transparent exopolymer particles (TEP) and their role in the sedimentation of particulate matter. *Continental Shelf Research,* 21**,** 327-346.

PATIL, S. M., MOHAN, R., SHETYE, S., GAZI, S. & JAFAR, S. 2014. Morphological variability of *Emiliania huxleyi* in the Indian sector of the Southern Ocean during the austral summer of 2010. *Marine Micropaleontology,* 107**,** 44-58.

PETERS, E. & THOMAS, D. N. 1996. Prolonged nitrate exhaustion and diatom mortality: a comparison of polar and temperate *Thalassiosira* species. *Journal of Plankton Research,* 18**,** 953-968.

PICKETT-HEAPS, J. D., CARPENTER, J. & KOUTOULIS, A. 1994. Valve and seta (spine) morphogenesis in the centric diatom *Chaetoceros peruvianus* Brightwell. *Protoplasma,* 181**,** 269-282.

PIONTEK, J., LUNAU, M., HÄNDEL, N., BORCHARD, C., WURST, M. & ENGEL, A. 2010. Acidification increases microbial polysaccharide degradation in the ocean. *Biogeosciences,* 7**,** 1615-1624.

PLUMLEY, F. G. & SCHMIDT, G. W. 1989. Nitrogen-dependent regulation of photosynthetic gene expression. *Proceedings of the National Academy of Sciences,* 86**,** 2678-2682.

RALPH, P. J. & GADEMANN, R. 2005. Rapid light curves: A powerful tool to assess photosynthetic activity. *Aquatic Botany,* 82**,** 222-237.

RAMANAN, R., VINAYAGAMOORTHY, N., SIVANESAN, S. D., KANNAN, K. & CHAKRABARTI, T. 2012. Influence of CO_2 concentration on carbon concentrating mechanisms in cyanobacteria and green algae: A proteomic approach. *Algae,* 27**,** 295-301.

RAVEN, J., CALDEIRA, K., ELDERFIELD, H., HOEGH-GULDBERG, O., LISS, P., RIEBESELL, U., SHEPHERD, J., TURLEY, C. & WATSON, A. 2005. *Ocean acidification due to increasing atmospheric carbon dioxide.* London, The Royal Society.

RAVEN, J. A. & WAITE, A. M. 2004. The evolution of silicification in diatoms: inescapable sinking and sinking as escape? *New Phytologist,* 162**,** 45-61.

REINFELDER, J., KRAEPIEL, A. M. L. & MOREL, F. M. M. 2000. Unicellular C4 photosynthesis in a marine diatom. *Nature,* 407**,** 996-999.

RIEBESELL, U. 1991. Particle aggregation during a diatom bloom. II. Biological aspects. *Marine Ecology Progress Series,* 69**,** 281-291.

RIEBESELL, U. 2004. Effects of CO_2 Enrichment on Marine Phytoplankton. *Journal of Oceanography,* 60**,** 719-729.

RIEBESELL, U., SCHULZ, K. G., BELLERBY, R. G. J., BOTROS, M., FRITSCHE, P., MEYERHOFER, M., NEILL, C., NONDAL, G., OSCHLIES, A., WOHLERS, J. & ZOLLNER, E. 2007. Enhanced biological carbon consumption in a high CO_2 ocean. *Nature,* 450**,** 545-548.

RIEBESELL, U., ZONDERVAN, I., ROST, B., TORTELL, P. D., ZEEBE, R. E. & MOREL, F. M. 2000. Reduced calcification of marine plankton in response to increased atmospheric CO_2. *Nature,* 407**,** 364-367.

ROBERTS, K., GRANUM, E., LEEGOOD, R. C. & RAVEN, J. A. 2007. C(3) and C(4) pathways of photosynthetic carbon assimilation in marine diatoms are under genetic, not environmental, control. *Plant Physiology,* 145**,** 230-235.

ROKITTA, S. D., JOHN, U. & ROST, B. 2012. Ocean acidification affects redox-balance and ion-homeostasis in the life-cycle stages of *Emiliania huxleyi*. *Plos One,* 7**,** e52212.

ROST, B. & RIEBESELL, U. 2004. Coccolithophores and the biological pump: responses to environmental changes. *Coccolithophores.* Berlin, Springer.

ROST, B., RIEBESELL, U. & SÜLTEMEYER, D. 2006. Carbon acquisition of marine phytoplankton: effect of the photoperiodic length. *Limnology and Oceanography,* 51**,** 12-20.

RUTTIMANN, J. 2006. Oceanography: Sick seas. *Nature,* 442**,** 978-980.

SARTHOU, G., TIMMERMANS, K. R., BLAIN, S. & TRÉGUER, P. 2005. Growth physiology and fate of diatoms in the ocean: a review. *Journal of Sea Research,* 53**,** 25-42.

SCIANDRA, A., HARLAY, J., LEFÈVRE, D., LEMÉE, R., RIMMELIN, P., DENIS, M. & GATTUSO, J.-P. 2003. Response of coccolithophorid *Emiliania huxleyi* to elevated partial pressure of CO_2 under nitrogen limitation. *Marine Ecology. Progress Series,* 261.

SHIFRIN, N. S. & CHISHOLM, S. W. 1981. Phytoplankton lipids: interspecific differences and effects of nitrate, silicate and light-dark cycles. *Journal of Phycology,* 17**,** 374-384.

SIMON, M., GROSSART, H.-P., SCHWEITZER, B. & PLOUG, H. 2002. Microbial ecology of organic aggregates in aquatic ecosystems. *Aquatic Microbial Ecology,* 28**,** 175-211.

SMAYDA, T. J. 1970. The Suspension and sinking of phytoplankton in the sea. *Oceanography and Marine Biology - An Annual Review* 8**,** 353-414.

SMAYDA, T. J. & BOLEYN, B. J. 1965. Experimental observations on the flotation of marine diatoms. I. *Thalassiosira cf. nana*, *Thalassiosira rotula* and *Nitzschia seriata*. *Limnology and Oceanography,* 10**,** 499-509.

SMAYDA, T. J. & BOLEYN, B. J. 1966a. Experimental Observations on the Flotation of Marine Diatoms. II. *Skeletonema costatum* and *Rhizosolenia setigera*. *Limnology and Oceanography,* 11**,** 18-34.

SMAYDA, T. J. & BOLEYN, B. J. 1966b. Experimental observations on the flotation of marine diatoms. III. *Bacteriastrum hyalinum* and *Chaetoceros lauderi*. *Limnology and Oceanography,* 11**,** 35-43.

SMETACEK, V. 1999. Diatoms and the ocean carbon cycle. *Protist,* 150**,** 25-32.

SMETACEK, V. 2000. Oceanography: The giant diatom dump. *Nature,* 406**,** 574.

SMETACEK, V. S. 1985. Role of sinking in diatom life-history cycles: ecological, evolutionary and geological significance. *Marine Biology,* 84**,** 239-251.

SOHM, J. A., WEBB, E. A. & CAPONE, D. G. 2011. Emerging patterns of marine nitrogen fixation. *Nature Reviews Microbiology,* 9**,** 499-508.

STOJKOVIC, S., BEARDALL, J. & MATEAR, R. 2013. CO_2-concentrating mechanisms in three southern hemisphere strains of *Emiliania huxleyi*. *Journal of Phycology,* 49**,** 670-679.

SUGIE, K. & KUMA, K. 2008. Resting spore formation in the marine diatom *Thalassiosira nordenskioeldii* under iron- and nitrogen-limited conditions. *Journal of Plankton Research,* 30**,** 1245-1255.

SUGIE, K., KUMA, K., FUJITA, S. & IKEDA, T. 2010. Increase in Si:N drawdown ratio due to resting spore formation by spring bloom-forming diatoms under Fe- and N-limited conditions in the Oyashio region. *Journal of Experimental Marine Biology and Ecology,* 382**,** 108-116.

SUNDA, W., KIEBER, D. J., KIENE, R. P. & HUNTSMAN, S. 2002. An antioxidant function for DMSP and DMS in marine algae. *Nature,* 418**,** 317-320.

TAKABAYASHI, M., LEW, K., JOHNSON, A., MARCHI, A., DUGDALE, R. & WILKERSON, F. P. 2006. The effect of nutrient availability and temperature on chain length of the diatom, *Skeletonema costatum*. *Journal of Plankton Research,* 28**,** 831-840.

TORTELL, P. D., PAYNE, C. D., LI, Y., TRIMBORN, S., ROST, B., SMITH, W. O., RIESSELMAN, C., DUNBAR, R. B., SEDWICK, P. & DITULLIO, G. R. 2008. CO_2 sensitivity of Southern Ocean phytoplankton. *Geophysical Research Letters,* 35**,** L04605.

TORTELL, P. D., RAU, G. H. & MOREL, F. M. 2000. Inorganic carbon acquisition in coastal Pacific phytoplankton communities. *Limnology and Oceanography,* 45**,** 1485-1500.

VAN DEN HOEK, C. M., MANN, D. G. JAHNS, H. M. 1995. *Algae : an introduction to phycology,* New York, Cambridge University Press.

WAITE, A., BIENFANG, P. & HARRISON, P. 1992. Spring bloom sedimentation in a subarctic ecosystem. *Marine Biology,* 114**,** 119-129.

WALSBY, A. E. & HOLLAND, D. P. 2006. Sinking velocities of phytoplankton measured on a stable density gradient by laser scanning. *Journal of the Royal Society Interface,* 3**,** 429-439.

WALSBY, A. E. & XYPOLYTA, A. 1977. The form resistance of chitan fibres attached to the cells of *Thalassiosira fluviatilis* Hustedt. *British Phycological Journal,* 12**,** 215 - 223.

WESTBROEK, P., BROWN, C. W., BLEIJSWIJK, J. V., BROWNLEE, C., BRUMMER, G. J., CONTE, M., EGGE, J., FERNÁNDEZ, E., JORDAN, R. & KNAPPERTSBUSCH, M. 1993. A model system approach to biological climate forcing. The example of *Emiliania huxleyi*. *Global and Planetary Change,* 8**,** 27-46.

WHITE, D. C., DAVIS, W. M., NICKELS, J. S., KING, J. D. & BOBBIE, R. J. 1979. Determination of the sedimentary microbial biomass by extractible lipid phosphate. *Oecologia,* 40**,** 51-62.

WIDJAJA, A., CHIEN, C.-C. & JU, Y.-H. 2009. Study of increasing lipid production from fresh water microalgae *Chlorella vulgaris*. *Journal of the Taiwan Institute of Chemical Engineers,* 40**,** 13-20.

WU, H., ZOU, D. & GAO, K. 2008. Impacts of increased atmospheric CO_2 concentration on photosynthesis and growth of micro- and macro-algae. *Science in China Series C: Life Sciences,* 51**,** 1144-1150.

WU, Y., GAO, K. & RIEBESELL, U. 2010. CO_2-induced seawater acidification affects physiological performance of the marine diatom *Phaeodactylum tricornutum*. *Biogeosciences Discussions,* 7**,** 3855-3878.

YOUNG, J., POULTON, A. & TYRRELL, T. 2014. Morphology of *Emiliania huxleyi* coccoliths on the northwestern European shelf – is there an influence of carbonate chemistry? *Biogeosciences,* 11**,** 4771-4782.

YOUNG, J. R. & ZIVERI, P. 2000. Calculation of coccolith volume and its use in calibration of carbonate flux estimates. *Deep-Sea Research Part II: Topical Studies in Oceanography,* 47**,** 1679-1700.

ZEEBE, R. E. & WOLF-GLADROW, D. A. 2001. *CO_2 in seawater: equilibrium, kinetics, isotopes*, Gulf Professional Publishing.

ZIVERI, P., DE BERNARDI, B., BAUMANN, K.-H., STOLL, H. M. & MORTYN, P. G. 2007. Sinking of coccolith carbonate and potential contribution to organic carbon ballasting in the deep ocean. *Deep Sea Research Part II: Topical Studies in Oceanography,* 54**,** 659-675.

ZONDERVAN, I., ROST, B. & RIEBESELL, U. 2002. Effect of CO_2 concentration on the PIC/POC ratio in the coccolithophore *Emiliania huxleyi* grown under light-limiting conditions and different daylengths. *Journal of Experimental Marine Biology and Ecology,* 272**,** 55-70.

ZONDERVAN, I., ZEEBE, R. E., ROST, B. & RIEBESELL, U. 2001. Decreasing marine biogenic calcification: A negative feedback on rising atmospheric *p*CO_2. *Global Biogeochemical Cycles,* 15**,** 507-516.